

# Journal of Energy

ISSN 1849-0751 (On-line)  
ISSN 0013-7448 (Print)  
UDK 621.31

**VOLUME 67 Number 3 | 2018 Special Issue**

---

- 03** A. Elez, J. Študir, S. Tvorčić  
Application of Differential Magnetic Field Measurement (DMFM method) in winding fault detection of AC rotating machines as part of expert monitoring systems
- 09** R. Sitar, Ž. Janić  
Determination of local losses and temperatures in power transformer tank
- 14** D. Gorenc, K. Flegar, I. Lončar, E. Plavec  
Simulation and Measurement of Pressure Rise in GIS 145 kV due to Internal Arcing
- 20** A. Foškulo, M. Kokoruš  
Streamlining the Decision-Making Process on Tubular Rigid Busbar Selection During the Planning / Designing Stage by Utilizing 3D Substation BIM Design Software
- 30** I. Ivanković, D. Peharda, D. Novosel, K. Žubrinić-Kostović, A. Kekelj  
Smart grid substation equipment maintenance management functionality based on control center SCADA data
- 36** I. Ivanković, V. Terzija, S. Skok  
Transmission network angle stability protection based on synchrophasor data in control centre
- 41** G. Majstrovic, D. Jaksic, M. Mikulic, D. Bajcs, W. Polen, A. Doub  
Impact of Adriatic submarine HVDC cables to South East European Electricity Market Perspectives
- 45** V. Komen, A. Antonic, T. Baricevic, M. Skok, T. Dolenc  
Coordinated TSO and DSO network development plan on the islands of Cres and Lošinj

# Journal of Energy

Scientific Professional Journal Of Energy, Electricity, Power Systems

Online ISSN 1849-0751, Print ISSN 0013-7448, VOL 67

## Published by

HEP d.d., Ulica grada Vukovara 37, HR-10000 Zagreb

HRO CIGRÉ, Berislavićeva 6, HR-10000 Zagreb

## Publishing Board

**Robert Krklec**, (president) HEP, Croatia,

**Božidar Filipović-Grčić**, (vicepresident), HRO CIGRÉ, Croatia

## Editor-in-Chief

**Goran Slipac**, HEP, Croatia

## Associate Editors

**Helena Božić** HEP, Croatia

**Stjepan Car** Green Energy Cooperation, Croatia

**Tomislav Gelo** University of Zagreb, Croatia

**Davor Grgić** University of Zagreb, Croatia

**Marko Jurčević** University of Zagreb, Croatia

**Mičo Klepo** Croatian Energy Regulatory Agency, Croatia

**Stevo Kolundžić** Croatia

**Vitomir Komen** HEP, Croatia

**Marija Šiško Kuliš** HEP, Croatia

**Dražen Lončar** University of Zagreb, Croatia

**Goran Majstrovic** Energy Institute Hrvoje Požar, Croatia

**Tomislav Plavšić** Croatian Transmission system Operator, Croatia

**Dubravko Sabolić** Croatian Transmission system Operator, Croatia

**Mladen Zeljko** Energy Institute Hrvoje Požar, Croatia

## International Editorial Council

**Anastasios Bakirtzis** University of Thessaloniki, Greece

**Eraldo Banovac** J. J. Strossmayer University of Osijek, Croatia

**Frano Barbir** University of Split, Croatia

**Tomislav Barić** J. J. Strossmayer University of Osijek, Croatia

**Frank Bezzina** University of Malta

**Srećko Bojić** Power System Institute, Zagreb, Croatia

**Tomislav Capuder** University of Zagreb, Croatia

**Ante Elez** Končar-Generators and Motors, Croatia

**Dubravko Franković** University of Rijeka, Croatia

**Hrvoje Glavaš** J. J. Strossmayer University of Osijek, Croatia

**Mevludin Glavić** University of Liege, Belgium

**Božidar Filipović Grčić** University of Zagreb, Croatia

**Dalibor Filipović Grčić** Končar-Electrical Engineering Institute, Croatia

**Josep M. Guerrero** Aalborg Universitet, Aalborg East, Denmark

**Juraj Havelka** University of Zagreb, Croatia

**Dirk Van Hertem** KU Leuven, Faculty of Engineering, Belgium

**Žarko Janić** Siemens-Končar-Power Transformers, Croatia

**Igor Kuzle** University of Zagreb, Croatia

**Niko Malbaša** Ekonerg, Croatia

**Matslav Majstrovic** University of Split, Croatia

**Zlatko Maljković** University of Zagreb, Croatia

**Predrag Marić** J. J. Strossmayer University of Osijek, Croatia

**Viktor Milardić** University of Zagreb, Croatia

**Srete Nikolovski** J. J. Strossmayer University of Osijek, Croatia

**Damir Novosel** Quanta Technology, Raleigh, USA

**Hrvoje Pandžić** University of Zagreb, Croatia

**Milutin Pavlica** Power System Institute, Zagreb, Croatia

**Robert Sitar** Končar-Electrical Engineering Institute, Croatia

**Damir Sumina** University of Zagreb, Croatia

**Elis Sutlović** University of Split, Croatia

**Zdenko Šimić** Joint Research Centre, Petten, The Netherlands

**Damir Šljivac** J. J. Strossmayer University of Osijek Croatia

**Darko Tipurić** University of Zagreb, Croatia

**Bojan Trkulja** University of Zagreb, Croatia

**Nela Vlahinić Lenz** University of Split, Croatia

**Mario Vražić** University of Zagreb, Croatia

## EDITORIAL

Journal of Energy special issue: Papers from 47. CIGRE Session, 26. – 31. August Paris/France.

Paris CIGRE Session is the world's number one global power system event. This event attracts members from across the whole CIGRE community and is the culmination of the previous two years of the CIGRE knowledge programme. The Paris Session is unlike any other conference. It offers an in-depth interactive congress, following a rigorous process where, rather than being presented, hundreds of papers are collaboratively debated.

At the Paris Session, Authors papers are circulated to delegates and carefully analysed in advance by the Study Committee 'Special Reporters'. Before the Paris Session, these Special Reporters prepare a series of questions addressed to the community in order to stimulate contributions.

The 'Group Discussion Meeting' of each Study Committee, managed by the Special Reporter, allows the selected 'Contributors' to present their point of view and experience, before an audience of experts. This way the collective expertise of the Contributors is harnessed to create new ideas that build on what the author presented in their paper under discussion.

New ideas and knowledge are synthesised the following day in what are called 'Daily Reports'. These, along with other Group Discussion Meeting inputs, form the basis of what the CIGRE Study Committees and their 'Working Groups' will focus on in the following two years.

In this special issue, 8 papers were accepted for publication in Journal of Energy after additional peer-review process.

The papers are from SC A1, PS2: Asset Management of Electrical Machines one paper, from SC A2, PS1: Thermal Characteristics of Power Transformers one paper, from SC A3, PS1: Requirements for AC and DC Transmission & Distribution Equipment one paper, from SC B3 PS2: Evolution in Substation Management two papers, from SC B5 PS1: Protection under System Emergency Conditions one paper and from SC C1 PS3: Coordinated Planning between Grid Operators across all Voltage Levels two papers.

Authors of these papers are mostly members of the Croatian National Committee of CIGRE, so this special edition gives in some way a current review of the projects and issues in the Croatian power system, Industry and Science community.

Guest Editor

**Prof. Viktor Milardić**

University of Zagreb, Croatia

Faculty of Electrical Engineering and Computing

Ante Elez, PhD\*  
Josip Študir, M.E.E.\*  
Stjepan Tvorčić, M.E.E.\*\*

\*KONČAR – Generators and Motors

\*\*KONČAR – Electrical Engineering Institute  
CROATIA

# Application of Differential Magnetic Field Measurement (DMFM method) in winding fault detection of AC rotating machines as part of expert monitoring systems

## SUMMARY

Stator and rotor winding damages in rotating machines are result of electrical, mechanical, and thermal stress. Online magnetic field monitoring via permanently installed measuring coils inside air gap is a well-established methodology which enables winding fault detection. The paper deals with a new method for detection of stator and rotor winding inter-turn short circuits of synchronous machines and slip rings induction machines, as well as rupture of rotor bars and cage ring of induction machines. The method novelty is based on differential measurement of magnetic field by using two serial connected measuring coils. They are installed on the places (stator or rotor teeth) in the machine which have, by absolute value, equal magnetic vector potential. The distance between the measuring coils is  $n \cdot \tau_p$ , where  $\tau_p$  is a pole pitch, and  $n = 1, 2, 3, 4, \dots$  is a multiple of the pole pitch. Measuring the coil-induced voltage enables us to detect stator and rotor winding faults, which means that measured voltage is approximately zero without fault and increases in the presence of fault. Analysis of the measuring signal allows us to detect and locate fault. With this new method it is possible with high sensitivity to determine winding fault, which enables more reliable fault detection. For example, in comparison with the motor current signature analysis method (the most widely used method for motor faults detection), this new method gives 200 times higher sensitivity to fault occurrence. Also, by using the DMFM method, faults can be detected in the time domain and there is no need for spectral or other complex signal analysis. This is very important because the measuring equipment used for machine fault detection can be simple and more economically acceptable. The DMFM method enables fault detection for even small machines with small expense in a very effective way. The only downside of the DMFM method is the fact that machine should be disassembled in order to install measuring coils. This problem is solved during the machine overhaul or during the manufacturing of the machine, when sensors can be easily implemented in the machine. For machines with large air gap, measuring coils can be installed without a machine disassembly. For the purpose of the method testing, numerous finite-element (FE) simulations on the 2- and 3-D machine models have been carried out to verify the method. Powerful numerical tools generate realistic results with properly selected starting and boundary conditions. By FEM models, actual machines with embedded measuring coils were created and simulated. The voltage induced inside the measuring coils is calculated for different machine states, load point and with and without a fault (broken rotor bar or inter-turn short circuit). Also, this method was experimentally validated via series of laboratory tests performed on the real electric machines specially designed for fault study (broken rotor bars, broken ring and inter-turn short circuits in a stator and rotor winding). Additionally, this method is applied on more than 20 real machines in industry. Due to the large amount of measured data, in this paper, it will be presented only one measurement performed on an induction motor on which we have

detected one broken rotor bar. The thickness of the measuring coil designed in the printed circuit board technique is 0.3 mm. The number of turns is from 3 to 10. This new method and performed FEM calculations together with the experimental measurements improve fault detection portfolio knowledge that can be used in monitoring and diagnostics of rotating machines. Furthermore, this patent-pending method is already implemented in three innovative products placed on market (expert monitoring systems), so this method is fully confirmed in practice.

## KEYWORDS

finite element, induction machine, inter-turn shorted circuits, rotor bars, rotor cage faults, synchronous generator, magnetic field, measuring coil, induced voltage, air gap

## INTRODUCTION

Stator and rotor winding damages in rotating machines are result of electrical, mechanical, and thermal stress. Online magnetic field monitoring via permanently installed measuring coils inside air gap is a well-established methodology which enables winding fault detection [1, 2, 3, 4, 5]. In the industry and according to the literature [6, 7, 8, 9], rotor winding faults are very common problem. Most commonly used method for detection of broken rotor bars is method based on current signature analysis (MCSA) [10, 11, 12, 13, 14, 15, 16, 17].

The novelty of DMFM method is differential measurement of the magnetic field in a rotating machine with two serial connected measuring coils, installed on the places in the machine which have, by absolute value, equal magnetic vector potential. The distance between the measuring coils is  $n \cdot \tau_p$ , where  $\tau_p$  is a pole pitch, and  $n=1, 2, 3, 4 \dots$  is a multiple of the pole pitch. A typical installation of measuring coils is presented in Figure 1. Measuring coils 1 and 2 are installed around stator tooth so that they encompass the whole stator tooth or just part of the tooth.

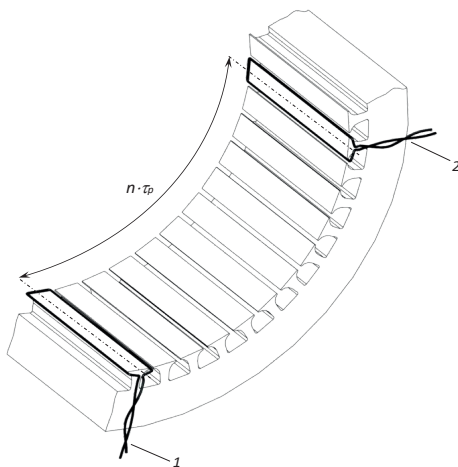


Figure 1. Principle of typical installation of measuring sensor on stator tooth: pos.1 measuring coil no. 1, pos. 2 measuring coil no.2.

The measuring coils 1 and 2 are installed on the stator tooth, and this way the area through which magnetic field is measured is strictly defined. With this type of installation, the area on which a magnetic field is measured is equal for both measuring coils, which is crucial for this differential measurement method.

In some cases, measuring coils can encompass only a section of the stator tooth for machines with radial ventilation gaps, or two identical measuring coils can be installed in the same position on the tooth. The measuring coils 1 and 2 are made in PCB technique, as shown in Figure 2 (installation on the stator tooth of the induction motor in the real condition).



Figure 2. Measuring coil in PCB technique installed on the stator tooth

The measuring coils 1 and 2 must be installed to such locations in the machine that have the same magnetic vector potential by absolute value. To meet this requirement and realize the measurement method, it is necessary to connect the measuring coils 1 and 2 with each other in series depending on the parity of the multiple of the pole pitch  $\tau_p$ .

If an odd multiple of  $n=1, 3, 5, 7 \dots$  of the pole pitch  $\tau_p$  is chosen for the distance between the measuring coils, then the measuring coils 1 and 2 should be connected as shown in Figure 3.

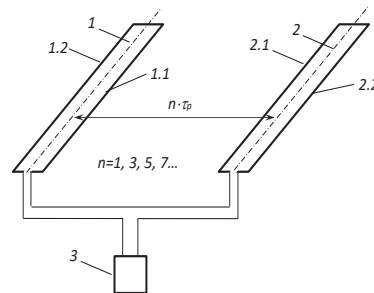


Figure 3. Typical measuring sensor installation if an odd multiple of the pole pitch is chosen for the distance between the measuring coils 1 and 2.

The inner side (pos.1.1 Figure 3) of the coil 1 connects with the inner side 2.1 of the coil 2. The outer side (pos.1.2 Figure 3) of the coil 1, through measuring system (pos.3 Figure 3), connects with the outer side (pos.2.2 Figure 3) of the coil 2. The measuring coils 1 and 2 connected in series according to Figure 3, whose mutual distance is an odd multiple  $n=1, 3, 5, 7 \dots$  of the pole pitch  $\tau_p$ , will have the same absolute value of a magnetic field, but the direction of the magnetic field lines will be different. The measuring coils connected and installed in this way allow mutual subtraction of the voltages that are induced in the measuring coils 1 and 2. If an even multiple of  $n=2, 4, 6, 8 \dots$  of the pole pitch  $\tau_p$  is chosen for the mutual distance of the measuring coils, then the measuring coils 1 and 2 should be connected as shown in Figure 4.

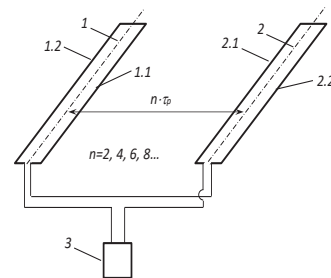


Figure 4. Typical measuring sensor installation if an even multiple of the pole pitch is chosen for the distance between the measuring coils 1 and 2

The inner side (pos.1.1 Figure 4) of the coil 1 connects with the outer side (pos.2.2 Figure 4) of the coil 2. The outer side (pos.1.2 Figure 4) of the coil 1, through measuring system (pos.3 Figure 4), connects with the inner side (pos.2.1 Figure 4) of the coil 2. The measuring coils 1 and 2 connected in series according to Figure 4, whose mutual distance is an even multiple  $n=2, 4, 6, 8 \dots$  of the pole pitch  $\tau_p$ , will have the same absolute value of a magnetic field and the same direction of the magnetic field lines. The measuring coils connected and installed in this way allow mutual subtraction of the voltages that are induced in the measuring coils 1 and 2. The measuring system (pos. 3 Figure 3 and 4) measures the total voltage  $U$  that is induced in two measuring coils 1 and 2, connected in series. In simple application, this method can be used in a following way: if the measured voltage  $U$  exceeds a predefined value, the measuring system can activate an output relay which signals the user that a winding fault is present in the machine. Figure 5 shows a simplified presentation of the magnetic field line distribution in a four-pole induction machine along with possible locations for installation of measuring coils.

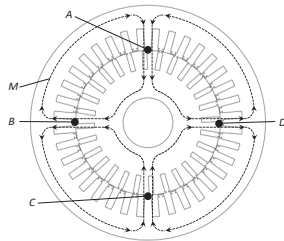


Figure 5. Simplified presentation of the magnetic field line distribution along with possible locations for magnetic field installation

Positions for installation of measuring coils in a four-pole machine, at a mutual distance of multiple pole pitch  $n \cdot \tau_p$ , where  $n=1, 2, 3, 4, 5, 6, 7, \dots$ , marked by positions A, B, C and D as presented in Figure 5, have by absolute value equal magnetic potential for one selected time point. However, the direction of the magnetic field lines (pos. M Figure 5) on the observed positions is not the same, but it differs on the positions A and C in relation to positions B and D. If the pole pitch  $\tau_p$  or odd multiple of pole pitch  $\tau_p$  is chosen as a mutual distance of the measuring coils during their installation in the machine, then the measuring coils 1 and 2 should be installed at the positions A and B or A and D or C and B or C and D; and connected according to Figure 3. If an even multiple pole pitch  $\tau_p$  is chosen as a mutual distance of the measuring coils during their installation in the machine, then the measuring coils 1 and 2 should be installed at the positions A and C or B and D and connected according to the Figure 4. In the case of a normal machine operation, in the measuring coils 1 and 2 installed in the corresponding places in the machine and connected according to the Figure 3 or Figure 4, the same voltage will be induced due to the changing magnetic field of the machine. Therefore, in the case of a normal machine operation (no fault), the total voltage of two measuring coils, connected in series, is approximately equal to zero for each selected time during one turn of the machine. In case of rotor winding damage, and at the moment of the arrival of the damaged rotor winding on one of the measuring coils 1 and 2, the voltages that are induced in the measuring coils 1 and 2 will no longer be equal. Thus, the total voltage of two measuring coils connected in series will not be equal to zero for any chosen moment during one turn of the machine. By measuring the total voltage of two measuring coils connected in series during one turn of the machine, one can unambiguously detect a rotor winding failure in induction and synchronous machines. In addition to winding failure detection, the number of rotor winding failures can be determined as well. By serial connection of the measuring coils 1 and 2, the magnetic field present in a machine operating without damage is eliminated from the measured value and the measured value depends only on the magnetic field caused by rotor winding damage. The method for rotor winding damage detection was tested by numerical calculations using Finite Element Method (FEM). Furthermore, the laboratory tests confirmed the effectiveness of this method through experiments on a synchronous and an induction machine.

## FEM ANALYSIS

For the purpose of the method testing numerous two and three-dimensional machine models were created. Powerful numerical tools generate realistic results with properly selected starting and boundary conditions. By FEM models, actual machines with embedded measuring coils were created and simulated. The voltage induced inside the measuring coils is calculated for different machine states, load point and with and without a fault (rotor bare rupture or inter-coil short circuit). Table 1 presents machine operating conditions for which calculations are performed.

No	Operating condition	Machine type	Machine operating condition for FEM calculations			No. of simulations
			Nominal load	Decreased load	With frequency converter	
1	No fault	Induction	•	•	•	4
2	With one broken rotor		•	•	•	10
3	With two broken rotor		•	•	•	20
4	With five rotor broken		•	•	•	20
5	With one broken rotor bar and eccentricity		•	•	•	20
6	With two broken rotor bar and eccentricity		•	•	•	20
7	No fault	Synchronous	•	•	•	4
8	With 1% of shorted		•	•	•	5
9	With 2% of shorted		•	•	•	5
10	With 5% of shorted		•	•	•	3
11	With 1% of shorted turns and eccentricity		•	•	•	10
12	With 2% of shorted turns and eccentricity		•	•	•	10

Table 1. Machine operating condition for FEM calculations

Figure 6 and Figure 7 present the magnetic field line distribution in the cross section of the induction machine with and without broken rotor bars acquired by FEM simulations. On Figure 7 machine cross section zone where rotor broken bars effect can be noticed is marked by white dashed line. Figure 8 presents calculated voltage waveform induced in two measuring coils connected in series and installed around stator tooth without fault and with one broken rotor bar.

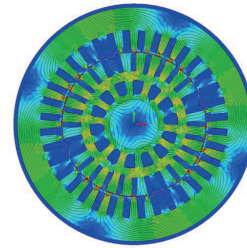


Figure 6. Presentation of the magnetic field line distribution in the cross section of four pole induction machine without broken rotor bars.

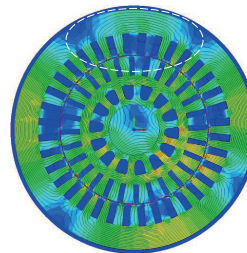


Figure 7. Presentation of the magnetic field line distribution in the cross section of four pole induction machine with broken rotor bars.

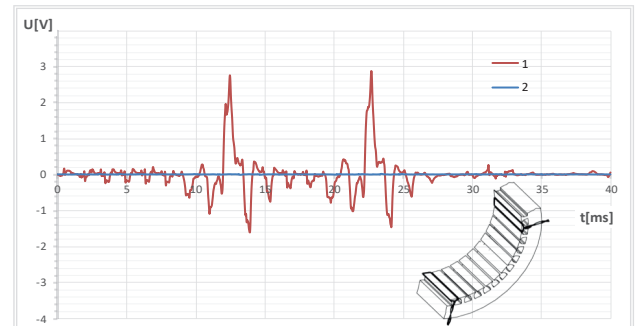


Figure 8. Calculated voltage induced in two measuring coils connected in series: 1 – with one broken rotor bar, 2 – without fault.

By observing the waveform of voltage induced in two measuring coils connected in series, presented in the Figure 8, the rotor winding damage is easy to detect. The measuring voltage is sensitive only to machine faults. In the Figure 8, winding damage is marked with voltage peak, which is repeated two times during a full turn in the case of one broken rotor bar. When the broken rotor bar comes across the measuring coil, one voltage peak appears. Therefore, in the measured waveform during one machine turn two extremely high voltage peaks will appear. Accordingly, the number of such measured peaks of the measured voltage during one full machine turn, divided by two, gives the number of broken rotor bars. Similar results were calculated for a synchronous machine with inter-coil short circuit in excitation winding.

## MEASUREMENT RESULTS AND APPLICATION

This method is verified experimentally via series of laboratory tests performed on the real machines specially designed for fault study of broken rotor bars, broken ring and inter-coil short circuit in a rotor winding. Additionally, this method is applied on more than 20 real machines in industry. Due to the large amount of measured data, in this paper we will present only one measurement performed on an induction motor on which we have detected one broken rotor bar. The rating of the machines where method

as applied are: 15, 65, 725, 800, 1200, 1250 kW. The thickness of the measuring coil designed in the PCB technique is 0,3 mm. The number of turns is from 3 to 10. From our experience the 1 turn is enough to obtain good signals, but our practice is to use 10 turns.

Figure 9 presents the measured induced voltage at the end of each measuring coil and also on the terminal of series connected coils for normal operation without fault. The voltage waveform is periodic and repeated for each turn of the machine, which corresponds to the time of 40 ms, i.e. 4 pole pitches, i.e.  $4\tau_p$ . It can be seen that the difference voltage for series connected coils are less than 0.5 V for healthy machine and the induced voltage waveform has the same shape for the measuring coil 1 and for the measuring coil 2.

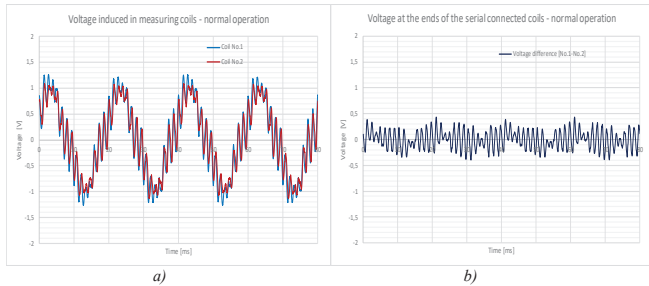


Figure 9. Voltage induced in coils without fault: a) voltage induced in each measuring coil without fault, b) voltage induced in series connected coils terminal

Figure 10 presents the measured induced voltage at the end of each measuring coil and also on the terminal of series connected coils for machine with one broken rotor bar. It can be seen that the difference voltage for series connected coils are now greater than 1.25 V for machine with one broken bar and could be detected.

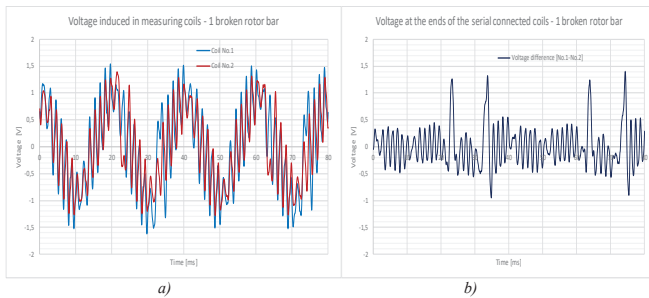


Figure 10. Voltage induced in coils with one broken bar: a) voltage induced in each measuring coil with fault, b) voltage induced in series connected coils terminal

Broken rotor bar detection based on the voltage waveform induced in one measuring coil, as presented in Figure 10.a), requires a complex signal processing. However, by observing the voltage waveform induced in two measuring coils connected in series, as presented in Figure 10.b), one can conclude that a rotor winding damage is easy to detect. The serial connection of two measuring coils cancels out a magnetic field present inside the machine without fault from the measuring signal. In that way two measuring coils connected in series measure the magnetic field caused only by rotor broken bar.

From Figure 10 it can be seen that the voltage peaks amplitude, caused by rotor broken bar, is between 1 V and 1.25 V. This level of signal is a sufficient for reliable damage detection and there is no need for amplification of the measured signal. This method, besides for broken rotor bar detection, can be used for determination of the number of the broken bars, but also for determination of their mutual positions. From Figure 10 it can be seen that the voltage of two measuring coils connected in series, for the rotor part without any winding damage, is not equal to zero. This occurs due to allowed tolerances in the machine manufacturing and assembly and imperfections of measuring coils installation. However, one can clearly see the change in the value of the measured voltage in the case of rotor broken bar, which is almost 150% for the presented machine. The method has been tested for the entire operating range of the machine and it successfully detects rotor winding damage in the entire operating range. The method has been tested and verified in the case when machine is powered from the frequency converter. Voltage oscillation around zero enables in combination with a key phasor sensor determination of the fault position. Each voltage oscillation represents one rotor bar.

The measuring system connected to measuring coils can be of different complexity level. The simplest type, presented in Figure 11, is basically a comparator which triggers an output relay when voltage exceeds the pre-set value.



a)



b)

Figure 11. a) measuring coil, b) FDSS (Fault Detecting Smart Sensor) enables detection of rotor broken bars and inter-coil short circuits in rotor winding

More complex product in which this patent-pending method is implemented is presented in Figure 12. This product enables fault detection, determination of number of faults and also fault positions. It can be applied for induction machine but also for synchronous hydro and turbo machines. Measurement can be permanent through an on-line measurement or users can periodically measure in order to locate rotor winding faults.



Figure 12. HG-WFD System (Hydro Generator Winding Fault Detection)

The concept of the EMCM system (Expert Machine Condition Monitoring) is presented in Figure 13. This system is specially designed for condition monitoring of the induction machines. The Figure 14 shows the web interface of the EMCM system. Through this interface the end user can monitor all relevant parameters of the induction motor, such as current, voltage, bearing vibrations, speed, temperatures, and especially the condition of the squirrel-cage winding. The condition of rotor winding (with or without fault) is monitored by application of the DMFM method. On the Figure 15 it is showed the measured induced voltage obtained by measuring coil embedded in the air gap of the motor and recorded by EMCM system. From the presented expert solutions, it can be seen that the DMFM method is fully confirmed in practice and has a significant industrial application in condition monitoring of rotating machines in various drives.

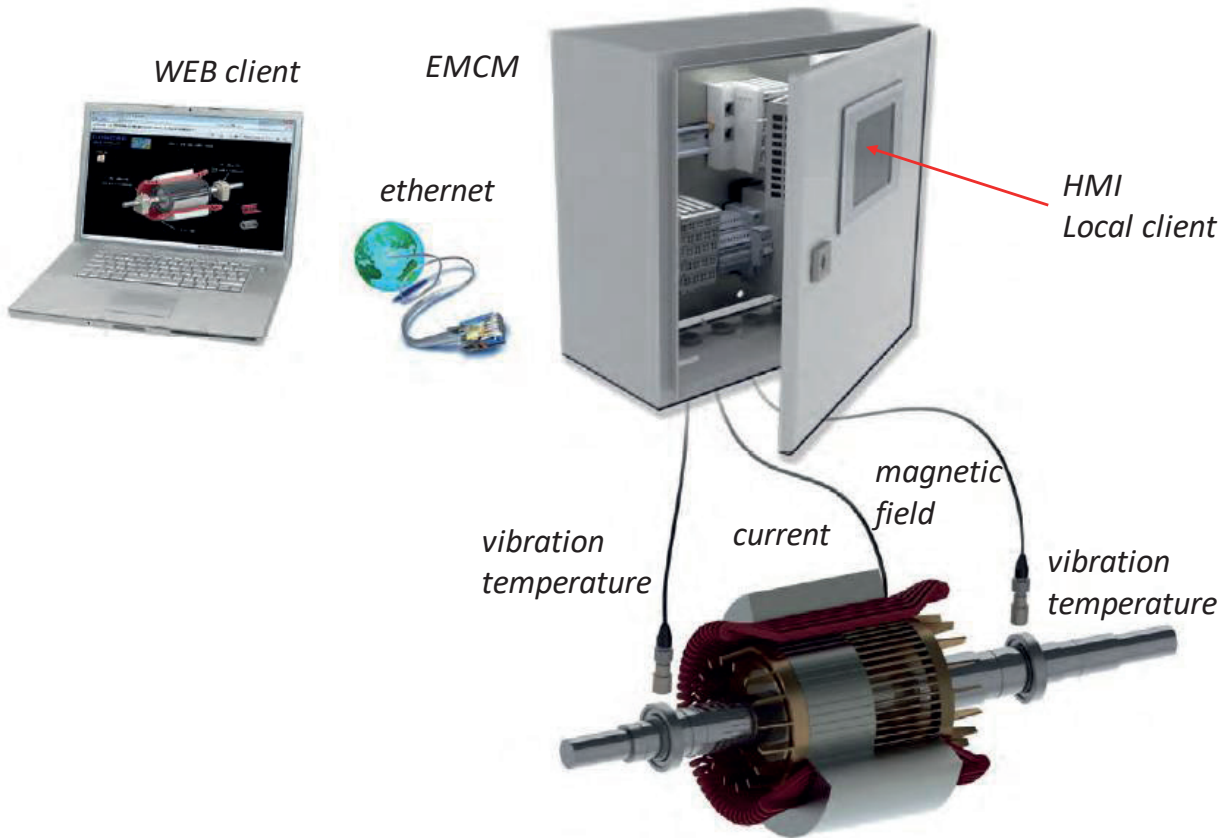


Figure 13. Concept of EMCM system

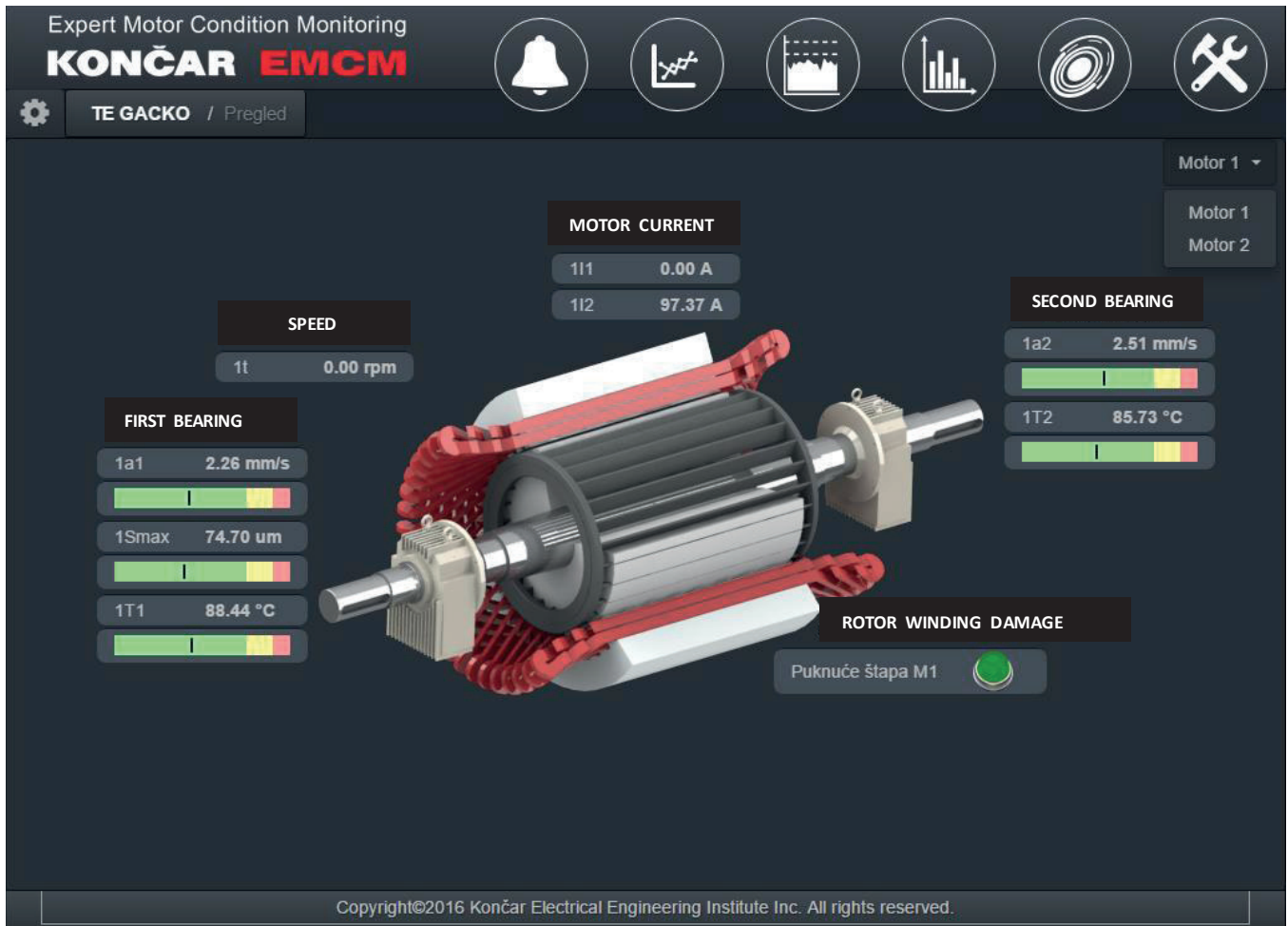


Figure 14. WEB interface of the EMCM system



Figure 15. The induced voltage signal from measuring coil recorded by EMC system

## CONCLUSION

This paper describes a new patent-pending method applicable for rotor winding inter-coil short circuit detection of synchronous machines and induction machines with slip rings, as well as rupture of one or more rotor bars and cage ring of induction machines. The DMFM method presented in this paper enables reliable detection of these faults. The technical novelty of this new method is a differential measurement of the magnetic field inside the machine. Measurement is performed by two serial connected measuring coils, installed on the stator tooth inside a machine air gap. Measuring coils must be installed on two stator teeth which, by absolute value, have equal magnetic vector potential.

A numerous FEM models have been developed to confirm this method. The method is tested for wide range of fault combinations but also for different machine operating conditions. Method is confirmed by the extensive laboratory tests on real models for various machine loads and for machines operating with and without a frequency converter. Method has already implemented on more than 20 machines in the industry and is tested and proven. From measuring results, one can conclude that this new DMFM method enables much simpler fault detection with significantly higher sensitivities.

Furthermore, this new method and performed FEM calculations improves fault detection portfolio knowledge that can be used in monitoring and diagnostics of rotating machines.

## BIBLIOGRAPHY

- [1] S. Nandi, H.A. Toliyat, X. Li: »Condition Monitoring and Fault Diagnosis of Electrical Motors«, IEEE transactions on energy conversion, Vol. 20, No. 4, December 2005.
- [2] D.R. Albright, "Inter turn Short-circuit Detector for Turbine-Generator Rotor Windings", IEEE trans. on power apparatus and systems, Vol. PAS-90 Number 2, March/April 1971.
- [3] M. Sasic, B.A. Lloyd, S.R. Campbell, "Flux Monitoring Improvement", IEEE industry applications magazine, Sept/Oct 2011
- [4] M. Šašić, L. Blake, A. Elez, »Finite Element Analysis of Turbine Generator Rotor Winding Shorted Turns«, IEEE trans. on energy conversion. 27 (2012), 4; 930-937.
- [5] A. Elez, S. Car, Z. Maljković, »A new method for inter-coil short circuit detection in synchronous machine armature winding«, The international review of electrical engineering (IREE). Vol. 7, N. 6 (2012).
- [6] H. C. Karmaker; - "Broken Damper Bar Detection Studies Using Flux Probe Measurements and Time-Stepping Finite Element Analysis For Salient - Pole Synchronous Machines", SDEMPED 2003, Symposium for Electric Machines, Atlanta USA August 2003.
- [7] O.V. Thorsen, M. Dalva: "A Survey of Faults on Induction Motors in Offshore Oil Industry, Petrochemical Industry, Gas Terminals, and Oil Refineries", IEEE transactions on industry applications, Vol. 31, No.5, September/October 1995.
- [8] O.V. Thorsen, M. Dalva: »Failure Identification and Analysis for High Voltage Induction Motors in Petrochemical Industry«, IEEE, 1998.
- [9] P. O'Donnell: »Report of Large Motor Reliability Survey of Industrial and Commercial Installations Parts I, II and III«, IEEE Transactions on Industry Applications, Motor Reliability Working Group, IEEE Industry Applications Society, July/August 1985, January/February 1987.
- [10] B.M. Ebrahim, J. Faiz, S. Lotfi-fard, P. Pillay: »Novel indices for broken rotor bars fault diagnosis in induction motors using wavelet transform«, Elsevier ScienceDirect, Journal of Mechanical Systems and Signal Processing 30, 131-145, February 2012.
- [11] C.C. Yeh, G. Sizov, A. Sayed-Ahmed, N.A.O. Demerdash, R.J. Povinelli, E.E. Yaz, D.M. Ionel: »A Reconfigurable Motor for Experimental Emulation of Stator Winding Interturn and Broken Bar Faults in Polyphase Induction Machines«, IEEE transactions on energy conversion, Vol. 23, No. 4, December 2008.
- [12] N.M. Elkasabgy, A.R. Eastham, G.E. Dawson: »Detection of Broken Bars in the Cage Rotor on an Induction Machine«, IEEE transactions on industry applications, Vol. 28, No.1, January/February 1992.
- [13] M.E.H. Benbouzid: »A Review of Induction Motors Signature Analysis as a Medium for Faults Detection«, IEEE transactions on industrial electronics, Vol. 47, No.5, October 2000.
- [14] G. Didier, E. Temisien, O. Caspary, H. Razika: »A new approach to detect broken rotor bars in induction machines by current spectrum analysis«, Elsevier, Mechanical Systems and Signal Processing, Vol.21, 2007.
- [15] Z. Ye, B. Wu, A. Sadeghian: »Current Signature Analysis of Induction Motor Mechanical Faults by Wavelet Packet Decomposition«, IEEE transactions on industrial electronics, Vol. 50, No.6, December 2003.
- [16] H. Douglas, P. Pillay, A. Ziarani: »Detection of broken rotor bars in induction motors using wavelet analysis«, IEEE International Electric Machines and Drives Conference, IEMDC'03, June 2003.
- [17] V.V. Thomas, K. Vasudevan, V.J. Kumar: »Online Cage Rotor Fault Detection Using Air-Gap Torque Spectra«, IEEE transactions on energy conversion, Vol.18, No. 2, June 2003.

R. SITAR  
Ž. JANIĆ

Končar - Electrical Engineering Institute  
Siemens EM TR LPT GTC RES  
Croatia

Končar Power Transformers - A joint Venture of Siemens AG and  
Končar d.d.  
Croatia

# Determination of local losses and temperatures in power transformer tank

## SUMMARY

Paper presents research of local losses and temperature rise in transformer steel tank. First experimental method based on initial rate of rise of temperature is presented. This is a direct method for determining distribution of losses in transformer structural steel parts. Technique relies on the fact that after a body has settled at a steady state temperature and the internal heat source is suddenly removed or applied, the initial rate of temperature change at any point is proportional to heat input (loss density) at that point. To test applicability of sensors and instrument for the local loss measurement method, measurement system was tested on conductors (strips) and magnetic steel rings.

Second part of experimental work consisted of investigations on model for tank local overheating. The model consisted of excitation windings that were sources of magnetic field. Existence of three separate windings gave the possibility to change value and position of magnetic field source inside the tank. Local losses in the tank were evaluated by proposed method of initial rate of rise of temperature. Heat-run tests were made on the model and local temperatures on the tank were measured. Measured local losses and local temperatures were used for determining local heat transfer coefficients on tank – oil interface. It was concluded that heat transfer coefficients can be presented as function of heat flux from tank to oil.

Finally, temperatures in transformer tank were calculated by finite element method. Losses calculated by electromagnetic calculation represented heat sources in thermal numerical model. Heat transfer equations were solved in solid domain (tank) while cooling conditions were defined by heat transfer coefficients checked experimentally. Calculated temperatures were compared to measured temperatures and gave good agreement.

## KEYWORDS

Power transformer - coupled calculation - local overheating - heat transfer coefficient

## INTRODUCTION

When testing power transformers, total value of stray losses in steel structural parts can be challenging to determine. Stray losses represent only a smaller part of total losses in transformers. Furthermore, if stray losses are concentrated in small areas that are not properly cooled, local overheating can arise, causing transformer operation failure. Experimental research of this whole coupled electromagnetic-thermal behavior is very hard to make on a real transformer unit.

In order to verify and improve the parameters to be used in simulations a detailed research on local overheating in transformer steel parts on experimental models has been conducted. First part of the research was focused on stray magnetic field losses solely. Such work on losses in magnetic material has been elaborated in many papers [1], [2]. It consisted of experimental work and calculation in numerical tools that can be used for more complex geometries.

Second part was oriented on a geometry that is similar to configuration of power transformer tank - configuration most often submitted to local overheating in power transformer and easily detected by measurement with thermal IR cameras in test bays. Experiments were done in laboratory using the method developed in first part of research. In the end numerical

tools were used to calculate temperature and compare calculated and measured temperature values. This made all stages of numerical modeling of real power transformers checked on an experiment.

## LOCAL LOSS MEASUREMENT

A possibility for determining local loss in constructional steel parts is to measure transient temperature-time curve and determine its initial slope. Example of determining the initial slope of a heated body is shown in Figure 1.

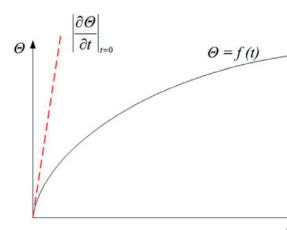


Figure 1.  
Principle of  
determining  
initial slope  
of a heating  
curve

The curve shown in Figure 1 can be mathematically expressed by heat diffusion equation

$$p = c\rho \frac{\partial \theta}{\partial t} + q \quad (1)$$

where  $p$  is generated heat (power loss),  $\rho$  body temperature,  $c$  thermal capacitance,  $\theta$  mass density and  $q$  heat dissipated to surrounding regions. Surrounding regions to which heat dissipates are cold metal bodies (where generated heat is much lower than at the measurement point) and surrounding fluids (which cool the heated body by convection or radiation). Dissipated heat highly depends on temperature differences between the measurement point and surrounding regions. As temperatures of heated bodies grow dissipated heat from measurement points become higher and cause the initial straight line to turn into an exponential curve. So, if initial conditions consider all metal parts and the surrounding fluid at equal temperatures, for  $t = 0$  it can be stated  $q = 0$ , and expression (1) can be written as

$$p = c\rho \left. \frac{\partial \theta}{\partial t} \right|_{t=0} \quad (2)$$

Therefore, heat loss at any point can be obtained by multiplying the initial rate of temperature rise, mass density and thermal capacitance of material under test. However, it is important to determine initial section where temperature-time curve can be considered as a straight line because of negligible heat dissipation. This will highly depend on how non-uniform power losses are in the body observed.

The first step when making a measurement system for local loss measurement method is to choose sensors for temperature measurements. The probes should be robust and have good thermal connection with the measurement point. Another important requirement is to be able to measure temperature instantly. Thus, sensors should have negligible heat capacity as recommended in [3]. To meet all of these requirements thermocouples were made from 0,08 mm thick constantan and copper wires. When working with AC power sources it is obligatory to twist the two wires together, so that AC pick-up in inductive loops of sensor leads is minimized.

The measurement junction was placed and fixed on a point where losses are to be measured, while the reference junction was inserted in a water bath at a stable and known temperature. The main disadvantage of thermocouples is that they have relatively weak signal. For example, copper-constantan (T-type) thermocouples have sensitivity of about 43  $\mu\text{V}/^\circ\text{C}$ . In order to detect temperature changes of 0,001  $^\circ\text{C}$ , a so-called nanovoltmeter with resolution of 1 nV was used. In order to test applicability of chosen sensors and instrument for the loss measurement method, measurement system was first tested on aluminium and copper strips. Thermocouple measurement junction was fixed in the middle of 1000 mm long copper and aluminium strips, as shown in Figure 2. Circuit breaker was used to apply a DC voltage source suddenly to the strips, while resistors were used to change current in the circuit.

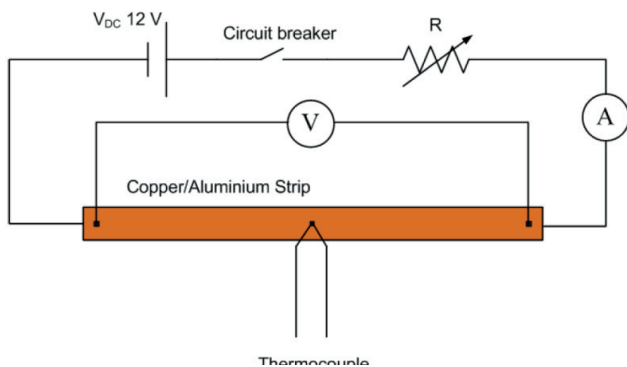


Figure 2. Measurement of losses on copper and aluminium strips

Initial rate of temperature rise was calculated from the temperature change in  $\Delta t = 1$  s after the voltage source was applied. From measured temperature rise and expression (2) value of local losses in  $\text{W}/\text{m}^3$  were evaluated.

Specific heat capacity of copper was 385  $\text{J}/\text{kgK}$  and of aluminium 890  $\text{J}/\text{kgK}$ . Mass density of copper was 8940  $\text{kg}/\text{m}^3$  and of aluminium 2700  $\text{kg}/\text{m}^3$ . At the same time current and voltage of tested conductors were measured. Total losses of conductors were evaluated by wattmeter and compared with results from the local loss measurement method in Table I.

Table I – Measured losses in copper and aluminium conductors

Conductor	Current, A	Measured initial slope, $^\circ\text{C}/\text{s}$	Total losses, W	Ratio (1)/(2)	
			Temperature-time method (1)	Wattmeter (2)	
Cu 1,0 x 15 $\text{mm}^2$	81,5	0,143	6,64	6,83	0,97
Cu 5,6 x 4,0 $\text{mm}^2$	98,3	0,098	6,80	6,80	1,00
Al 2,0 x 15 $\text{mm}^2$	80,8	0,088	5,71	5,51	1,04

Results from both measurement methods showed good agreement. Experiment has confirmed the suitability of thermocouples as sensors and nanovoltmeter as instrument for local power loss measurement.

Here it should be emphasized that losses that were measured were distributed uniformly inside the heated object (copper/aluminium conductors). This is not the case when losses are caused by eddy currents in thick magnetic materials. Due to small skin depth (from 1 to 3 mm) of magnetic steel parts, losses are localized in a thin layer at surface of a magnetic part. Cold metal interior cools the surface layer, making value of the dissipated heat from equation (1) substantial.

## EXPERIMENTAL RINGS

When heat sources are non-uniform, errors in measured losses will occur if the temperature rise being measured is not completed before appreciable heat diffuses to or from other parts of different temperatures. The errors in these cases can be estimated by experimental and numerical analysis of heat transfer on a simple geometry.

An experimental ring made of magnetic steel wound throughout its circumference with a copper conductor was considered as a model for evaluating possible measurement errors. Configuration is shown in Figure 3. Inner ring diameter  $D_i$  was 325 mm, outer diameter  $D_o$  385 mm and thickness  $b$  8 mm. Coil wound around the ring was excited by a sinusoidal current source of frequency 50 Hz. Magnetic permeability of magnetic steel was modeled as a single-valued  $B-H$  curve as in [4], while electrical conductivity was  $6,56 \times 10^6$   $\text{S}/\text{m}$  (value at 20  $^\circ\text{C}$ ).

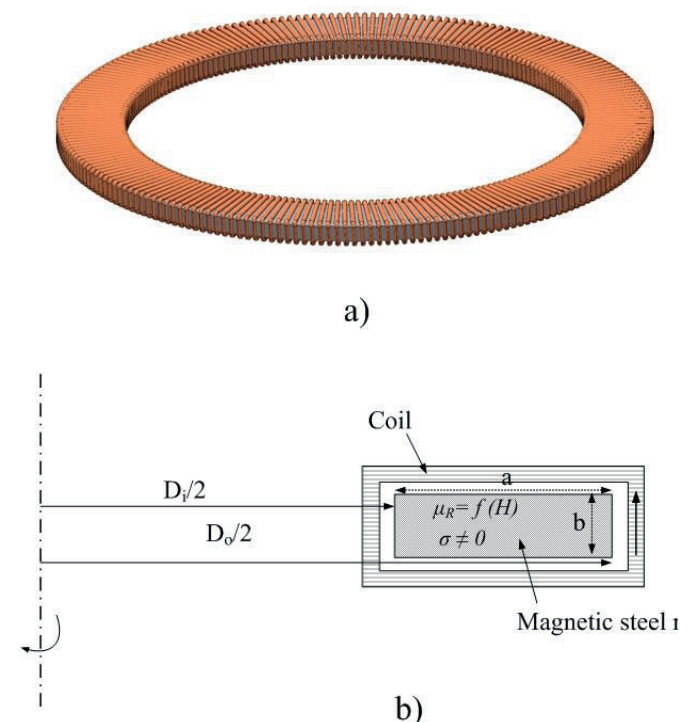


Figure 3. Experimental ring a) 3D view and b) 2D model with dimension description

Generally, depending on amount of magnetic flux penetrating into steel ring, loss distribution along skin depth varies. For 50 Hz sinusoidal source and stated material properties most of the losses are concentrated in 1 to 3 mm surface layer of steel [1]. Due to the fact that losses are not distributed uniformly along steel ring depth, problems in application of proposed local loss measurement method can occur.

Measurement results obtained by the method of initial rate of rise of temperature and wattmeter were compared to calculation results by numerical tool MagNet. Figure 4. shows comparison of total losses (W) and local surface losses (W/m<sup>2</sup>) to calculated losses obtained by nonlinear electro-magnetic calculation.

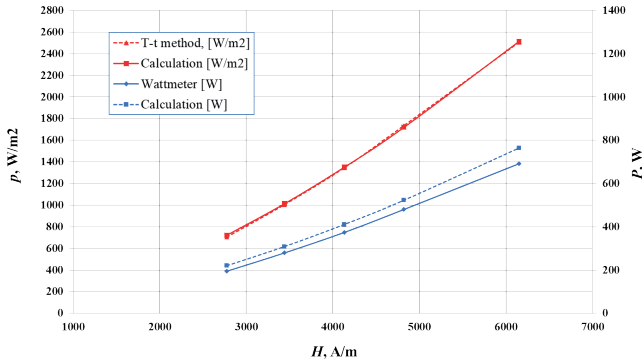


Figure 4. Comparison of loss measurement methods and calculation

It can be stated that nonlinear electromagnetic calculation by FEM can be used for estimation of local and total losses in nonlinear magnetic material. If only local surface losses are examined, difference of calculated and measured values on magnetic steel ring can be less than 3%. This leads to a conclusion of applicability of proposed local loss measurement method. Although losses are distributed non-uniformly along magnetic steel depth, surface local losses (W/m<sup>2</sup>) can be determined with high precision.

## MODEL FOR TANK LOCAL OVERHEATING

In order to investigate high local loss densities and consequent temperature rises a simple one phase experimental model was created. Steel tank was made of magnetic (carbon) steel, except one wider side that was made from nonmagnetic steel. For regulation of applied magnetic field model had three windings inside the tank that were concentric with separated leads. Magnetic flux would close through steel tank in such way that it would be highly localized and therefore could create temperature rises critical from perspective of power transformer operation. Also, a cooling system for the model was designed in such way that oil temperature inside the tank could be controlled and maintained at usual oil temperature in a power transformer. Experimental model is shown in Figure 5. Details of windings in experimental model are shown in Figure 6.

In order to determine local losses and temperatures on tank wall, thermocouples were installed on tank wall. Thermocouples on tank wall are shown in Figure 7. Such experimental model is used as a benchmark model for coupled electromagnetic-thermal numerical analysis.

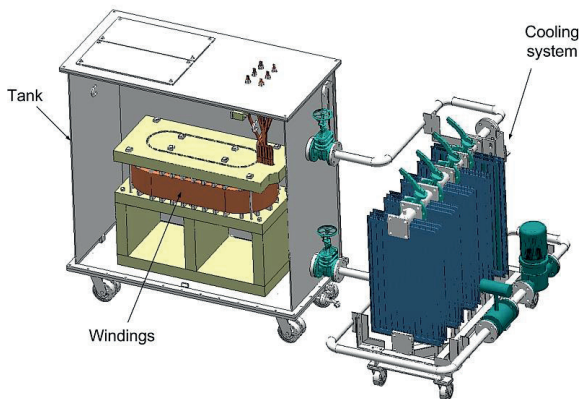


Figure 5. Experimental model for tank local overheating

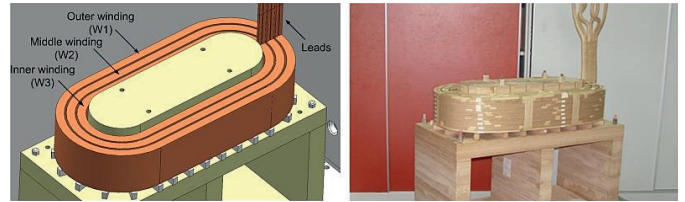


Figure 6. Windings used in experimental model

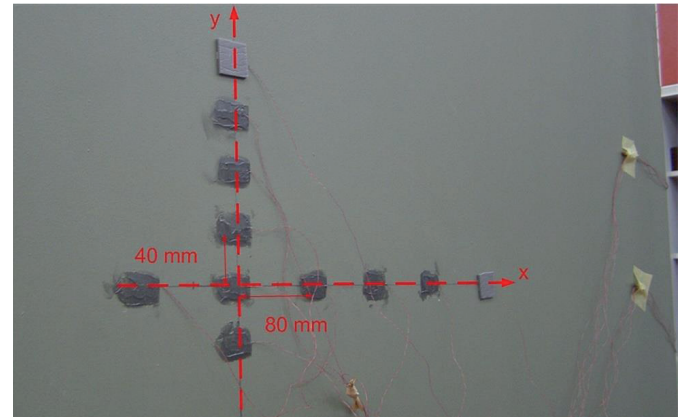


Figure 7. Thermocouples fixed on tank surface

## COUPLED ELECTROMAGNETIC-THERMAL MODELING IN FEM

Numerical calculation of losses in transformer steel tank is done in Infolytica's finite element software MagNet using the so-called time-harmonic solver. MagNet uses the edge element version of  $T-\Omega$  method to solve Maxwell's equations and calculate losses in transformer metal parts. Calculation was performed at a single frequency (50 Hz) in complex domain with fields represented as phasors. Principles of the method are described in paper by Webb [5]. For the plate made from magnetic steel surface impedance boundary condition was used. No mesh was generated inside the plate, but the ratio of the tangential components of electric field  $E_t$  and magnetic field  $H_t$  was equal to the value of the surface impedance:

$$Z = \frac{E_t}{H_t} = \frac{1+j}{\delta\sigma} \quad (3)$$

where  $\sigma$  is electric conductivity of magnetic steel and  $\delta$  skin depth:

$$\delta = \frac{1}{\sqrt{\pi f \mu \sigma}} \quad (4)$$

where  $f$  is the frequency and  $\mu$  magnetic permeability of magnetic steel. For calculation of losses in nonmagnetic steel (one wider side of the tank) mesh was generated and calculated by expression

$$p = \int_V \frac{J^2}{\sigma} dV \quad (5)$$

For calculation of losses in magnetic steel electrical conductivity  $\sigma$  was  $4,5 \times 10^6$  S/m, while for nonmagnetic steel  $1,3 \times 10^6$  S/m (values for 75 °C). Nonlinear  $B-H$  curve was used for modeling magnetic permeability of magnetic steel. Nonlinearities in the MagNet models were handled by the Newton-Raphson linearization method. Although it was not theoretically correct to use nonlinear materials with phasor calculation, time-harmonic solvers could take into account saturation effects approximately. After losses were calculated, it was possible to conduct a temperature

(heat transfer) FEM calculation. Local losses in the tank represented heat source in the heat transfer equation that was solved by Infolytica ThermNet software

$$-\nabla \cdot (k \nabla \theta) = p \tag{6}$$

where  $k$  is thermal conductivity,  $\theta$  temperature, and  $p$  power loss density. Value of thermal conductivity for magnetic steel was 40 W/mK and for nonmagnetic steel 20 W/mK. Cooling of metal parts was defined as a boundary condition on a surface in contact with the coolant (air/oil)

$$-\alpha(\theta - \theta_a) = k \frac{\partial \theta}{\partial n} \tag{7}$$

where  $\alpha$  is the heat transfer coefficient and  $\theta_a$  ambient temperature. In short it can be stated that thermal computation was a conduction problem where convection was taken into account via heat transfer coefficients. In case of air-tank interface, heat transfer coefficient was given constant value 10 W/m<sup>2</sup>K. However, dependence of heat transfer coefficients on heat flux is usually modeled using expression from literature. Such dependence is proposed in [6].

In this paper, availability of local losses and temperatures gave an opportunity to experimentally determine heat transfer coefficients and check such empirical expressions.

## EVALUATION OF HEAT TRANSFER COEFFICIENTS

Heat transfer coefficient is defined as heat flux at fluid-soil boundary divided with temperature rise of solid above fluid:

$$\alpha = \frac{q_{oil}}{\Delta \theta} \tag{8}$$

Temperatures rise can be measured with thermocouples while heat flux  $q$  is more complicated to determine. With the initial rate of temperature rise method local losses were determined according to Figure 8:

$$P = \iint_{\Delta V} q dS \tag{9}$$

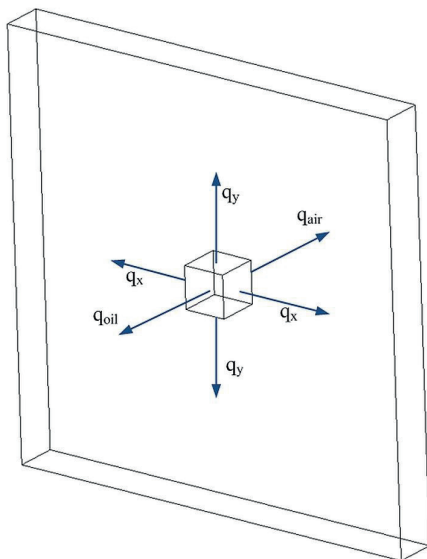


Figure 8. Heat transfer in steel wall at measurement point

Heat flux  $q_{oil}$  is only one part of generated heat (losses)  $p$  at measurement point. Therefore in order to evaluate local heat transfer coefficients from measured local losses it is important to check impact of local conditions and parameters at measurement location. In thermal stagnation there are high differences in tank temperatures where local overheating is taking place. To take into account this local heat transfer to surroundings ( $q_x, q_y, q_{air}$ ), numerical model of tank was made. By calculating temperatures for different loss and  $\alpha$  values, family of curves for determination of local heat transfer coefficients was created. Such curve family is shown in Figure 9.

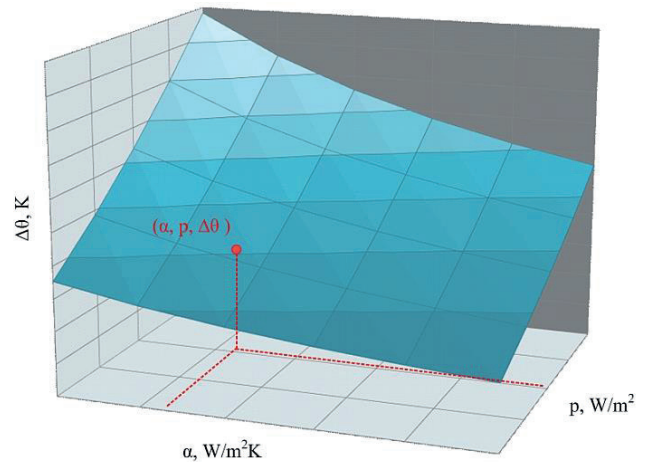


Figure 9. Family of curves for determination of heat transfer coefficients from measured losses  $p$  and temperature rise  $\Delta \theta$

Heat transfer coefficients for measured cases of local losses and temperatures on nonmagnetic and magnetic steel tank were determined. Obtained heat transfer coefficient values were compared to analytical expression according to literature [6]. Comparison is shown in Figure 10.

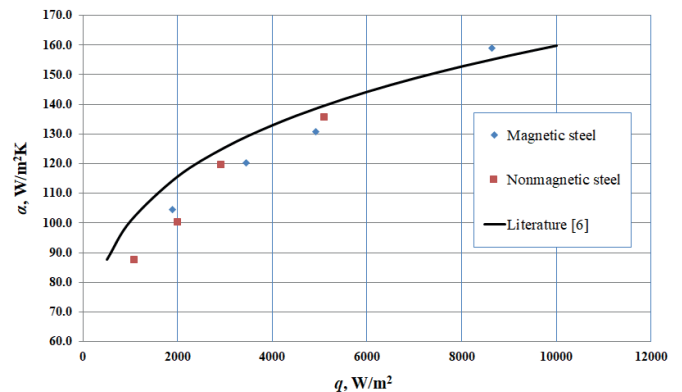


Figure 10. Comparison of experimentally determined heat transfer coefficients to empirical expressions

Differences were up to 15 %. It is important to note that heat transfer coefficients do not depend on steel type – magnetic or nonmagnetic. Experimental analysis on the benchmark model has shown that it is justified to use empirical expressions as in [6] for modeling of heat transfer coefficients.

## TEMPERATURE MEASUREMENT VS CALCULATION

### A - EXPERIMENTAL MODEL

Described modeling approach is used for calculation of losses on the experimental model. Figure 11. gives the comparison. All three windings of the model were connected in series and supplied with 250 A. This created high local losses in the middle of the tank causing high local temperatures. Temperature measurements with IR camera FLIR 460 were performed and compared to calculation. Emissivity for measurements with IR camera was set to 0.95. Difference between calculated and measured temperatures on magnetic side of the tank are not higher than 3 K.

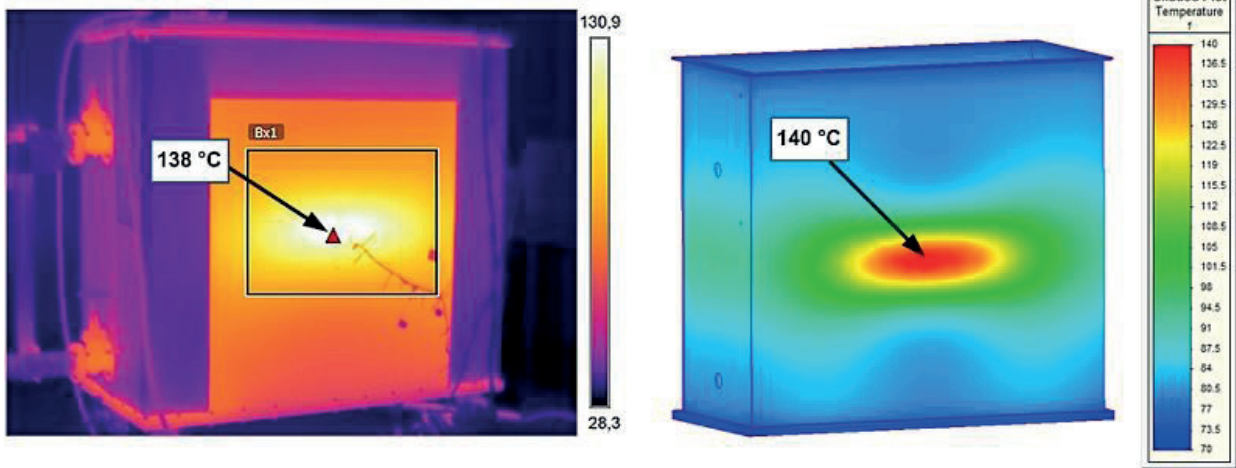


Figure 11. Comparison of measured and calculated temperatures on experimental model

### B - 280 MVA THREE PHASE TRANSFORMER

Modeling approach is also checked on a real three-phase transformer. On a 280 MVA three phase transformer unit measurement of tank temperatures were made during heat run test. Phase current on LV side was 5,2 kA. Both winding and LV leads were modeled. Including leads in a transformer model made the model very demanding as the number of elements increase and computational time increases drastically. In this paper tank was modeled without additional details what made calculation results not fully accurate but comparable to a real transformer. It should be pointed out that tank magnetic shield on tank wall were also considered in this case. In Figure 12. measured temperatures by IR camera in the test bay are shown and compared to calculation. Temperature distribution fits very well with the measurements. Hotspots on tank are located correctly. Calculated hotspot value is 102 °C while measured 103 °C.

## CONCLUSION

Reliable measurement for verification of numerical software is very hard to make on real transformer units. In case of stray losses it is not easy to extract measured stray losses from total losses. In order to have reliable loss measurements and consequent temperature rises on configurations such as transformer tank, it is easier to make investigations on an experimental model. Local losses were measured using special method based on initial rate of rise of temperature. Method was tested on simple configurations (models) before it was successfully employed on a configuration of transformer steel tank. Using such technique tank local losses and temperature rises were measured on an experimental model and heat transfer coefficients were determined.

Heat transfer coefficients were used in coupled electromagnetic-thermal numerical model. Numerical calculation of experimental model and real three phase transformer showed good agreement with measurements. Therefore presented research in the paper has give a reliable modeling method for tank temperature determination.

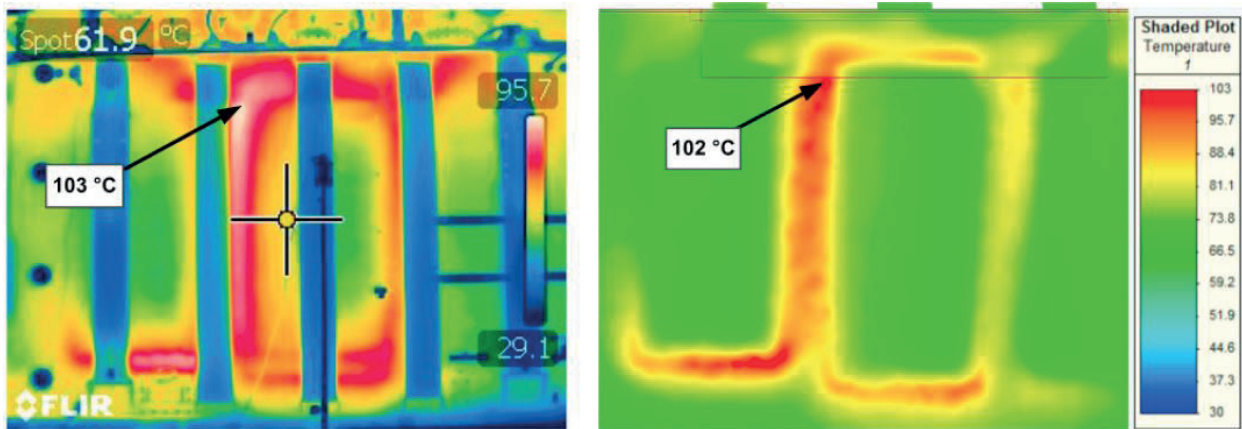


Figure 12. Comparison of measured and calculated temperatures on three-phase transformer

## BIBLIOGRAPHY

- [1] N. Niewierowicz, J. Turowski, "New thermometric method of measuring power losses in solid metal elements", Proc. IEE Vol 119, No. 5, May 1972.
- [2] H. Hamzehbahmani, A. J. Moses, F. J. Anayi, "Opportunities and Precautions in Measurement of Power Loss in Electrical Steel Laminations Using the Initial Rate of Rise of Temperature Method", IEEE Transactions on Power Delivery, vol 29., no. 2, pp.651-659, April 2014
- [3] A. J. Gilbert, "A method of measuring loss distribution in electrical machines", Proceedings of the IEE, 1961, Vol A 108, p. 39, pp. 239-244, 1961.
- [4] R. Sitar, I. Šulc, Ž. Janić "Prediction of local temperature rise in power transformer tank by FEM", Procedia Engineering 202, pp. 231-239, 2017.
- [5] J. P. Webb, b. Forghani, "T-Ω method using hierarchical edge elements", IEE Proceedings – Science, Measurement and Technology, Volume 142, Issue 2, pp. 133-141, March 1995
- [6] K. Preis, O. Biro, G. Buchgraber, I. Tičar, "Thermal-Electromagnetic Coupling in the Finite-Element Simulation of Power Transformers", IEEE Transactions on Magnetics, vol. 42, no. 4, pp. 999-102, April 2006.

**D. GORENC**  
**K. FLEGAR**  
**I. LONČAR**

KONČAR – Apparatus and Switchgear  
CROATIA

**E. PLAVEC**

KONČAR – Electrical Engineering Institute  
CROATIA

# Simulation and Measurement of Pressure Rise in GIS 145 kV due to Internal Arcing

## SUMMARY

Internal arc testing of metal-enclosed, SF<sub>6</sub> gas insulated switchgear (GIS) is defined by IEC 62271-203 and is not a part of mandatory type tests. However, due to the increasing demands on the safety of personnel, more often the implementation of this test is required in the tender documentation. According to IEC, the duration of the electric arc is related to the performance of the protective system determined by the first and second stage of protection. For the rated short-circuit current equal or higher than 40 kA, during the first stage of protection (0.1 s), no external effects on enclosure other than the operation of pressure relief device is permitted. During the second stage of protection (≤0.3 s) no fragmentation is permitted, but burn-through is acceptable. The test should be carried out on the GIS compartment with the smallest volume at nominal gas pressure. Since a newly developed GIS 145 kV is designed as a three-phase encapsulated, arc initiation is achieved by short connecting of all three phase conductors in the vicinity of a partition by means of a thin metal wire. This ensures that two electric arcs burn simultaneously commutating between the phases, so the possibility of enclosure burn-through in this type of GIS is minimized. In order to prevent the release of SF<sub>6</sub> gas in the atmosphere during the testing, a test enclosure should be placed in a protective gastight enclosure filled with air or more often SF<sub>6</sub> gas at pressure of 0.1 MPa. This test object configuration significantly complicates the pressure rise calculation and increases the testing cost. In order to prevent enclosure fragmentation, the pressure difference between the test enclosure and the protective enclosure during the test should always be less than the bursting pressure of test enclosure. Also, the protective enclosure should be designed to withstand the maximum pressure rise that may occur after pressure relief device opens. In order to assess the likelihood of passing the upcoming type test for newly developed GIS, a computer program for calculation of pressure and temperature in the test enclosure and protective enclosure was developed. The mathematical model is based on the paper of the working group CIGRE A3.24, published in 2014. The basic model shown in the paper is enhanced by the real properties of the SF<sub>6</sub> gas/plasma, evaporation of the electrode material and the insulator ablation. The contribution of exothermic/endothermic reactions between the gas and the electrode material on the pressure and temperature rise was also considered. At the same time, the measurements of pressure rise in GIS enclosure and protective enclosure were carried out in Končar High Power Laboratory. The experiments performed on a copper and aluminum electrodes in SF<sub>6</sub> gas confirmed significantly higher contribution of aluminum electrodes to the pressure and temperature rise compared to the copper electrodes. The computer program is verified by measurement results.

## KEYWORDS

GIS, internal arc test, protective enclosure, pressure rise, test enclosure

## INTRODUCTION

Internal arc testing of metal-enclosed, gas insulated switchgear (GIS) 145 kV is defined by IEC standard [1] and is not a part of mandatory type tests. However, due to the increasing demands on the safety of personnel, more often the implementation of this test is required in the tender documentation. According to IEC, the duration of the electric arc is related to the performance of the protective system determined by the first stage (main) and second stage (back-up) protection. For the rated short circuit current equal or greater than 40 kA, the recommended current duration is 0.1 s for the first protection stage and less than or equal to 0.3 s for the second protection stage (Table I). The criteria for a successful test are that there is no external effect other than the operation of pressure relief devices in the first 0.1 s of current duration and that there is no fragmentation of enclosure after 0.3 s of current duration, burn-through is acceptable.

Table I Recommended arc duration and the criteria for passing the test according to [1]

Rated short-circuit current	Protection stage	Duration of current	Performance criteria
<40 kA r.m.s.	1	0.2 s	No external effect other than the operation of suitable pressure relief devices
	2	≤0.5 s	No fragmentation (burn-through is acceptable)
≥40 kA r.m.s.	1	0.1 s	No external effect other than the operation of suitable pressure relief devices
	2	≤0.3 s	No fragmentation (burn-through is acceptable)

The compartment of GIS which appear to have the least likelihood of withstanding the pressure and temperature rise in the event of arcing shall be selected for test. In practice, this means the compartment with the smallest volume. The testing is performed at nominal SF<sub>6</sub> gas pressure in the test enclosure. The specified standard allows the test results obtained in a single compartment to be used in calculating and proving the resistance of other gas compartments on internal arc.

## PHYSICAL PROCESSES IN GIS COMPARTMENT DUE TO INTERNAL ARC

When the arc burns between the phase conductors, evaporation of the electrode material occur. The specific energy of evaporation for various electrode materials are given in Table II [2], they include the energy required for heating to the melting temperature, melting, heating to the evaporation temperature and evaporation. The evaporated electrode material is mixed with SF<sub>6</sub> gas in arc compartment and the chemical reactions occur. In the exothermic chemical reaction between evaporated aluminum and SF<sub>6</sub> gas (or oxygen) more heat is generated than it is required for evaporation of the same amount of aluminum (Table II). On the other hand, in the reaction between the evaporated copper and the oxygen, less heat is developed than it is required for copper evaporation, because of that the reaction is endothermic. The data for the reaction between evaporated copper and SF<sub>6</sub> gas were not found in the references.

If the arc burns in the vicinity of bushing plate, ablation or evaporation of the insulation material occurs. The bushing plates are mainly made of epoxy resin and glass-based fillers. It is assumed that methane gas (CH<sub>4</sub>) is the only gaseous product of bushing plate ablation [3]. If the gas temperature in the arc compartment is sufficiently high, gas degradation occurs and at the highest temperatures plasma formation occurs. Between the products of gas degradation and evaporated electrode material chemical reactions and formation of new products occur. This also leads to the change in thermodynamic properties of gas/plasma. Assuming the local thermodynamic equilibrium (all gas/plasma particles are at the same temperature), thermodynamic properties of gas/plasma are the functions of temperature, pressure and mass concentration of individual reactants.

Table II Specific energy of evaporation, chemical reactions and generated specific heat for various electrode materials and surrounding gas

Electrode material	Specific energy of evaporation [MJ/kg]	Molar mass [g/mol]	Exothermic/endothermic reactions	Specific generated heat [MJ/kg]
Al	13.73	26.98	$Al + \frac{3}{2} SF_6 \rightarrow AlF_3 + \frac{3}{2} SF_4 + 850 \text{ kJ}$	31.5
			$Al + \frac{3}{4} O_2 \rightarrow \frac{1}{2} Al_2O_3 + 837 \text{ kJ}$	31
Cu	6.18	63.54	$Cu + \frac{1}{4} O_2 \rightarrow \frac{1}{2} Cu_2O + 75 \text{ kJ}$	1.2
Fe	8.04	55.85	$Fe + \frac{1}{2} O_2 \rightarrow FeO + 250 \text{ kJ}$	4.5

## MATHEMATICAL MODEL

The basic layout for calculation of pressure and temperature rise in GIS enclosure and protective enclosure is shown in Fig. 1 [3]. The GIS test compartment is represented by arc compartment, and the protective enclosure with exhaust compartment. Between the arc and exhaust compartment there is a bursting disc which opens at predefined pressure. Although there can also exist bursting disc between the exhaust compartment and installation room/environment, its function is solely for safety, i.e. under normal conditions during the testing no opening is expected.

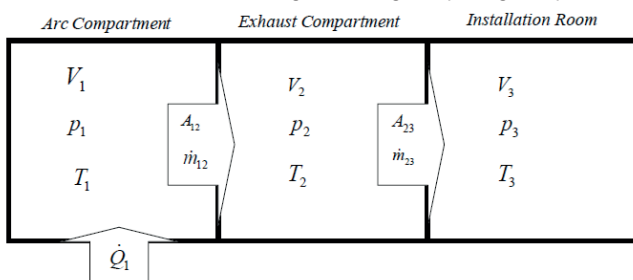


Fig. 1 Basic layout and variables used in calculation [3]

Several computer programs have been made for calculation of pressure and temperature rise due to internal arcing inside the test compartment and protective enclosure. Mathematical models are based on the report of the working group A3.24 CIGRE [3]. This paper presents two models: the basic model with constant properties of gas already shown in [3] and enhanced model with real gas/plasma properties which considers evaporation of electrodes material, ablation of an insulators and the contribution of exothermic/endothermic reactions to pressure and temperature rise. Both models assume the uniformly distribution of temperature, pressure and other gas parameters in the arc compartment and exhaust compartment, respectively. Along with known initial conditions, the Euler's method was used to integrate ordinary differential equations. The total phenomenon duration is divided into a series of short intervals  $\Delta t$  in which calculation of temperature and mass change of gas are performed, and at the end of each interval the new values of temperature, pressure and mass of gas in the enclosures are calculated. The described computer program was made in Matlab.

## The basic model with constant gas properties

The equations for pressure and temperature rise in arc and exhaust compartments are based on the assumption of ideal gas, meaning that the thermodynamic properties of gas,  $C_p$ ,  $C_v$ ,  $R_s$  and  $k$ , are constant and taken at gas temperature of 300 K and a pressure of 0.1 MPa (Table III). Since in reality the thermodynamic properties of gas/plasma change with the temperature, pressure and mass concentration of individual reactants, this model is applicable for SF<sub>6</sub> gas temperature up to 2000 K and air temperature up to 6000 K. The model does not consider the evaporation of electrode material neither the ablation of an insulation material. The contribution of exothermic/endothermic reaction to the temperature and pressure rise is considered by "artificial" increase of  $k_p$  factor, which shows how much electrical energy is consumed to heat the gas. According to [3], for copper electrodes, the value of  $k_p$  factor is between 0.5 and 0.7, while the value for aluminum electrodes can be significantly higher than 1 (up to 1.6).

Table III Thermodynamic properties of air and SF6 gas at T=300 K and p=0.1 MPa [3]

Thermodynamic properties of gas	Label	Air	SF <sub>6</sub>	Measurement unit
Specific heat capacity at constant volume	$C_v$	716	608	J/(kgK)
Specific heat capacity at constant pressure	$C_p$	1005	665	J/(kgK)
Heat capacity ratio	$k$	1.403	1.0936	-
Specific gas constant	$R_s$	287	56.9	J/(kgK)

The temperature change in the arc compartment, in interval  $\Delta t$ , is calculated according to:

$$\Delta T_1 = \frac{\Delta Q_1 - \Delta m_{12}(C_p - C_v) \cdot T_1}{m_1 \cdot C_v}, \quad (1)$$

with following notations:

$\Delta Q_1$  – the portion of electric energy used to heat the gas, including the exothermic reaction between the evaporated electrode material and gas,

$C_p$  – specific heat capacity at constant pressure [Jkg<sup>-1</sup>K<sup>-1</sup>],

$C_v$  – specific heat capacity at constant volume [Jkg<sup>-1</sup>K<sup>-1</sup>],

$m_1$  – mass of the gas [kg],

$\Delta m_{12}$  – mass flow from the arc compartment into the exhaust compartment after the opening of the bursting disc [kg].

The portion of electric arc energy used to heat the gas in this model also considers the energy of exothermic/endothermic reaction between the gas and evaporated electrode material. It is calculated using the following equation:

$$\Delta Q_1 = k_p \cdot P_{el} \cdot \Delta t, \quad (2)$$

Where  $k_p$  is the heat transfer coefficient and  $P_{el}$  is the electrical arc power.

The temperature of gas  $T_1$  in the arc compartment after time  $t$  is obtained by summing up all the changes of temperature  $\Delta T_1$ . The gas pressure in arc compartment after time  $t$  is calculated from the equation of the ideal gas state:

$$p_1 = \frac{(\kappa-1)}{V_1} \cdot m_1 \cdot C_v \cdot T_1, \quad (3)$$

Where  $\kappa$  is the heat capacity ratio and  $V_1$  is the volume of the arc compartment.

After opening of bursting disc, the mass flow from the arc compartment, in interval  $\Delta t$ , is calculated according to:

$$\Delta m_{12} = \alpha_{12} \cdot A_{12} \cdot \rho_{12} \cdot w_{12} \cdot \Delta t, \quad (4)$$

with following notations:

$\alpha_{12}$  – discharge coefficient (considering the contraction of gas flow through an opening),

$A_{12}$  – bursting disc opening cross-section area [m<sup>2</sup>],

$\rho_{12}$  – gas density within the opening [kg/m<sup>3</sup>],

$w_{12}$  – gas velocity within the opening [m/s].

The total mass flow (kg) from the arc compartment after time  $t$  is calculated by summing up all the changes while the remaining gas mass in arc compartment is calculated by subtraction of the total mass flow from the initial mass. The temperature change in the exhaust compartment after opening of the bursting disc is calculated using the following equation:

$$\nabla \Delta T = \frac{w^3 \cdot C^h}{\nabla w^{1.5} (C^b \cdot \Delta T - C^h \cdot \Delta T^2) - \nabla w^{3.5} \cdot (C^b - C^h) \cdot \Delta T^3}, \quad (2)$$

Where  $\Delta T$  is the gas mass and  $\nabla \Delta T$  is the gas mass flow from the exhaust compartment into the environment.

## The enhanced model with real gas/plasma properties, evaporation, ablation and exothermic reaction

The equations for temperature and pressure rise in the arc and exhaust compartment are derived with the assumption of ideal gas. The model is considering the real properties of gas/plasma which, in this case, consist of SF<sub>6</sub> gas and evaporated electrode material. For this purpose, tables with thermodynamic properties of gas/plasma for pure SF<sub>6</sub> and mixtures of SF<sub>6</sub> and evaporated copper at concentrations of 10%, 20%, 30%, 50% and 100% were prepared. The same was made for the mixture of SF<sub>6</sub> and evaporated aluminum. The influence of evaporated methane CH<sub>4</sub> on the thermodynamic properties of mixture is neglected due to low expected concentration. The temperature range in the tables is between 300 K and 10000 K, the pressure range is between 0.1 MPa and 10 MPa. The tables were prepared using the software named "Chemical Equilibrium with Applications" (CEA) [4]. For illustration, Fig. 2 shows C<sub>p</sub> for the pure SF<sub>6</sub> gas and also for the mixture of SF<sub>6</sub> and evaporated Cu and Al, respectively. The curves are illustrated at pressure value of 1 MPa. The enhanced model is applicable for the temperatures up to 10000 K.

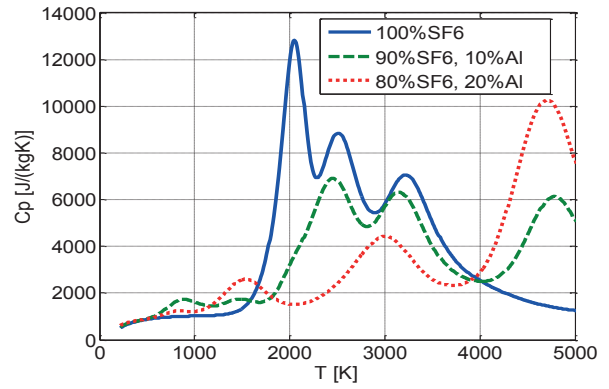
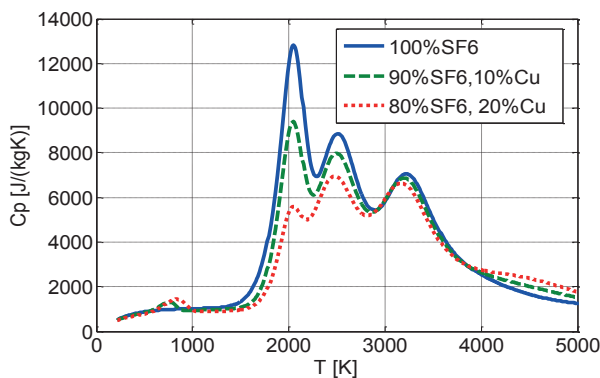


Fig. 2 C<sub>p</sub> for pure SF<sub>6</sub> gas and mixture of SF<sub>6</sub> gas and evaporated Cu/Al at pressure of 1 MPa

The mass of evaporated electrode material, in interval  $\Delta t$ , is calculated using the following equation:

$$\Delta m_{evap} = \frac{k_{evap} \cdot P_{el} \cdot \Delta t}{W_{evap}}, \quad (6)$$

Where  $k_{evap}$  is the evaporation factor which shows the portion of electric arc energy consumed on the electrode evaporation and  $W_{evap}$  is the specific energy required for evaporation of electrode material (Table II).

The mass of evaporated insulation material from the bushing plate in interval  $\Delta t$  is calculated using equation:

$$\Delta m_{abl} = \frac{k_{abl} \cdot P_{el} \cdot \Delta t}{W_{abl}}, \quad (7)$$

Where  $W_{abl}$  is the ablation factor which shows the portion of electric arc energy consumed on the ablation of insulation material and  $W_{abl}$  is the specific energy required for ablation of insulation material.

Evaporation factor and ablation factor depend on material and they are determined experimentally i.e. by measuring the mass of evaporated material and electric arc energy, both of them are less than 1. The contribution of exothermic/endothermic reaction between the gas and the electrodes material on the temperature rise considers the additional energy source in arc compartment:

$$\Delta Q_{ex} = W_{ex} \cdot \Delta m_{evap}, \quad (8)$$

Where  $\Delta Q_{ex}$  is the specific generated heat of exothermic/endothermic reaction [J/kg] (Table II).

If  $k_{evap}$  and  $W_{evap}$  are known and the contribution of exothermic/endothermic reaction is calculated according to (8), then the factor  $W_{ex}$  in this model cannot be greater than 1 as it was the case in the basic model with the constant gas properties. Namely, the sum of  $W_{evap}$  and  $W_{abl}$  should be equal to 1 and it represents the law of conservation of energy, if the losses are neglected. The evaporated electrode material and the evaporated insulation material represent the heat source or heat sink when mixing with the gas. Therefore the temperature change in arc compartment is calculated according to:

$$\Delta T_1 = \frac{\Delta Q_1 + \Delta Q_{ex} - \Delta m_{12} \cdot (h_1 - u_1) + \Delta m_{evap} \cdot (u_{evap}(T_{evap}) - u_{evap}(T_1)) + \Delta m_{abl} \cdot (u_{abl}(T_{abl}) - u_{abl}(T_1))}{m_1 \cdot C_{v1}}, \quad (9)$$

with the following notations:

$h_1$  – specific enthalpy of gas/plasma in arc compartment [J/kg],

$u_1$  – specific internal energy of gas/plasma in arc compartment [J/kg],

$u_{evap}$  – specific internal energy of the evaporated electrode material [J/kg],

$T_{evap}$  – evaporation temperature of electrode material [K],

$u_{abl}$  – specific internal energy of the evaporated insulation material [J/kg],

$T_{abl}$  – ablation temperature of the insulation material [K].

Neglecting the chemical reactions between the gas from the arc compartment and the gas in exhaust compartment, the temperature change in exhaust compartment, in the interval , is calculated using the equation:

$$\Delta T_2 = \frac{\Delta m_{12} \cdot (h_1 - u_2) - \Delta m_{23} \cdot (h_2 - u_2)}{m_2 \cdot C_{v2}} \quad (10)$$

Where  $h_2$  is the specific enthalpy of the gas in exhaust compartment [J/kg] and  $u_2$  is the specific internal energy of the gas in exhaust compartment [J/kg].

## INTERNAL ARC DEVELOPMENT TESTS

### Test model

For the purpose of verifying the mathematical model, two configurations of the test model were designed and tested (Fig. 3). A total of 4 tests were performed. In the first two tests the arc has been initiated between the electrodes with the round cross-section (Fig. 4a) using the test configuration illustrated in Fig. 3a. In the first test the copper electrodes were used, while in the second they were replaced with the aluminum electrodes. Since the voltage source in the test laboratory was limited to about 600 V, the initial spacing between the electrodes, on which the arc was initiated, was only 3-4 mm. The initial SF<sub>6</sub> gas pressure in the test compartment was 0.6 MPa, while the pressure in the protective enclosure was 0.1 MPa. The volume of the test compartment is 0.3 m<sup>3</sup>, while the volume of the protective enclosure is 2.4 m<sup>3</sup>. The disc bursting pressure is 0.9 MPa ±5%, and the cross-section area is 0.009 m<sup>2</sup>. During the test, arc voltage and current, the pressure in test compartment and protective enclosure, were measured. After the test, electrode material erosion was measured. The erosion of insulation material (in the tests no. 3 and 4) could not be accurately measured due to relatively large weight of the bushing plate compared to the amount of eroded insulation material, and also because of the fact that at the same time the erosion of cast copper electrodes in the bushing plate occurred. After the test, based on the measurements of the arc voltage and current, the electrical power and total arc energy were calculated.

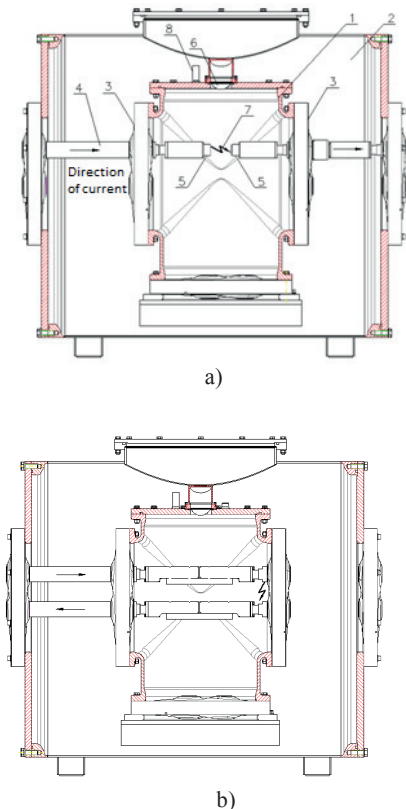
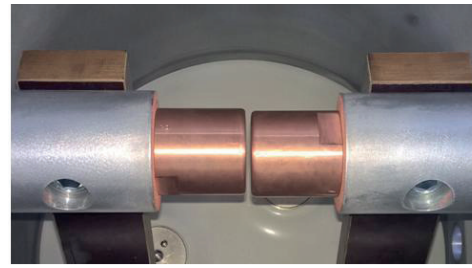
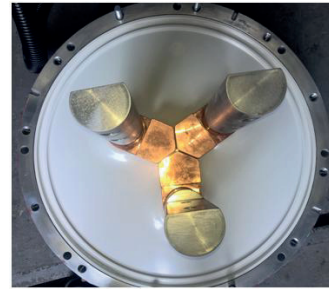


Fig. 3 The cross-section of the test configurations for development testing on internal arc (1. test compartment, 2. protective enclosure, 3. bushing plate, 4. conductors, 5. changeable electrodes, 6. bursting disc, 7. electric arc, 8. pressure sensors)



a)



b)



Fig. 5 Internal arc development testing in Končar – High Power Laboratory

### Test results

The test results are shown in Table IV and figure 6.

Table IV Test results

Test no.	1	2	3	4
Test configuration	Figure 3a)	Figure 3b)		
Electrode material	Cu	Al	Cu	Al
Arc fault type	Single-phase	Three-phase		
Arc current [kA]	40	40	40	40
Arc duration [s]	0.36	0.114	0.42	0.37
Electric arc energy [MJ]	1.42	0.52	2.6	2.95
Max. pressure rise in test compartment [MPa]	0.35	0.32	0.4	0.85
Max. pressure rise in protective enclosure [MPa]	-	0.15	0.15	0.3
Bursting disc opening time [s]	0.65	0.6	0.38	0.18
Electrodes material erosion [g]	347.5	34.5	773.5	505.5

Fig. 4 Electrodes for single-phase fault a) and three-phase fault b)

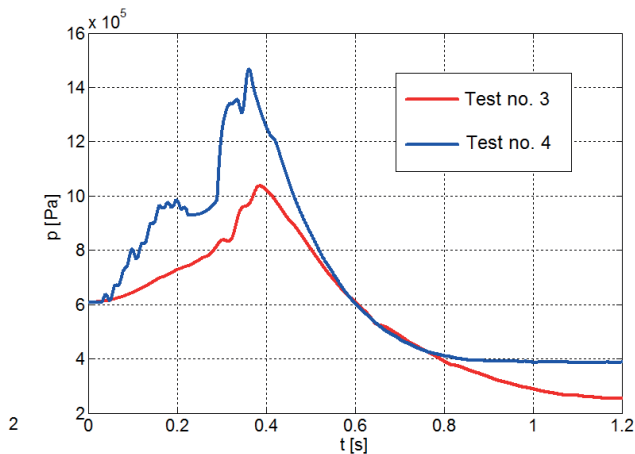
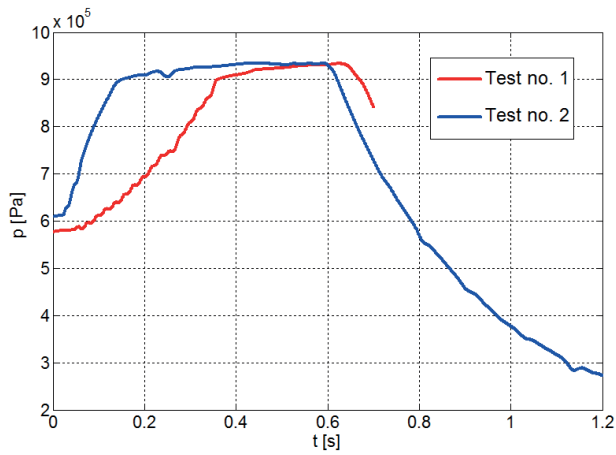


Fig. 6 Measured pressure in the test compartment

By analyzing the pressure curves in the tests no. 1 and 2, it can be seen that the maximum pressure rise is almost the same for copper and aluminum electrodes although the electric arc energy was 2.7 times smaller in the test with aluminum electrodes. The pressure gradient is also significantly higher in the test with aluminum electrodes. The bursting disc in both tests operated long after the arc was extinguished, which can be explained by the fact that for equalizing of the temperature, and thus the gas pressure, throughout the test compartment take some time.

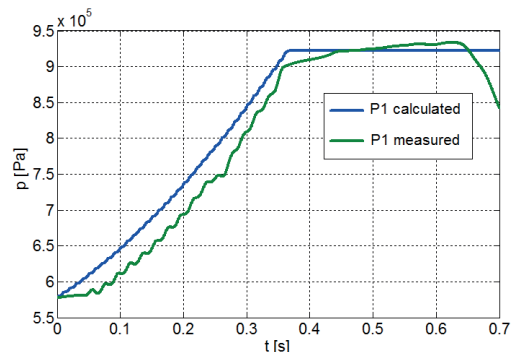
In the tests no. 3 and 4, for approximately the same amount of electric arc energy, the double increase in pressure rise was obtained in test with aluminum electrodes. Although the bursting disc operated, the pressure continued to increase until the arc was extinguished. This is especially emphasized in the test no. 4 with aluminum electrodes.

The equalization of the pressure in the test compartment and protective enclosure after the arc is extinguished and the disc opened, will take less in the tests with higher maximum pressure (and higher maximum temperature) due to higher speed of sound at higher temperatures. Except in test no. 2, in all other tests, a significant erosion of the electrodes occurred. Erosion is partly a consequence of melting and partly of evaporation of electrode material. Due to the erosion of the electrodes, the distance between the electrodes increases, which increases the arc voltage. At the moment when the arc voltage value approaches to the maximum source voltage, the arc is extinguished. It should be noted that in the case of type test, due to greater distance between the electrodes, it is possible to expect up to ten times greater electric arc energy than it was achieved on the development test.

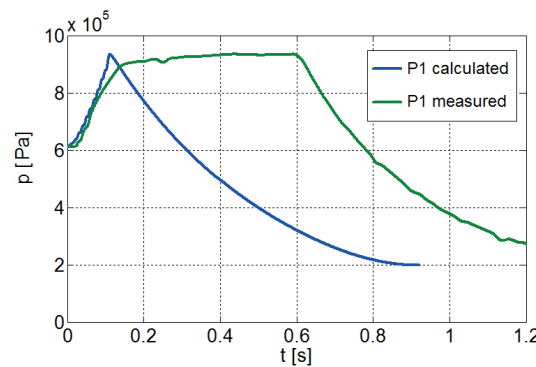
## VERIFICATION OF THE MATHEMATICAL MODEL WITH THE TEST RESULTS

As it is shown in [3], verification of the mathematical model comes down to determination of the heat transfer factor and discharge coefficient for which a good correlation between the measured and calculated pressure P1 in the test compartment is obtained (Fig. 7). Unlike [3], where the basic model with constant gas properties was used to verify the results of the calculation, an improved model with real gas/plasma properties is used

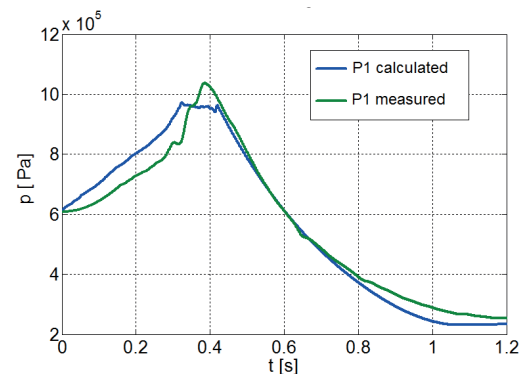
in this paper. By changing the factor in the calculation, the increase rate of pressure is adjusted, and by changing the discharge coefficient the downstream of pressure curve after the disc bursting. Since the erosion of electrodes is simultaneously the result of melting and evaporation of the material, it was not possible to determine the evaporation factors of electrode material or ablation factors of insulation material from the results of the tests. Therefore, in this case, the factor also includes the contribution of the exothermic/endothermic reaction to the pressure rise and the factors and are set to zero.



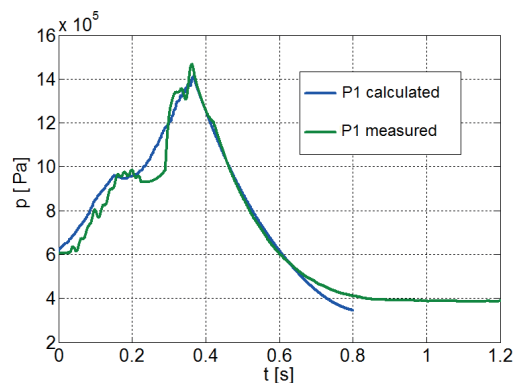
a) Test no. 1:  $k_p=0.9$



b) Test no. 2:  $k_p=2.35$ ,  $\alpha_{12}=0.7$



c) Test no. 3:  $k_p=0.9$ ,  $\alpha_{12}=0.7$



d) Test no. 4:  $k_p=2.3$ ,  $\alpha_{12}=0.7$

Fig. 7 Verification of the mathematical model with the test results

For the electric arc on the copper electrodes (tests no. 1 and 3), a very good correlation of the calculation results with the measurement results for the factor of 0.9 is achieved. On the other hand, for the electric arc on the aluminum electrodes (tests no. 2 and 4), the factors are 2.3 and 2.35 respectively. The discharge coefficient in test no. 1 was not possible to determine, since the downstream pressure curve, after the bursting disc operated, was not recorded to the end. In other tests, a good correlation of the calculation results with the measurement results was achieved for the discharge coefficient of 0.7.

## CONCLUSION

In order to assess the GIS enclosure resistance on the internal arc at the upcoming type test, a program for the calculation of the pressure and temperature rise in the test compartment and protective enclosure due to an internal arc was developed. The basic model with constant gas properties shown in the A3.24 working group report was enhanced by the real gas/plasma properties, evaporation of electrodes material and ablation of insulation material. The contribution of the exothermic/endothermic reaction to the pressure and temperature rise was also taken into account. Unlike the basic model with constant gas properties applicable to the SF<sub>6</sub> gas temperature of 2000 K, the enhanced model is applicable to the temperature of 10000 K. The mathematical model is verified on the basis of the results of the GIS enclosure development test on internal arc. Satisfactory accuracy has been achieved in determining the maximum pressure and gradient of pressure rise in the test compartment and protective enclosure.

## BIBLIOGRAPHY

- [1] IEC 62271-203:2011 „High-voltage switchgear and controlgear – Part 203: Gas insulated, metal enclosed switchgear for rated voltages above 52 kV“
- [2] M. Binnendijk, G.C. Schoonenberg, A.J.W. Lammers, »The Prevention and Control of Internal Arcs in Medium-Voltage Switchgear“, CIREC 97, 2-5 June 1997, Conference Publication No. 438 IEE, 1997.
- [3] N. Uzelac, M. Glinkowski, L. del Rio, M. Kriegel, J. Douchin, E. Dullni, S. Freitoza Costa, E. Fjeld, H-K. Kim, J. Lopez-Roldan, R. Pater, G. Pietsch, D. Reiher, G. Schoonenberg, S. Singh, R. Smeets, T. Uchii, L. Van der Sluis, P. Vinson, D. Yoshida „Tools for the Simulation of the Effects of the Internal Arc in Transmission and Distribution Switchgear“, Working Group A3.24 CIGRE, December 2014.
- [4] <https://www.grc.nasa.gov/WWW/EAWeb/ceaguiDownload-win.htm>

The tests performed on the copper and aluminum electrodes in SF<sub>6</sub> gas confirmed a significantly higher contribution of aluminum electrodes to the pressure and temperature rise in GIS enclosure (), compared to copper electrodes (). It can be concluded that for the same electric arc energy, in the case of aluminum electrodes, SF<sub>6</sub> gas receives up to 2.5 times more heat than it is the case with the copper electrodes. Higher values of the factor in regards to the references can be explained by applying a mathematical model with the real gas properties. Namely, the increase of the gas temperature results in an increase in the specific heat capacity and the gas can absorb more heat with a lower temperature rise and pressure, respectively. In the model with the constant gas properties, which is mostly used in the references for the verification of calculation results with the measurement results, this effect is not considered.

For discharge coefficient the pressure drop curves have been calculated after the disc bursting and arc extinguishing and they are well matched with measured curves, indicating that gas flow through the opening and the pressure rise are well modeled.

However, the evaporation factor for electrode material could not be determined from the test results because the erosion of the electrodes is simultaneously the result of melting and evaporation of material. The ablation factor also was not possible to determine from the test results since it was not possible to precisely measure the erosion of insulation material from the bushing plate. Nevertheless, a computer program based on the presented mathematical model can be used to calculate the pressure and temperature rise in the test compartment and protective enclosure during the preparation of the test object for type test on internal arc.

**A. FOŠKULO \***

KONČAR – POWER PLANT AND ELECTRIC TRACTION  
ENGINEERING INC.  
CROATIA

**M. KOKORUŠ**

ENTEGRA EYRICH + APPEL GMBH  
GERMANY

# Streamlining the Decision- Making Process on Tubular Rigid Busbar Selection During the Planning / Designing Stage by Utilizing 3D Substation BIM Design Software

## SUMMARY

For Utilities, each substation is regarded as an asset. Managing of assets is one of domains of Asset Management including Life Cycle Costing (LCC) as a decision-making criterion. However, LCC as a decision-making criterion should be applied on an entire substation taking into account all of the potential cost influences for the purpose of achieving of an effective substation management. Asset management as a decision-making process should be observed within a larger context and should be more focused on risk management, as all real decisions include an element of risk due to present uncertainties.

Two promising avenues are explored in regards to more comprehensive and rigorous up-front planning through usage of Information Technology (IT). While up-front planning falls under the domain of Lean philosophy, Building Information Modeling (BIM) falls under the category of agile decision-support tools. Utilization of both is explored from a perspective of design-uncertainties under both product and process design.

Standard specifications and standard designs are another form of applied Lean Philosophy that reduces design-uncertainty and variability. However, a range of technical solutions stemming out of the standardization can be quite wide. Customization involves specification and design of new / innovative designs with wide range of technical solutions as well. Due to external pressures focused on shortening of the project delivery time, there is a need for a faster project time throughput. This is reflected in the form of a requirement for more rapid engineering decision-making and faster decision cycles.

Streamlining of a decision-making process related to the engineering is all about engineers' awareness of the situation from the project level perspective coupled with utilization of decision-support tools for creation and reuse of knowledge. Plan – Do – Study – Orient (PDSO) cycle is a decision-making model that supports creation and reusability of knowledge along with providing an explanation in regards to the time dimension relating to decision-making, and as such is presented in this paper.

The rigid busbar system design is an iterative process influenced by many factors, defined either as design variables or design constraints. As rigid busbars are gaining more popularity for both greenfield and brownfield investments, the rigid busbar system design is explored from a perspective of decision-making streamlining. The case of the rigid busbar system design of El Chaparral project in El Salvador is given.

## KEYWORDS

Lifecycle – Decision – Design – Standardization – Customization – Lean - Agility – Calculation – BIM - Busbar

# INTRODUCTION

As forecasted in [1], the demand for electricity is expected to increase by more than two-thirds between 2011 and 2035. Utilities are already under pressure to extend the useful life of aging assets beyond their original expected life time [2]. As reported by [2], improvements regarding cost, time and quality during the project delivery are required, thus leaving space for improvements for making right decisions and to deliver projects more efficiently across an array of asset types.

For Utilities, each substation is regarded as an asset. Managing of assets is a domain of Asset Management with Life Cycle Costing (LCC) as a decision-making criterion [3]. Doing so, the main goal is to minimize the total cost of a substation [4]. However, LCC as a decision-making criterion should be applied on an entire substation taking into account all of the potential cost influences, as opposed to its often application on substations individual components, with the purpose to achieve an effective substation management [5]. These additional cost influences are related to land costs [5] [6], but also to costs for the balance of the plant as well, representing steel structures, concrete elements, transport and installation, among all others [6]. Engineering should also be included as a cost into the system and equipment cost [6]. The same relates to renewal costs [7]. The following figure represents a LCC basic structure for high voltage (HV) substations.

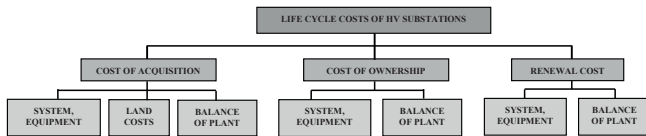


Figure 1. Prime levels of the basic structure of the LCC assessment for HV substations [6]

Asset management, in general, as a decision-making process should be observed within a larger context and should be more focused on risk management [8]. According to [9], risk management is defined as “a decision-making to balance risk and risk mitigation”.

All real decisions include an element of risk as all decisions are usually made under uncertainty [10]. Uncertainty in engineering can be classified either as content-uncertainty (incompleteness, imprecision and vagueness) or as context-uncertainty (unreliability, invalidity and instability) in regards to information quality [11]. In order to make rational decisions, information needs to be full, current and reliable [12]. Apart from advising improvements in decision making, improvement of the information flow is also advised. An effective information flow represents a basis for an effective decision-making [13]. Two defined promising avenues are, according to [14], the introduction of more comprehensive and rigorous up-front planning, and enhancement of Information Technology (IT) capabilities.

Section 2 of this paper represents a literature review section in which following topic are covered:

- Design-uncertainties from a process design perspective;
- Design-uncertainties from a product design perspective;
- Pursuing optimization through utilization of decision-support tools;
- Decision-making models from the lens of agility, and;
- Rigid busbar design process, variables and constraints.

Inside section 3, a recapitulation of the literature review section is presented before defining research questions as a part of the problem statement. Section 4 relates to the presentation of up-front Building Information Modeling (BIM) utilization as a solution of a problem. A busbar system design example from the recent project El Chaparral in El Salvador is given and described inside Section 5 of this paper, before setting forth a discussion relating to the busbar design example from a perspective of utilization of up-front BIM engineering inside Section 6. A conclusion is presented inside Section 7 relating to streamlining of decision-making process for the rigid busbar system design. Such a conclusion can be generalized and applied to other parts of power substations as well. Last sections of this paper are related to the presentation of recommendations and acknowledgements before outlining references.

# LITERATURE REVIEW

## DESIGN UNCERTAINTIES FROM PROCESS PERSPECTIVE

As decision-making is an integral part of any design process [9], uncertainty in the design process is referred to as design-uncertainty [15], which will, if not addressed, ultimately lead to engineering reworks and project delays [16]. According to [17], a general view is that uncertainty is the highest at the beginning and then it is reducing during time with generation of relevant information that is made available. Resolving of uncertainties early in the project is highly advised [16]. In general, dealing with uncertainties is labeled as “Lean” [18]. Lean can be defined as an early project planning process for elimination of all non-value added work which is regarded as waste [19]. Delays, waiting, and misused resources are just a few types of waste [20], and all of these can be translated directly to engineering. Lean Project Delivery System (LPDS) is a framework comprising five traditional project phases as triads linked in such a manner to enable cross-functional teams to be involved early in planning and design [21], and is depicted on Figure 2.

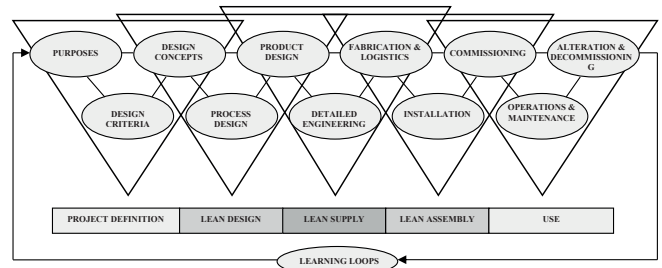


Figure 2. Triads of the Lean Project Delivery System (LPDS) [22]

Utilization of Concurrent Engineering (CE) is advised for dealing with engineering reworks and uncertainty [16]. According to [20], CE is a systematic approach where integrated teams consider more relevant information at the right time for decision-making [19].

Lean design phase is critical due to the following tools and techniques:

- Involve downstream players in upstream decisions, to participate in key decisions [23];
- Share incomplete information for each level of decision making [23], thus enabling CE;
- Selecting alternatives at the last responsible moment, thus reducing negative design iterations as an example of waste reduction [23], providing more time for exploring alternatives [22];
- Shifting early design decisions to a point where they can be made in the most efficient manner [23];
- Consider the influence of installation, logistics, procurement, detailed engineering, maintenance, and commissioning on design [23];
- Reduce batch sizes of information between project participants, thus speeding up design process allowing dividing of decision-making into several segments [23], thus enabling CE;

all for the purpose of designing the final product under the Design for X (DFX) concept, where X marks an ability downstream in the supply chain [23], to achieve a time compression.

Early identification of suppliers and their involvement gives rise to the concept of the Design for Procurability, as designs are to be made with the procurement in mind [23], as the procurement of materials / equipment impacts the detail engineering [24], and it is a critical element for the project success [25]. The design for Constructability [23], focuses on the ease of installation [24], but also on transportability [26]. The supply chain should be involved in the design, construction and in definition of client’s requirements.

Figure 3. depicts interrelationships among project requirements and it puts client’s requirements with identified requirements stemming out from the supply chain and construction into perspective.

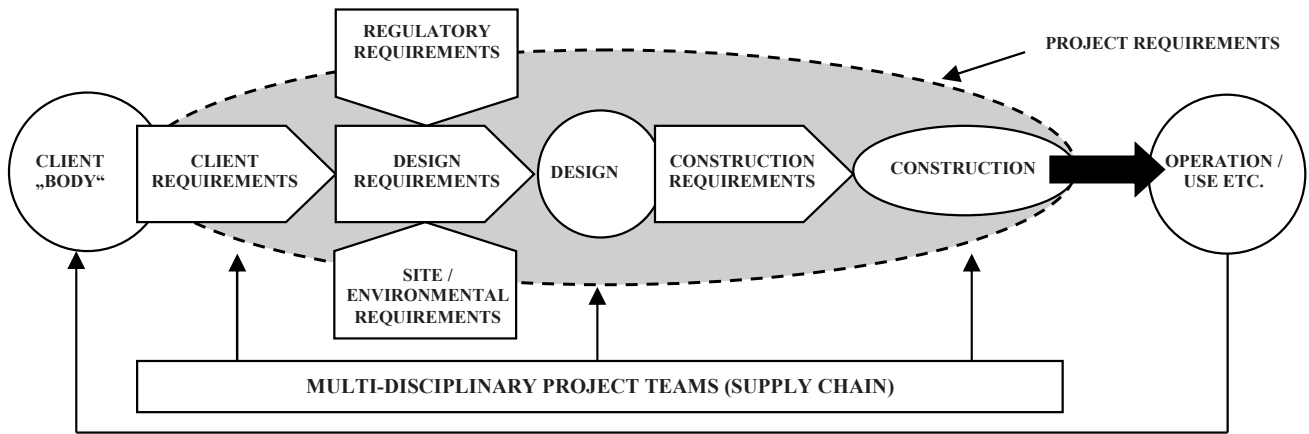


Figure 3. Interrelationships among project requirements [27]

According to Figure 3., the designer needs to translate the “voice of the client” defined inside client requirements successfully into the “voice of the designer” that is aligned with project requirements [27]. In essence, decisions are to be made on what exactly represents client’s requirements (seen as a problem), and the representation of those requirements in design terms (seen as the solution) [27].

Less experienced clients tend to provide unclear and ambiguous requirements as input information in the design process [27], increasing design-uncertainty. Satisfaction of all project requirements according to Lean principles becomes a daunting task that requires, according to [19], a high level of engineering effort that is between two to three times higher compared to the traditional non-lean project delivery.

A higher level of required engineering up-front effort in the design process is depicted on Figure 4. as a curve No. 4. The ratio of a higher engineering effort can be extrapolated between curve No. 4 and curve No. 3 during the detailed design stage, as it closely resembles to the ratio between 2:1 and 3:1 as stated earlier.

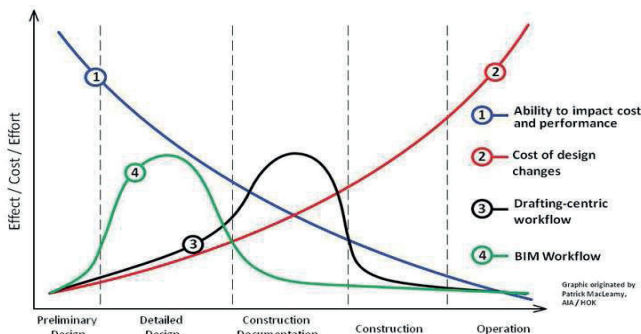


Figure 4. MacLeamy's curve, as adapted from [28]

## DESIGN UNCERTAINTIES FROM PRODUCT VARIABILITY PERSPECTIVE

According to Figure 2., the Lean Design comprises both, the process design and the product design. While the process design determines how to produce, the product design determines what is to be produced [23]. Utilities tend to standardize, practicing utilization of standardized specifications and standardized designs [29]. According to [30], standardization is one of the methods of the applied Lean Philosophy that reduces variability. In simple words, the Lean Design is about design standardization reducing variability of potential design solutions, generally enabling reductions in time and cost [30]. However, standardization itself does not guarantee any significant reduction in variability of possible technical solutions, as according to [31]; the range of possible technical solutions can be wide even with standard technical specifications, advising the generation of more thorough and precise specifications even for minor requirements.

Customization is opposite to standardization [30]. In general, and according to [32], Pareto's principle or 80-20 rule can be applied on substations,

as “at least 80% of substation projects can use predefined standardized designs while 20% or fewer will require some form of customization”. Customized designs are referred to as being innovative designs representing tomorrow standards [29].

The decision process is translation of inputs (requirements and constraints) into an output (decisions) [9]. To correlate with Figure 3., all project requirements are treated as inputs into the decision process for the designer as additional constraints, while client’s requirements are treated as requirements. Figure 5. is given for that purpose to illustrate the design decision process.

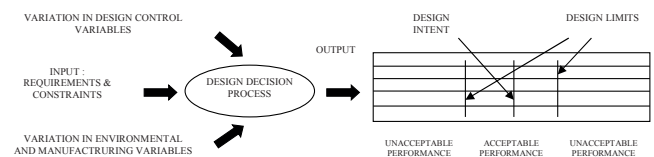


Figure 5. Design decision process in the context of variability [9]

Variation may exist in the form of information fed as an input, but primary variations are stemming out of the design and environmental / manufacturing variations [9]. While design variations can be controlled by affecting design parameters, environmental / manufacturing variations cannot be controlled, as these are based on factory product ranges [9], and they are represented as standard material / equipment properties.

That results in variations around the mean acceptable performance of the design intent [9], and usually involves several acceptable potential product solutions as alternatives [10]. These are designer’s preferences that single out one alternative among the others [10], and seek out the best design as a solution following the rule of optimization [10].

## PURSuing OPTIMIZATION WITH DECISION-SUPPORT TOOLS

The iterative design process is an example where making of structure decisions is required which is custom to engineering, as a route between the current and a desirable future state comprising multiple nodes of which each node has multiple options to be chosen [33]. According to [34], engineers have been lately forced to make decisions with incomplete sets of information due to time constraints, and rapid decision-making under these conditions represents one of the most difficult tasks for engineers. Calculations are an integral part of the design process for various selections and verifications [35], and engineers preferred to make them only once [36]. Although important decisions need to be made early and they need to be made firmly [24], sometimes decisions are to be made just-in-time (JIT) [37].

In general, the quality of decisions can be improved by utilization of computer-based tools, such as knowledge-based systems (KBS) [9]. KBSs are categorized as decision-support tools [27]. Benefits include a support for key decisions to be made earlier along with an exploration of alternative solutions faster thus streamlining the design process [38]. Streamlining of the design process is also achieved through automation of various engineering calculations ensuring efficiency and accuracy [39].

Three-dimensional (3D) models also enable exploration of alternatives for preparation of more effective designs [40], but also enable reduction in

engineering man-hours and thus a faster throughput of projects [41]. Faster throughput of projects is enabled due to the design automation but is also due to rapid evaluation of design alternatives [42]. 3D models are also being referred to as knowledge repositories supporting standardization [43], under which the equipment is grouped into blocks [44], thus further enhancing reusability of same knowledge. In order to benefit from the 3D approach, the process of creating both standardized designs for re-usage and unique designs based on advanced 3D modelling techniques must be automated [42]. Generally, reusing previously captured solutions is a base for “delta engineering” which allows execution of processes starting from specifications up to delivery of final documentation, reducing times of engineering tasks through central project database [45]. According to [46], the substation model in 3D can embrace all aspects of the substation project lifecycle, and as such is depicted inside Figure 6.

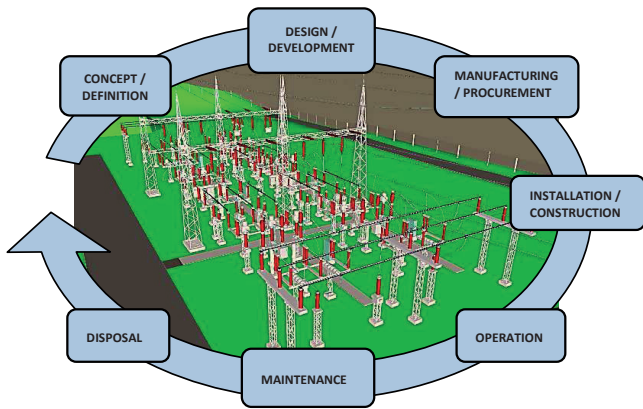


Figure 6. Lifecycle of a substation in a 3D environment with image of El Chaparral station

Building Information Modeling (BIM) is seen as a bridge between decision-support tools as engineering calculations and standardized designs in 3D, with data bases in the background [47].

BIM as “Building Information Modeling is the development and use of a computer software model to simulate the construction and operation of a facility. The resulting model, a Building Information Model, is a data-rich, object-oriented, intelligent and parametric digital representation of the facility, from which views and data appropriate to various users’ needs can be extracted and analyzed to generate information that can be used to make decisions and improve the process of delivering the facility” [48]. BIM as a Building Information Model is being referred to as a “shared knowledge resource for information about a facility forming a reliable basis for decisions during its lifecycle from inception onwards” [49].

From a project perspective, BIM stands to enable better decision-making shifting the effort to determine critical cost factors early in the design process [50], as depicted inside Figure 4. as a curve No. 4 compared to a traditional workflow given as curve No. 3. That means that decisions will be made faster and earlier in the process, as making specifications of materials and brand selection can start earlier as opposed to the traditional way to identify suppliers and conducting a pre-selection of brands later on [51]. BIM models comprise “smart” objects containing project-relevant information, among others, calculations [52]. Substation specific calculations can be integrated with 3D substation model, as depicted on Figure 7. Such an approach of having integrated calculations allows analysis and optimization of the design continuously during the entire design and planning phase [50], [53].

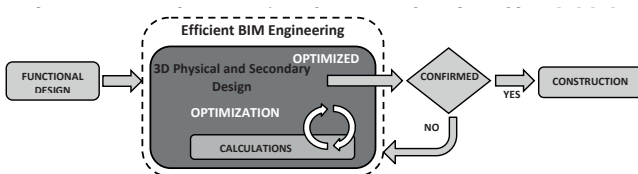


Figure 7. Concept of Efficient BIM Engineering – Integrated Calculations [53]

In general, if performed by a computer, calculations and recalculations are conducted more quickly, allowing further exploration of alternatives [36], and the decision-making is improved through simulations and analyses [54]. BIM therefore could also stand for as a lean framework enabling concurrent engineering, driving agility, and increased accuracy of estimations, designs and calculations with 3D representation defined as a key for en-

gineering decision-making during the entire lifecycle [55]. Decisions are often made, however, without considering of the effects on the project level [56].

## DECISION-MAKING MODELS THROUGH THE LENS OF AGILITY

Agility is defined as “the ability of a system to thrive in an uncertain and unpredictable evolving environment; deploying effective response ...” [57]. The effective response is related to the decision-making and the decision-implementation [58] due to the constantly increasing demand for faster decision cycles [59].

While Simon’s model of problem solving is considered to be suitable for engineering problems, it does not include time as an attribute [60], which as a tempo or the decision cycle time is a unique feature of Boyd’s Observe – Orient – Decide – Act (OODA) decision making model [61].

Faster cycle times in OODA loop are instrumental for perception of the concept of agility [62]. OODA loop is a single-agent model [63], and as such it is fully aligned with the argument that decisions are always made by individuals and individuals alone [10]. OODA loop is depicted as a cycle at the top of Figure 8.

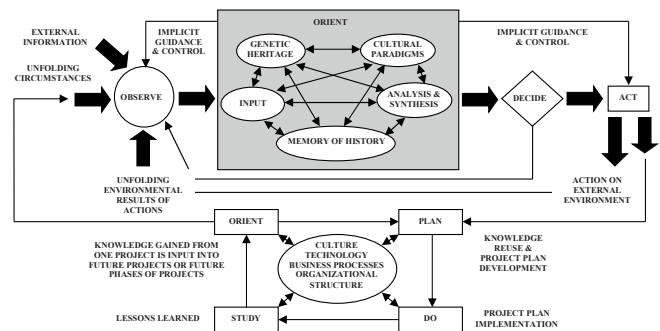


Figure 8. Linked OODA loop and PDSO cycle based on [63] with correction based on [64]

Steps of OODA are described as follows [63]:

- Observe step observe current environment and data / information gathered from both external and internal sources;
- Orient step enable orientation to current situation based on information fed, past experiences and analysis / synthesis for creation of new knowledge and allowing knowledge to be reused;
- Decide step develops hypotheses in order to identify and derive one solution over others, thus representing an identification of a course of action; and
- Act step allows testing of hypothesis by acting on a decision previously made [61].

Main focus of OODA loop is put on the Orient step [61]. It is impacted by employees’ keen understanding of the “big picture” [62], or by keeping a broad perspective [63]. It is a “mental thing” [64], shaping observation, decision and action [62].

Knowledge management is one cornerstone of agility [37]. OODA loop lacks planning stage and ability to store / recall data [61]. Remedy is achieved by linking OODA loop with Plan – Do – Study – Orient (PDSO) cycle, thus enabling decision-making cycling for knowledge creation inside OODA loop to be combined with knowledge storage / retrieval within PDSO cycle [63]. PDSO cycle is depicted as a cycle at the bottom of Figure 8.

According to [63], from engineering standpoint, PDSA / PDSO cycling can be described as:

- Plan step for project scoping and developing a project plan along with reusing explicit knowledge from previous projects by means of project documentation;
- Do step deals with implementation of project plan along with reusing both explicit and tacit knowledge from previous projects;
- Study step enables assessment and reflection onto what has occurred in the project and deals with lessons learnt;
- Act step deals with decision whether to reuse previous knowledge on new project or to abandon it.

Act step also represent a link to Observe step of OODA loop for the purpose of orientation whether or not to reuse previous project knowledge, thus PDSA cycle is renamed as PDSO cycle [63].

According to [63], PDSO cycle from a perspective of the project level and the project knowledge:

- Starts with Orient step toward Plan step where specific knowledge is carried
- Knowledge reuse occurs at Plan steps by means of reusing project documentation, from earlier projects thus representing explicit knowledge;
- Knowledge reuse occurs at Do step from previous projects on both explicit and tacit level, including lessons learnt;
- Study steps deals with reflecting and assessing what has occurred in the project;
- PDS steps are related to knowledge flow during project completion or stage completion;
- Knowledge flows from Orient step of PDSO cycle to Observe step of OODA loop.

Operated within OODA loop, information is processed into knowledge (knowledge created) and reused, saving rework [63]. Decisions as such are a commitment to action, but not action itself [61].

Action can flow from two directions, namely from Decide and from Orient through Implicit Guidance and Control (IG&C) link [64]. Later on, one enables more rapid flow as the Decide step if skipped [64], as opposed to the flow from Decide which is required when one is unsure about the course of the action or when there is no plausible action that can be inferred via IG&C link [62].

As a rapid execution of OODA loop is essential for the overall project success [62], this can be achieved in two ways, either using IG&C link and skipping the Decide stage, or speeding up the Decide stage, but for both keeping our observation better matched to the reality is a key prerequisite for both ways [64].

According to [64], different ways of executing OODA loop deal with:

- Usage of existing repertoire of actions directly through IG&C link when faced with low levels of uncertainty, and
- Creating new repertoire of actions through the Decide stage employing a circular process through the feedback of unfolding interaction with environment.

Standardization is seen as a method for creation of repertoires of action from perspectives of both OODA loop and Lean philosophy [64]. A successful organization is described as one being able to employ the existing repertoire, create a new repertoire through circular OODA loop, and update orientations [64].

Figure 8. presents such linked OODA and PDSO cycles based on [63] with deleted input into the Decision from the Implicit Guidance & Control as non-existent according to [64].

A prime example of an Agile enterprise is an Agile Utility. Such an Utility is able to:

- Streamline the design process and automate it [66], [67];
- Standardize the process [68];
- Design in parallel [69], thus employing Concurrent Engineering;
- Define and employ standardized designs for each voltage level [67], [68], thus developing standard layouts [66] and applying it [67], [68];
- Utilize IT [66] through utilizing automated design tools [68] based on 3D models [66];
- Employ designs for procurability and designs for constructability [66] and final solution optimization [68];
- Always looking for more innovative ways to deliver future projects under seemingly impossible time restraints [69];
- Reuse existing standardized designs as a jumpstart for each new project also involving customized configurations [67];
- Form alliances with vendors thus enabling shorter lead-times [66] and cost reductions [68].

According to [57], Agile principles can be incorporated into Lean principles without a compromise. While Lean principles ultimately come down to optimize the project and not its piece [30], and to ensure that once made

decisions would never be revisited [64], Agile principles ultimately induce the speed and thus, faster response times.

## RIGID BUSBAR DESIGN PROCESS, VARIABLES AND CONSTRAINTS

In general, the rigid buswork design process involves selection of the minimum bus size required for ampacity, insulators, hardware, electrical clearance, and determining the short-circuit fault current [70].

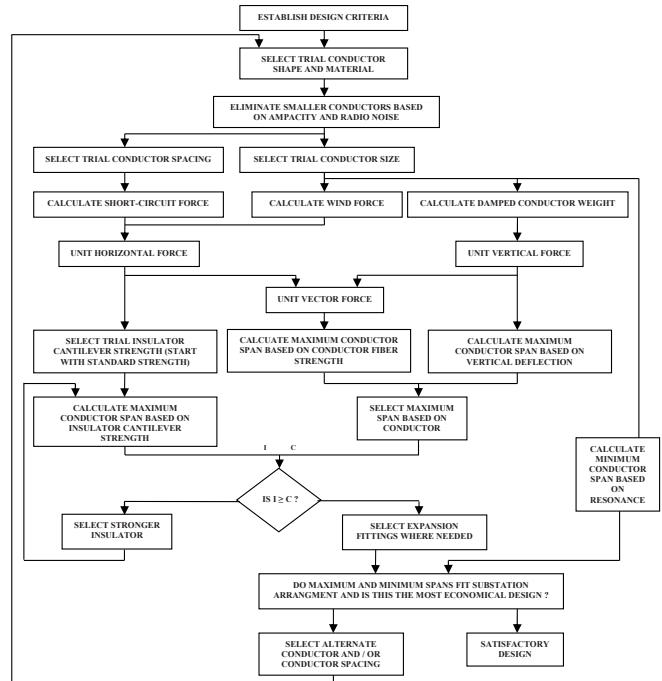


Figure 9. Flowchart for the rigid buswork design process based on [71]

The flowchart of the horizontal rigid busbar design process is given in Figure 9, with a made assumption that the maximum span length is not limited by the aeolian vibration. According to [72], the procedure for rigid bus design is the following: (1) material and size selection based current-carrying requirements, (2) determine bus centerline-to-centerline spacing, (3) calculate the maximum short-circuit force for bus to withstand, (4) determine the total bus conductor loading including environmental factors, (5) calculate the maximum bus span / support spacing, (6) calculate the maximum vertical deflection, (7) determine the minimum required support insulator cantilever strength, (8) provide thermal expansions for conductors, (9) adequately position bus couplers / fittings, and (10) verify the presence of aeolian vibration.

To illustrate a relationship between design variables and environmental / manufacturing variables to constraints, Figure 10 is given representing an interaction of design variables and constraints.

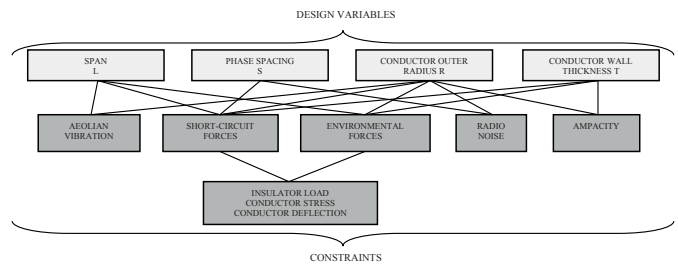


Figure 10. Interaction of design variables and constraints for the rigid buswork selection [71]

Inside the first row of design variables, span and phase spacing are clearly design controllable variables, while the conductor outer radius and conductor thickness are an example of environmental / manufacturing variables, which can be theoretically regarded as uncontrollable if unprocurable, due to the availability of materials that changes from a country to

a country [73]. Two bottom rows inside Figure 10 represent constraints for the rigid buswork selection. In the isolation, each of constraints can be easily satisfied [36]. However, the selection of the design variable to satisfy one constraint will not necessarily satisfy other constraints, thus making the rigid buswork design as an iterative process [71], involving excessive calculations [74]. Minimum electrical and structural requirements are usually defined inside company standards [75], and thus they have an anchor in the practice of standardized designs. Standardization can also be reflected into environmental / manufacturing design variables such as the conductor outer radius and its wall thickness being design controllable variables if indeed such materials are procurable, thus further reducing variability on the input side of the design decision process. Customization can be manifested inside Figure 10. as:

An addition of new types of constraints such as physical site constraint [71], and due to upgrading [76] among others;

- Harsher existing types of constraints such as the deflection limit due to aesthetics [77], due to capacity increase [7], and / or due to the new substation location among others;
- A change in one or in all existing design variables, due to upgrading among others [7], [76];
- or it can encompass a new rigid buswork concept such as the A-frame arrangement whose calculations are not covered by relevant standards [78].

All in all, both standardized and customized designs for the rigid busbar selection require undertaking of several design iterations before an optimized technical solution can be identified as the best option.

## PROSPECTIVES FOR STREAMLINING OF AN ENGINEERING DECISION-MAKING PROCESS

Reviewing the literature in the previous section, the following has become evident:

- Lean design stage should produce designs that are construction and procurement-driven;
- Design-uncertainties should be dealt up-front for both standardized and customized designs;
- Optimization should be pursued for both product and process design having the project level in mind;
- Design and decision-making processes are complementary and they can be streamlined with BIM;
- BIM is a decision-support tool enabling both Lean and Agile principles to design;
- Agile enterprises utilize IG&C link inside PDSO cycle for deploying existing repertoires of the action based on a range of standardized designs reducing the decision cycle time, while all other companies have to create new repertoires of the action before being able to utilize such an IG&C link;
- Orientation step is the critical step inside the decision-making process;
- Rigid bus system design is a typical example of an iterative process.

The concept model presented on Figure 11 takes into account requirements to include procurability and constructability up-front in the design process, before undertaking a quest for optimization of the functional design. Once optimized and conforming to all project requirements, the functional design is confirmed before its components are ready to be procured and henceforth installed / constructed.

Giving a timely input to design engineers up-front, the following is argued:

- Variation in manufacturing variables is reduced through an early identification of suppliers (perspective of procurability);
- Variation in design controllable variables is reduced through an early incorporation of principles of constructability (which may or may not be grounded into principles of standardization);
- Reduction in variation in both manufacturing and design controllable variables reduces the total number of technical solutions (design alternatives) of the acceptable performance;
- The reduced total number of design alternatives with acceptable performance makes the identification of a best solution easier among the rest based on designer's preferences.

Having integrated calculations incorporated into BIM, the following is argued:

- Time required to single out the best solution is reduced;
- Time required to verify the best solution is reduced;
- Time required to verify any solution is reduced.

While integrated calculations with BIM contribute to agility through speeding up of the verification process by automation and to the selection of an optimized solution from the perspective of the design, lean principles contribute to the time reduction through a filtration of numerous design alternatives by focusing on best suited ones when observed from the project level. A question can be asked regarding possible differences in cycling within a PDSO cycle between an Agile enterprise and other enterprises.

Would such differences be grounded in the standardization and customization? And if they are, how these differences are manifested from a perspective of a decision-making process? What stages of the decision-making process contribute to the final streamlining of a decision-making process? Subsequently, how does this relate to the rigid busbar system design process and from the context of BIM? Answers to these questions shall be put forward by observing *modus operandi* of an Agile Utility as presented inside section 2.4 of this paper, in contrast to the usability test performed on the rigid busbar system design falling under the category of a customized design from the company's perspective.

## TUBULAR BUSBAR SYSTEM DESIGN EXAMPLE FROM EL CHAPARRAL PROJECT

The Company ongoing project consists of a 115 kV switching station, El Chaparral, as a greenfield investment and of a 115 kV substation, 15 de Septiembre, as a brownfield investment, both in El Salvador. Both stations are of breaker-and-a-half arrangement.

Some of client's initial design requirements relating to the busbar system of El Chaparral station were ambiguous in regards to:

- Basic Insulation Level (BIL) between 550 kV and 650 kV, representing a parallel requirement for both highest voltage for equipment of 123 kV and 145 kV respectively;
- Aluminum rigid tube properties as Standard Pipe Size (SPS) 3.5 inch was stated but with no other defined requirements relating to its schedule type (outer radius and wall thickness), nor related to alloy type.

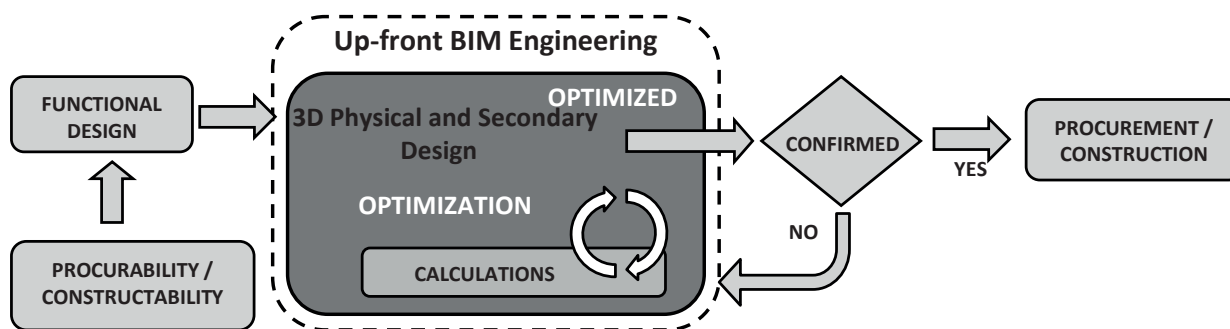


Figure 11. Upgraded concept of Efficient BIM Engineering – Integrated Calculations with timely input regarding procurability / constructability fed up-front

Form a perspective of refurbishment of existing station, 15 de Septiembre, not directly related to the busbar system, following ambiguities were related to:

- A new rigid tube to be installed between two existing 115 kV disconnectors required a rigid tube SPS 2.5 inch, schedule 40 of alloy 6063-T6 type, while electrical DC resistance @ 20°C parameter stated was referring to a SPS 3 inch, schedule 80, alloy 6061-T6 tube;
- No initial requirements for post insulators were stated. However, as existing steel gantries were initially dimensioned as not being able to receive additional gravitational loads of line traps, each new line trap had to be installed on pedestal and supported with additional steel adapter installed between tops of two post insulators. The existing rigid tube goes between these two post insulators slightly beneath the bottom of such a steel adapter while satisfying the minimal phase-to-ground voltage clearance towards the top of the steel support supporting this entire assembly. This solution is depicted in Figure 12. b).

The rigid buswork system at El Chaparral switching station supports currently two diameters and it is depicted in Figure 12.a).

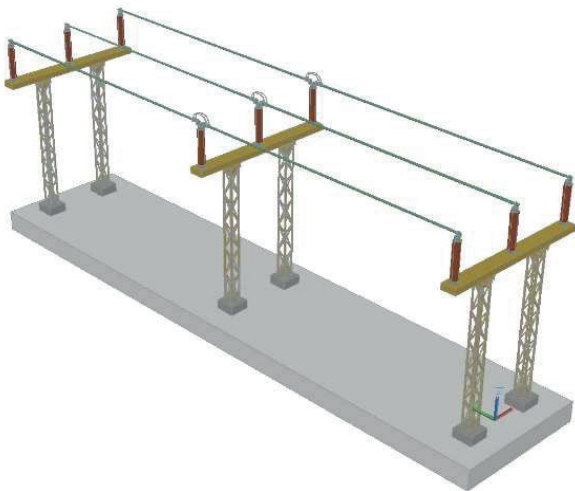


Figure 12. (a) Isometric view of the rigid tubular buswork system, (b) Tubular rigid conductor installed between two disconnectors and going in-between two post insulators for line trap installation

Other atypical client's requirement were related to:

- Standardization of equipment / materials between both stations;
- Steel structure designs to follow the foundation design, as foundations were previously designed by one of Client's subcontractor.

Project requirements were related mostly to procurability of rigid tube

conductors according to ANSI H35.2 standard, as suppliers failed to provide exact specifications especially regarding the value of electrical DC resistance @ 20°C parameter. Encountered engineering challenges were related to:

- Inability to timely define procurability of tubular conductors early in the design stage;
- Designing both stations in parallel with definition regarding the installation of line traps and eventual usage of post insulators still lagging behind the design of the buswork system;
- First time dealing with IEEE 605-2008 standard, as all calculations were conducted manually;
- Resolution of the requirement stating BIL 650 kV over 550 kV, thus influencing the buswork system as the tube conductor centerline-to-ground height has increased;
- Downstream steel support engineering required timely inputs for their part of engineering in order to fit in to the previously locked solution for the foundation design.

All of these requirements had put a great deal of pressure on the electrical design engineer (representing up-stream engineering) to make timely decisions in a short period of time whilst limited information of high levels of uncertainty at engineers' disposal. Upstream engineering thus had to be conducted by observing multiple "what-if" scenarios involving calculations and analyses as a part of the multi-iterative design process, before relevant information could be passed downstream.

During upstream engineering decisions were made by following Lean principles of optimizing the project and not its piece, and by ensuring decisions once made are never revisited again from the upstream engineering standpoint:

- Type TR-289 post insulators were specified instead of type TR-286 at both stations, as requirement for BIL 650 kV ultimately prevailed over BIL 550 kV,
- Type TR-288 post insulators were discarded as a solution due a lesser cantilever strength when compared to type TR-286, as type TR-286 post insulators were a strict tender requirement;
- Upgraded version of type TR-289 post insulators were specified with regards to greater permissible tensile, torsion and compression forces;
- All rigid tubular conductors were defined as SPS 3.5 inch, schedule 40, alloy type 6063-T6 over alloy type 6061-T6 due to better volume electrical conductivity at 20°C percent IACS;
- Volume electrical conductivity at 20°C percent IACS for alloy type 6063-T6 inside calculations was fixed at the typical value of 53 as according to IEEE 605-2008, rather than applying allowed value of 55 to be utilized, as allowed by NEMA standard [74];
- Damping rope due to Aeolian vibration was specified on an entire span length, instead on only its two thirds, and of type procurable falling into weight range advised by IEEE 605-2008;
- Clamps / fittings with current links were specified supporting busbar expandability through single spans, therefore concept of continuous busbars was not followed.

In essence, these decisions made aimed at worst case scenario due to weights and forces transferred onto steel structures, in order to pass downstream batches of information relevant for the steel structure design, all for the purpose of both minimizing number of iterations both upstream and downstream, but also for streamlining downstream engineering process. However, even though design variables of span length and phase-to-phase distance (initially already supporting a value of 2.44 meters based on BIL 650 kV as according to [79], [80]) were locked, that still has not relieved design requirement to satisfy all constraints as indicated inside Figure 10., thus requiring exploration of several alternatives including calculations before turning to the validation of selection for both equipment and materials inside the buswork system. Conducting these calculations and generation of subsequent drawings manually proved to be an undertaking wasting engineering resources. Solution for streamlining both the design process and decision-making process has been sought in the meantime by the company, and by following current industry trends, company has acquired "primtech" solution for the smart substation design which was later utilized on entire HV equipment on a station including verification of results on busbar conductor selection as well. "Primtech's" integrated calculations were conducted according to IEC 60865-1 in which the accuracy of calculations has been previously already established. Obtained results confirmed that our designs according to IEEE 605-2008 were on the safe side of the calculation. The most important is that calculations were per-

formed much faster as being automated, thus enabling a faster selection of the best / optimal solution.

## DISCUSSION

Drawing on the problem statement brought forward inside Section 3, example of the *modus operandi* of an Agile Utility defined in Section 2.4, and on the described usability test set forth in Section 4 of this paper, this section presents a discussion about relevant questions asked in Section 3 from a perspective of a PDSO cycle.

Agile Utilities are able to use existing repertoires of action skipping the Decide stage through standardized layouts, answering the question whether the current design is the best solution or not. This path is given with blue color inside the Figure 13. All non-Agile enterprises and Agile Utilities dealing with innovative / customized designs must follow an entire sequence from Observe to Act marked with red arrows. In all cases, Act step cannot be skipped as it is related to undertaking of analysis / calculations as a prerequisite for a solution capture and justification.

New repertoires of action are created by cycling within a bigger loop between Observe step and Act step through feedback #2 with possibility of several iterations to be conducted by cycling through smaller loop between Observe and Decide through feedback #1. Once new repertoire is defined as the best solution under required conditions and it is verified through running analysis / calculations, such a solution is saved as a 3D BIM model for future knowledge reuse. Saving a solution as a 3D model applies also to each new reused standardized solution stemming from IG&C link.

Figure 13. presents a new conceptual model of a PDSO cycle based on the depicted one in Figure 8.

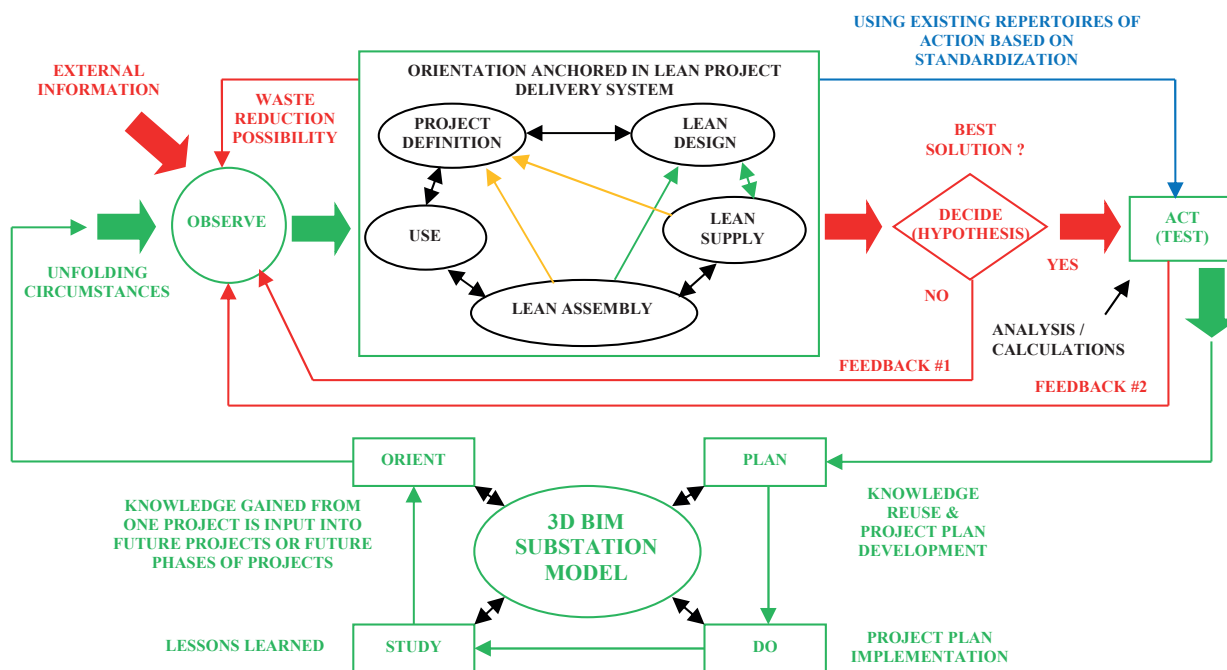


Figure 13. PDSO cycle with indicated differences between an Agile and non-Agile enterprise in respect to the design process based on utilization of BIM models, as adapted from Figure 8.

The Orient step is based on five triads of LPDS. The Lean Design is impacted by the Lean Supply through procurability, and by the Lean Assembly through constructability. These influences are marked with green arrows inside the Orient step. Same can be applied to the Project Definition step of LPDS as indicated with orange arrows. The Orient step as such, and if based on LPDS, enables pro-active search for waste reduction possibilities during the Observe step. The Observe step enables a correlation of design requirements and constraints with project requirements. While design requirements and constraints are fed from the Orient step of PDSO cycle through Unfolding Circumstances, the input enabling constant correlation with project level is fed through External Information input into Observe.

As Figure 13. is defined from a design engineer's perspective, the External information input is a direct correlation to project management through

which up-front project related information is being fed. Elements marked with the green color belong to both paths of the repertoire definition / usage.

Streamlining of a decision-making process is conducted through all steps of OODA loop combined with a 3D BIM model as a heart of a PDSO cycle: the Observe step through utilization of the Lean principles, and for the Decide and Act steps through agility due to integrated calculations. The prerequisite for both is a 3D BIM model as a knowledge repository.

## CONCLUSION

During Plan, Do and Study steps of a PDSO cycle, knowledge from previous project flows into the new project, meaning that design variables and constraints relevant for buswork design are taken from previous projects as relevant ones during the first iteration. Up-front input must be given from project management level regarding availability of materials / equipment that impact final buswork design. Procurability and constructability concepts must be taken into an account during the design stage. This reduces the total number of alternative solutions, thus faster and more accurate identification of a best optimal solution from a project level is supported. Reduction in number of iterations reduces the number of engineering man-hours required. Through usage of software with integrated calculations, verification of design solutions is conducted much faster and more accurate. Streamlined design process has a direct impact on streamlining of an engineering decision-making process. Streamlined and more accurate information flow is a key for streamlining the engineering decision-making process.

## RECOMMENDATIONS

Future papers leaning on this topic could relate to the decision-making for the design of other switchgear parts inside the power substation. Also, future papers could relate to an extension of 3D modeling with BIM in regards to the construction sequencing through utilization of four-dimensional (4D) BIM models (3D space + time), and / or utilization of five-dimensional (5D) BIM models involving 3D space + time + cost as additional dimensions, thus examining the engineering decision-making process from both levels of overall project optimization and design solution optimization.

## ACKNOWLEDGEMENTS

It is often believed that tender requirements correlate fully to client's requirements. However, such a belief is a mistake. Unless tender requirements are fully unambiguous, the client is more likely to hint what it does not want

## BIBLIOGRAPHY

- [1] International Energy Agency. "World Energy Investment Outlook 2013", Special Report, 2014.
- [2] McDonnell Group. "2014 Global Utility Evolution", Benchmark Study, 2014.
- [3] Working Group C1.25 CIGRE. "Asset Management Decision Making Using Different Risk Assessment Methodologies", Technical brochure 541, June 2013.
- [4] M. Hinow. "Genetic Algorithm based Methodology for Optimization of Innovative Switchgear Design" (IEEE International Symposium on Electrical Insulation 2008, June 2008, Paper B31, pages 437-440).
- [5] M. Hinow, M. Waldron, L. Muller, H. Aeschbach & K. Pohl. "Substation Life Cycle Cost Management Supported by Stochastic Optimization Algorithm" (CIGRE Session 2008, August 2008, Paper B3-103, pages 1-9).
- [6] G. Balzer & C. Neumann. "Asset Simulation and Life Cycle Assessment for Gas Insulated Substation" (CIGRE 2011 Recife Symposium, April 2011, Paper 87, pages 1-10).
- [7] Working Group B3.03 CIGRE. "Guidelines to an Optimized Approach to the Renewal of Existing Air Insulated Substations", Technical brochure 300, August 2006.
- [8] L. Willis & R. E. Brown. Substation Asset Management, in: J. D. McDonald, ed. *Electric Power Substations Engineering*, 2<sup>nd</sup> edition, CRC Press, chapter 19, 2007.
- [9] National Academy of Sciences. "Theoretical Foundations for Decision Making in Engineering Design", 2001, National Academy Press.
- [10] G. A. Hazelrigg. Fundamentals of Decision Making for Engineering Design and Systems Engineering, 2012, self-published by Dr. George Hazelrigg Jr.
- [11] K. Grebici, Y. M. Goh & C. McMahon. "Uncertainty and risk reduction in engineering design embodiment process" (International Design Conference – Design 2008, May 2008, pages 143-156).
- [12] P. Nowak, M. Ksaizek, M. Draps & J. Zawistowski. "Decision Making with use of Building Information Modeling" (Procedia Engineering, Vol. 153, 2016, pages 519-526).
- [13] A. Floros Phelps. The Collective Potential: A Holistic Approach to Managing Information Flow in Collaborative Design and Construction Environments, February 2012, Turning Point Press.
- [14] Accenture. "Developing Strategies for the Effective Delivery of Capital Projects – Accenture global survey of the energy industry", Report, 2012.
- [15] I. Xenakis & A. Arnellos. "Reducing Uncertainty in the Design Process: The Role of Aesthetics" (Proceedings of 8<sup>th</sup> International Design and Emotion Conference, September 2016, pages 1-8).
- [16] V. L. Mitchell & B. R. Nault. "Cooperative Planning, Uncertainty, and Managerial Control in Concurrent Design" (Management Science, Vol. 53, No. 3, March 2007, pages 375-389).
- [17] K. Samset. Projects, Their Quality at Entry and Challenges in the Front-end Phase, in: T. M. Williams et al., eds. *Making Essential Choices with Scant Information: Front-End Decision Making in Major Projects*, Palgrave MacMillan, pages 18-37, 2009.
- [18] R. N. Anderson, A. Boulanger, J. A. Johnson & A. Kressner. Computer-Aided Lean Management for the Energy Industry, 2008, PennWell.
- [19] R. M. Patty & M. A. Denton. The End of Project Overruns: Lean and Beyond for Engineering, Procurement and Construction, 2010, Universal-Publishers.
- [20] A. R. Rumane. Quality Tools for Managing Construction Projects, 2013, CRC Press.
- [21] L. H. Forbes & S. M. Ahmed. Modern Construction: Lean Project Delivery and Integrated Practices, 2011, CRC Press.
- [22] G. Ballard & G. A. Howell. "Lean project management" (Building Research & Information, Vol. 31, No. 1, 2003, pages 1-15).
- [23] G. Ballard, I. D. Tommelein, L. Koskela & G. A. Howell. Lean construction tools and techniques, in: R. Best & G. de Valence, eds. *Design and Construction: Building in Value*, Butterworth-Heinemann, pages 227-255, 2002.
- [24] M. E. Roos & K. Kallis. Building "Constructability" into the Design, in: A. D. Pugh, ed. *Proceeding of the Electrical Transmission and Substation Structures Conference 2012: Solutions to Building the Grid of Tomorrow*, ASCE, pages 323-335, November 2012.
- [25] K. T. Clebak Jr, B. A. Nelson, B. Shvartsberg & J. Solinski. "Federal square 138/4 kV substation as an example of modern distribution substation constructed on a design/build basis" (Proceedings of the 33<sup>rd</sup> Annual PMI Seminars, October 2001).
- [26] S. Rajendran. Constructability Review Process – A Summary of Literature, in: J. A. Gambatese et al., eds. *Constructability: Concepts and Practice*, ASCE, pages 6-25, 2007.
- [27] J. M. Kamara, C. J. Anumba & N. F. O. Ebuomwan. Capturing client requirements in construction projects, 2002, Thomas Telford.
- [28] P. MacLeamy. "Collaboration, integrated information and the project lifecycle in building design, construction and operation", The Construction Users Roundtable (CURT), White Paper 1202, August 2004.
- [29] Working Group B3.11 CIGRE. "Combining Innovation with Standardization", Technical brochure 389, August 2009.
- [30] S. Nekoufar & A. Karim. "Lean Project Management in Large Scale Industrial Project via Standardization" (Project Perspectives 2011, Vol. 33, IPMA, pages 72-77).
- [31] B. Shvartsberg. "PSE&G Howell Street substation – the example of a successful turn-key utility project" (Proceedings of the PMI Global Congress, October 2008).
- [32] G. Wolf. "Substation Design in the Third Dimension" (Transmission & Distribution World Magazine, April 2012, pages 28-34).
- [33] Y. Hatamura. Decision-Making in Engineering Design, 2006, Springer.
- [34] J. K. Yates. Productivity Improvement for Construction and Engineering: Implementing Programs That Save Money and Time, 2014, ASCE Press.
- [35] Z. Stojković. Computer-Aided Design in Power Engineering: Application of Software Tools, 2012, Springer / Academic Mind.
- [36] M. Sun & R. Howard. Understanding I. T. in Construction, 2004, Spon Press.
- [37] R. Dove. "Enterprise Agility – Managing Risk with Agility", February 2005, pages 1-3.
- [38] L. D. Helwig. "Automating Substation Design in Times of Extreme Load Growth" (DistribUTECH 2005 Conference & Exhibition, January 2005, pages 1-9).
- [39] S. Sheffield. Custom Software Development: Automating Transmission Line Design Processes for Improved Efficiency and Accuracy, in: R. E. Nickerson, ed. *Electrical Transmission Line and Substation Structures: Structural Reliability in a Changing World*, ASCE, pages 298-303, 2007.
- [40] J. Quintana & E. Mendoza. 3D virtual models applied in power substation projects, in: *15<sup>th</sup> International Conference on Intelligent Systems Applications to Power Systems ISAP 2009*, IEEE, pages 616-618, 2010.
- [41] E. Islas Perez, J. Bahena Rada, J. Romero Lima & M. Molina Marin. Design and Cost Estimation of Electrical Substations Based on Three-Dimensional Building Blocks, in: G. Bebis et al., eds. *Advances in Visual Computing: 6<sup>th</sup> International Symposium on Visual Computing, Part III*, Springer, pages 574-583, 2010.
- [42] M. Lambert. "Computer Aided Substation Design – Why 3D Modelling?" (DistribUTECH 2005 Conference & Exhibition, January 2005, pages 1-5).
- [43] S. Lamothe & P. Graveline. "3D Substation Design: Better, Easier, Faster" (CIGRE Canada Conference on Power Systems 2009, October 2009, Paper #132, pages 1-6).
- [44] S. Lamothe & P. Graveline. "Advances in 3D Substation Design at Hydro-Quebec" (CIGRE Canada Conference on Power Systems 2008, October 2008, Paper #508, pages 1-6).
- [45] G. Lingner. "3D Engineering of High Voltage Substations" (IET Substation Technology Europe, October 2010, pages 1-7).
- [46] D. R. Lemelin, C. Bege, C. Benavides, C. Lacroix & Y. Drolet. 3D Automated Design of Substations, in: M. W. Vogt, ed. *Proceeding of the Electrical Transmission and Substation Structures Conference 2009: Technology for the Next Generation*, ASCE, pages 153-160, November 2009.
- [47] J. Correa & J. Garcia. "Software for optimization and time reduction in substation design, using BIM Technologies, advanced information systems and knowledge management" (CIGRE Session 2014, August 2014, Paper B3-101, pages 1-8).
- [48] The Associated General Contractors of America. "The Contractor's Guide to BIM", 1<sup>st</sup> edition, 2006.
- [49] U.S. Army Corps of Engineers. "Building Information Modeling (BIM): A Road Map for Implementation to Support MILCON Transformation and Civil Works Projects within the U.S. Army Corps of Engineers", October 2006.
- [50] S. Heuser, W. Eyrich & M. Kokoruš. "Smart substation information model – challenges in the development of a Building Information Modeling (BIM) based software for substation design" (CIGRE International Colloquium "Building smarter substations", November 2016, Paper 106, pages 1-12).
- [51] Roland Berger. "Building material industry potential upsides in an uncertain market: North America building materials winner and industry outlook", Report, August 2017.
- [52] Roland Berger. "Turning point for the construction industry: The disruptive impact of Building Information Modeling (BIM)", Report, September 2017.
- [53] S. Heuser, W. Eyrich & M. Kokoruš. "Optimization of effort and cost structures in substation design using a 3D substation engineering software with integrated design calculations" (17<sup>th</sup> Ibero American Regional Council of CIGRE-RIAC, May 2017, pages 1-8).
- [54] M. Kokoruš, W. Eyrich & R. Gačanović. "Implementation of Building Information Modelling (BIM) process in substation design software to increase design quality" (CIGRE Session 2016, August 2016, Paper B3-209, pages 1-10).
- [55] Accenture. "Building for Success", Report, 2017.
- [56] C. Berggren, J. Soderlund & C. Anderson. "Clients, Contractors, and Consultants: The Consequences of Organizational Fragmentation in Contemporary Project Environments" (Project Management Journal, Vol. 132, No. 3, September 2001, pages 39-48).
- [57] R. Dove. "Agile and Lean SE: Complimentary and Contradictory Relationship" (Lean and Agile Systems Engineering Conference, January 2014, pages 1-53).
- [58] R. Dove. "Utility Agility – An Oxymoron?" (UtiliPoint's Client Conference, August 2005, pages 1-46).
- [59] B. Baker. "Timely decisions" (PM Network, Vol. 19, No. 6, October 1996, pages 20-21).
- [60] T. Kuusisto, R. Kuusisto & L. Armistead. System Approach to Information Operati-

- ons, in: A. Jones, ed. *Proceedings of the 3<sup>rd</sup> European Conference on Information Warfare and Security*, Academic Conferences Limited, pages 231-239, 2004.
- [61] T. Grant & B. Kooter. "Comparing OODA & other models as Operational View C2 Architecture" (Proceedings of the 10<sup>th</sup> International Command and Control Research Technology Symposium: The Future of C2, June 2005, Paper 196, pages 1-14).
- [62] T. S. Abdelhamid, D. Schafer, T. Mrzowski, V. Jayaraman, G. A. Howell & M. A. El-Gafy. Working Through Unforeseen Uncertainties Using the OODA Loop: An Approach for Self-Managed Construction Teams, in: Y. Cupeus & E. Hirota, eds. *Proceedings of the 17<sup>th</sup> Annual Conference of the International Group for Lean Construction*, Chien-Ho Ko, pages 573-582, 2009.
- [63] J. Owen, F. Burstein & W. P. Hall. Knowledge Reuse in Project Management, in: H. Lingner *et al.*, eds. *Constructing the Infrastructure for the Knowledge Economy*, Kluwer Academic / Plenum Publishers, pages 443-454, 2004.
- [64] C. Richards. "Boyd's OODA Loop (It's Not What You Think)", March 2012.
- [65] R. Wilson & H. Younis. Business Strategies for Electrical Infrastructure Engineering: Capital Project Implementation, 2013, IGI Global.
- [66] G. Wolf & G. Garcia. "The "Point and Click" Distribution Substation" (Transmission & Distribution World Magazine, March 1999, pages 90-100).
- [67] G. Garcia. "The Design Tool of the Future - Today" (Transmission & Distribution World Magazine, November 2017, pages 21-26).
- [68] G. Wolf. "The Point-and-Click Substation Matures" (Transmission & Distribution World Magazine, November 2004, pages 26-32).
- [69] G. Wolf. "Wind Power" (Transmission & Distribution World Magazine, November 2003, pages 20-25).
- [70] American Society of Civil Engineers. Substation structure design guide: ASCE manuals and reports on engineering practice no. 113, 2008, ASCE.
- [71] G. J. Anders, G. L. Ford, M. Vainberg, S. J. Arnot & M. D. Germani. "Optimization of Tubular Rigid Bus Design" (IEEE Transactions on Power Delivery, Vol. 7, No. 3, July 1992, pages 1188-1195).
- [72] USDA / RUS. "Design Guide for Rural Substations", RUS Bulletin 1724E-300, June 2001.
- [73] Working Group 23.03 CIGRE. "General Guidelines for the Design of Outdoor AC Substations", Technical brochure 161, August 2000.
- [74] The Aluminum Association. Aluminum Electrical Conductor Handbook, 3<sup>rd</sup> edition, November 1989, The Aluminum Association.
- [75] IEEE 605-2008. "Guide for Bus Design in Air Insulated Substations", December 2008.
- [76] Working Group B3.23 CIGRE. "Substation Uprating and Upgrading", Technical brochure 532, April 2013.
- [77] K. Malmedal & J. Wendelburg. Substation Bus Design: Current Methods Compared with Field Results, in: M. W. Vogt, ed. *Proceeding of the Electrical Transmission and Substation Structures Conference 2009: Technology for the Next Generation*, ASCE, pages 143-152, November 2009.
- [78] B. Sedaghat & A. Nabatchian. "Engineering Method for Calculation of Short-Circuit Mechanical Effects in HV Substations with A-frame Arrangements Using FEM" (CIGRE Canada Conference on Power Systems 2011, September 2011, Paper 127, pages 1-7).
- [79] ANSI C37.32-2002. "American National Standard for High Voltage Switches, Bus Supports, and Accessories Schedules of Preferred Ratings, Construction Guidelines, and Specifications", 2003.
- [80] NEMA SG6-2000. "Power Switching Equipment", 2001.

**IGOR IVANKOVIĆ**

HOPS  
CROATIA

**DOMAGOJ PEHARDA**

KONČAR-KET  
CROATIA

**DAMIR NOVOSEL**

QUANTA TECHNOLOGY  
USA

**KSENIJA ŽUBRINIĆ-KOSTOVIĆ**

HOPS  
CROATIA

**ANA KEKELJ**

HOPS  
CROATIA

# Smart grid substation equipment maintenance management functionality based on control center SCADA data

## SUMMARY

Classic approach to preventive maintenance of equipment in power system substations was based on periodical maintenance according to regulations and best practices recommended by vendors. SCADA system in HOPS is used primary for real-time monitoring and control of the equipment in substations. Real time data available in SCADA databases contain useful information for substation maintenance optimization based on operational conditions. Malfunctions and failures in the substations are monitored via SCADA system. Analyses of these data can be used to evaluate maintenance strategy and plan the reconstructions and replacement of the equipment.

This article presents current maintenance management approach in HOPS, which is the only transmission system operator in Croatia, and possible improvements in efficiency of equipment maintenance using SCADA data. Prerequisite for the analyses of these kinds of data is standardization and unification of information names and structures. HOPS put a lot of effort in standardization of SCADA data during last refurbishment of control centers. Use of SCADA data for analysis drives the need for standardization and vice versa.

Examples of statistical analyses of the SCADA data are done on multiple levels. High level analyses is used to provide the global overview of the real time data. It can point to suspicious information that require detailed analyses. The signals that appear often in the list can indicate that there is a problem in the primary equipment, monitoring system or alarm configuration. Low level analyses can be done on target information important for equipment maintenance. In this paper some low level analyses are presented for switching equipment, transformer lifetime, equipment in operation, and tap changer operation. An analysis is made for number of switching operations for breakers and disconnectors in different operational conditions. Preventive maintenance should be done based on number of switching in normal operations and even more often for breakers that are often interrupting fault current. SCADA data can be used for availability of the equipment and duration of failures thus providing valuable information to managers. An analysis on RTU communication availability is shown.

## KEYWORDS

SCADA data – Equipment maintenance – Maintenance management – Smart grid – SCADA data standardization – Analyzing alarms and events – Analyzing measurement – Key performance indices.

# INTRODUCTION

Transmission System Operator Company (HOPS) has two major criteria for defining company efficiency, technical and economic criteria. New smart grid and information-based applications can be suitable to create, trace and analyze those criteria [1][2]. Maintenance management for substation equipment is crucial one in accomplishing both technical and economic efficiency criteria. Former periodic maintenance process can be enhanced towards more preventive and condition based maintenance. To make this shift possible it is important to collect and correlate data from substations and direct consequence of this process is gathering of substantial amount of data in control center [3].

Main role of control centers is monitoring and control the power system but beside that, modern centers should have new additional roles and one of these roles will be smart grid platform for maintenance functionality in TSO. To achieve that, station SCADA systems gather as much data as possible from each piece of substation equipment and then that data is being forwarded into control centers' SCADA systems. Almost all acquired data is stored in central utility data warehouse at TSO. Smart grid applications should process those data in centers for maintenance purposes assisting preventive and conditions based management for substations equipment maintenances.

## DATA POINTS AVAILABLE IN CONTROL CENTRE SCADA SYSTEM

HOPS is only transmission system operator in Croatia and is responsible for operation, maintenance and construction of entire high voltage transmission network (400kV, 220kV and 110kV) as presented in figure 1. Peak load of Croatian power system network is 3 GW. Production installed capacity is 4.5 GW. Transmission network is controlled remotely through modern SCADA system. All internal transmission substations and numerous substation in neighboring TSOs are connected to that system

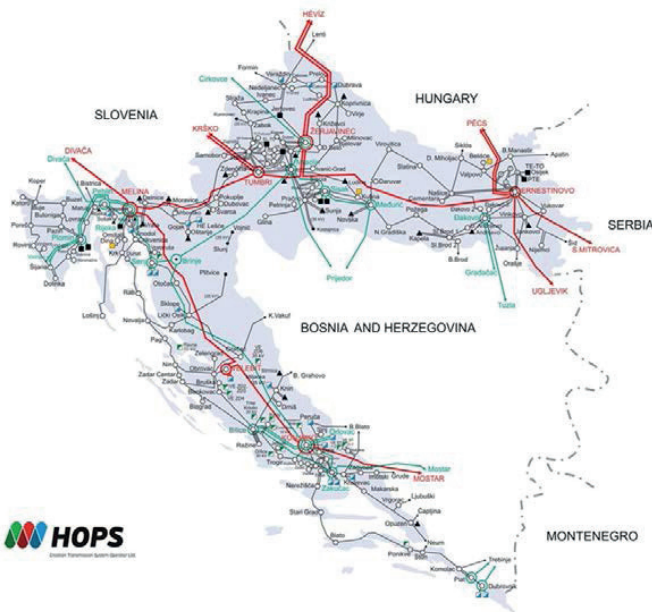


Figure 1. Detail schemes of Croatian transmission network with substations and power plants.

Station computers and RTUs in transmission object collect all local information and transfer most of it to the SCADA in control center. HOPS SCADA aggregate all information in database. General data in SCADA is as follow:

- 185 substations and power plant switchyards on 110, 220 and 400 kV voltage level,
- 84.000 indications,
- 9000 measurements.

SCADA in control center is a fundamental application and it is a source for many others. One of important applications is Energy Management System (EMS). Some general data that described the size of HOPS EMS

model is presented in Table 1.

Table 1. Size of the EMS model.

Region	Station	Sub-net	Bay	Generator	Transformer	Line	Load	Capacitor	Reactor
OSIJEK	25	75	420	3	56	52	50	3	1
RIJEKA	45	123	818	14	106	73	90		
SPLIT	55	174	1198	41	121	90	86		
ZAGREB	60	182	955	28	169	112	145	3	1
<b>Total</b>	<b>185</b>	<b>554</b>	<b>3391</b>	<b>86</b>	<b>452</b>	<b>327</b>	<b>371</b>	<b>6</b>	<b>2</b>

HOPS has been created from four companies that are now four regions within HOPS. Besides historical differences, there are other big differences between regions:

- Geographically differences (lowland, seaside region, mountain region, islands),
- Very different climate,
- Different structure of generation and load,
- Some specifics in operations rules, control and protection equipment.

Each of the transmission region is operated by its own regional control center. Therefore, data in SCADA databases are different. Some of the regional centers took more generalized approach where they send grouped data from substation indicating that there is an error on particular part of the equipment, while other regional centers send detailed data describing the type of the error. This can be shown on example of breaker failure indication. In some regional control centers there is only a group signal named "Breaker failure" while in other regional control centers individual signals like "Loss of SF6" can be found.

Table 2 presents an average number of indication and measurement per equipment in database. Individual number of indications differs based on age of equipment in substations. Newer substations have significantly larger number of information in database.

Table 2. Average number of indications and measurements per equipment.

Voltage	Generator	Capacitor	Reactor	Bus	Transformer	Line
0-110 kV	5,8	17,0	1,1	0,2	9,1	
110 kV	3,0	20,0	86,0	0,4	53,6	95,2
220 kV	1,9			0,5	60,6	50,0
400 kV	3,2		4,7	0,6	28,2	31,1
<b>Total</b>	<b>4,5</b>	<b>18,5</b>	<b>3,8</b>	<b>0,3</b>	<b>45,9</b>	<b>74,7</b>

SCADA database contains real time information for the following equipment:

- Operational data for primary equipment (active and reactive power measurements, current and voltage, switching status, transformer regulating control operation, etc.),
- Protection relay operation data,
- Primary and secondary equipment failures and warnings,
- Communication information (RTUs, switches, SCADA).

EMS system is integrated in SCADA system and contains data on power system equipment operating limits. In addition, EMS uses network model builder for calculating current topological state of the network.

## CURRENT PROCESS FOR PLANNING OF MAINTENANCE AND STATISTICS

ISOHOPS is programming system created in 1993 and last updated in 2011. The main purpose of the system is asset management and maintenance planning based on the HOPS' "Maintenance Rule Book" for the transmission network. It consists of two parts: technical database and maintenance rules. Technical database lists, categorizes and describes all equipment in HOPS' ownership. Maintenance rules proscribe schedules, type of work, authorization and accountability.

Independently another program system "Operating Events Statistics" (OES) monitors the availability of transmission network units over a one-year period. Flowchart for generating OES and collecting data with Yearly

report, which result, is presented on figure 3. Operator in Control Center manually input data in application DOR (Daily Operating Report). Expert for operational analysis validates and checks data and after they are automatically transferred to program and database for OES.

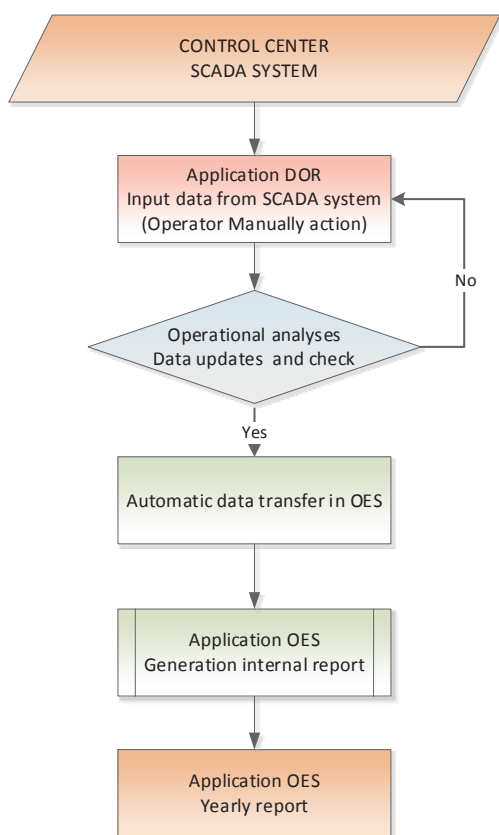


Figure 2. Basic flow chart for creating Operating events statistic (OES) from Daily operating report (DOR).

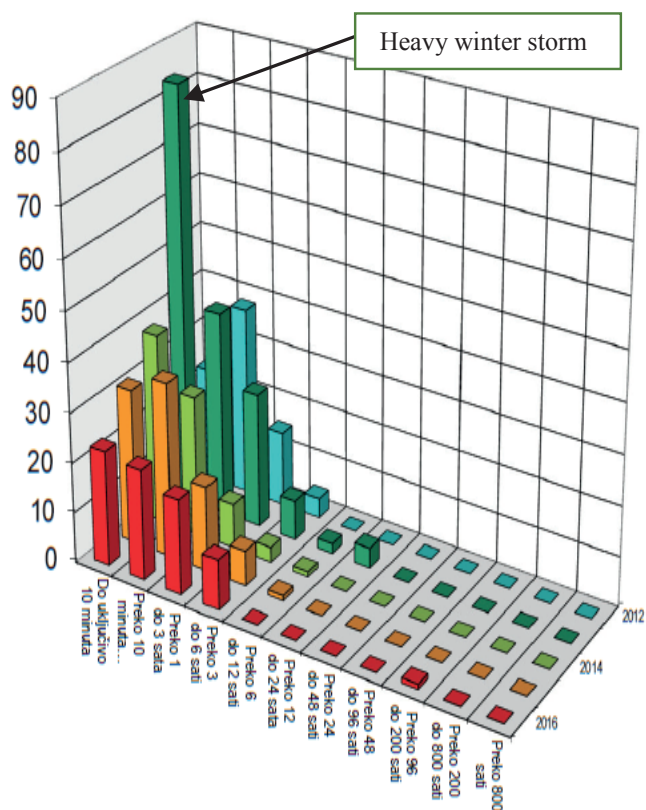


Figure 3. Details of yearly forced outages for Yearly report in period of 2012-2016.

Data collected is used to create a yearly report that consists of equipment statistics e.g. total number of transformers, transmission lines length, forced and planned outages of equipment broken down by various criteria. One of the indicators of company maintenance and business efficiency that derives from the "Operating Events Statistics" is in figure 3, and shows the number of forced outages for one year. The x-axis lists time intervals (up to 10 minutes, over 10 minutes to 1 hour etc.) On axis y forced outages are broken down by years.

Present-day approach to planning of maintenance results from compliance with existing regulation and internal maintenance procedures. Apart from reports on problems found during scheduled maintenance, there is no correlation with actual failure rate.

"Operating Events Statistics" is useful tool for analyzing key performance indicators but since it is compiled as an official yearly report, its use is limited because of lateness of the report and inflexibility of analysis.

Idea is to move more towards conditions based maintenance utilizing data collected in SCADA system in control center. Preventive maintenance, which relies on periodic maintenance work on equipment, can be improved with a new way of using SCADA data. First step is a work to have internal standardization of data point naming in company. Second step is analyses of alarms, events and measurements to create proactive maintenance.

## NEW PROCESS FOR ADVANCED EQUIPMENT MANAGEMENT

### Standardization of data points naming

A great challenge for HOPS has been the standardization of data points in SCADA database. Standardization has been done with utmost dedication and precision especially considering that both primary and secondary equipment in substations are diverse across regions and across time of installation. This affected naming, classification and grouping of signals in station SCADA, and consequently in control center.

Unification began in 2012 with refurbishment of SCADA systems in control centers. Figure 4 shows the number of indications per unique name for each area. Total number of indications per unique name is 14. The result of unifying effort is a catalog of unified process information that has decreased from 6500 unique names to 1500 names recommended for use in 185 stations. That corresponds to around 50 indications per unique name.

Catalog contains many information on each individual processing signal, and point name is a key to get all properties for this signal. Figure 5 shows hierarchical structure, classification and location of indication. For each type of equipment like relay protection, breaker, disconnecter transformer, measurement, process information, auxiliary systems there are point classes (trip, alarm, failure, control etc.). This classification and unique information is good base for operational system analyses. The catalogue contains information of processing of signal, states of signals, place of delivery etc. Also suggested are the addresses according to IEC61850 for SIPROTEC 5 generations. For others types of IED it needs to be further defined [4].

Area name	Number of indications	Number of names	Number of ind. per unique name
NCC_Supervision	42	8	5,3
NCC_Command	8	7	1,1
NCC	3979	164	24,3
RCC OSIJEK	12935	1557	8,3
RCC RIJEKA	19178	1507	12,7
RCC SPLIT	22929	2443	9,4
RCC ZAGREB	23054	2628	8,8
Training	6	3	2,0
<b>Total</b>	<b>82131</b>	<b>5885</b>	<b>14,0</b>

Figure 4. Number of indications per unique name before work on unification.

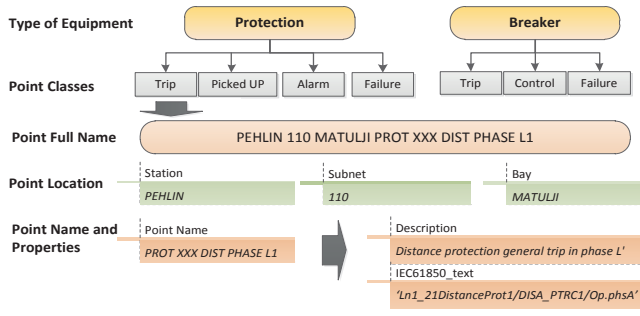


Figure 5. An example of indication classification and location.

Standardized SCADA database can be used for improvements in maintenance process and for monitoring of Key Performance Index (KPI). SCADA database comprise important information on operational state of equipment in substations, diverse malfunctions in power system elements and power system information (alarms, events, measurements, etc.). When smart analytics are applied on raw SCADA data, a lot of useful information can be found and used for improving overall reliability of the system and at the same time optimizing maintenance costs.

## Analyses of number of events per signal and per type of signal

Figure 6 contrasts number of data points in the database with number of events for name/type of indication. Ideal case would be that each bay has the same names/types of indications, which would make comparison and analysis trivial. Figure 6 in lower right corner lists a number of indication names/types that have small number of data points in database but large number of events associated with them. There is continuous work on decreasing these kind of data.

Total number of indications in SCADA system is close to 90.000. In operational use, there are more than 5.500 different names/types. Those large number of signal names/types have historical causes. So for the all refurbishment process and new substations "Catalog of unified process information" is used to implement all signals in station computer and SCADA.

Analysis and reporting work is rather complex and to be effective it is essential to have standardized signal names. Process of standardization is important for itself but is also needed to be carried out for better equipment maintenance management. Without standardization it is impossible to implement advanced management application based on SCADA data in control center.

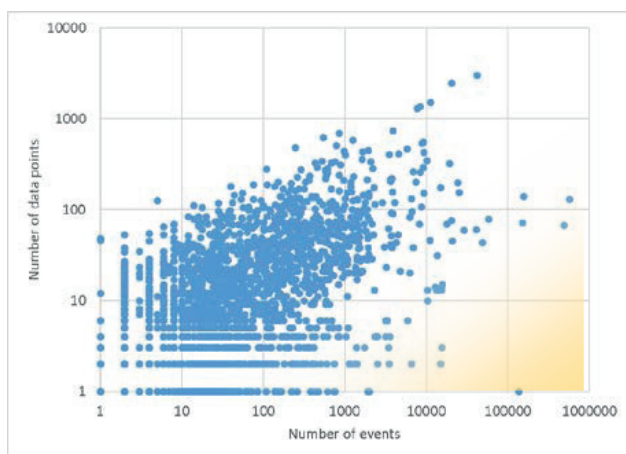


Figure 6. Number of data points in database vs number of events for name/type of indication.

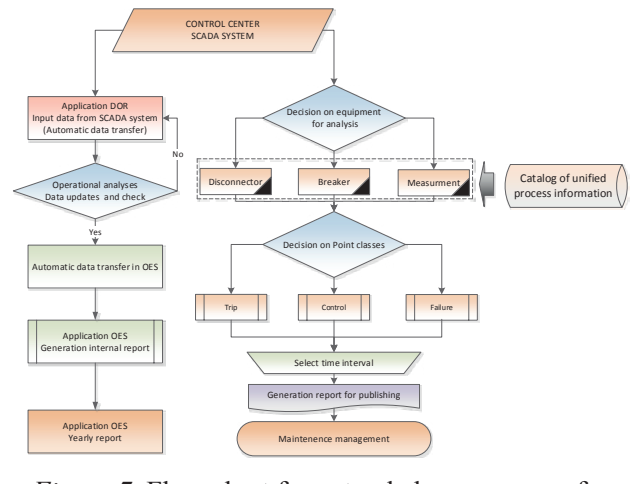


Figure 7. Flow chart for extended new process for maintenance based on SCADA data

## New Process for Maintenance

New process for maintenance relies on SCADA data to adapt planned maintenance schedule to respond to operational state of equipment. Decision on time interval for maintenance schedule is created after analysis of certain groups of data. The flow chart of this decision is on the right side of figure 7.

## ANALYZING ALARMS AND EVENTS

Application deployed at HOPS gathers data from SCADA and correlates it with information from catalog of process information to create analysis and reports for various time periods. Analysis and reports are used for various purposes and one of them is maintenance management.

## Monitoring the operation of switching devices in network

SCADA system monitors 6278 switches in the internal network of HOPS. These switches are not operated with equal frequency. Figure 8 shows a number of switching operations for individual switches, grouped by type of switch (circuit breaker, disconnector and grounder switch), during a period of six months. It is indicative that there are 6278 switches monitored and only 2500 had at least one operation during that time period.

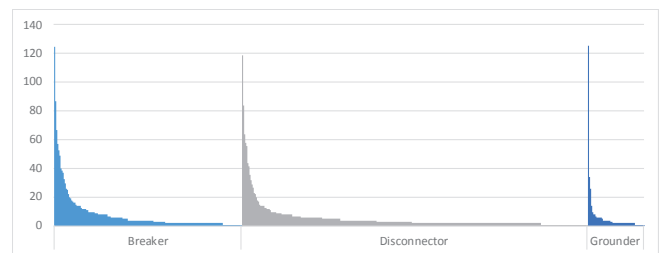


Figure 8. Switching operations for 2500 switches that had at least one switching operation during the period of six months.

Switching operations are one of components of evaluating the condition of the switch. Using the switching operations it is possible to plan proactive maintenance schedules for individual switches.

## Breaker Interrupting Fault Current

Data points are mostly contained in bays that can be topologically assigned to equipment. It is possible to correlate equipment in operation with data coming from data points. For identification of breaker interrupting fault current, it is necessary to determine if protected equipment was in ope-

ration prior to the outage and if they were, a trip protection signal needs also to be associated with breaker interruption.

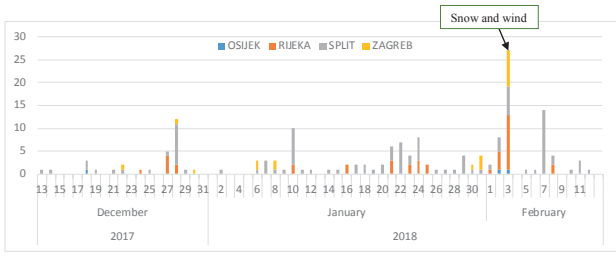


Figure 9. Number of circuit breaker interrupting fault current during period of two months.

Figure 9 shows daily number of breaker interrupting fault current per region for two months. When planning proactive maintenance breakers that interrupted fault current should be checked and appropriate service actions should be performed. Additionally the number of circuit breaker interrupting operational current should be added multiplied by factor determined by supplier of the breaker. Cumulative number of fault current interrupted by breaker is calculated.

### RTU communication

SCADA alarms and events can be also used to trace the efficiency of maintenance and availability of certain part of system. Figure 10 presents an analysis of communication loss alarm that is active in cases when there is no communication to RTU-s, figure on the left shows the number of times communication with RTU was lost, and figure on the right shows the duration of the loss of communication.

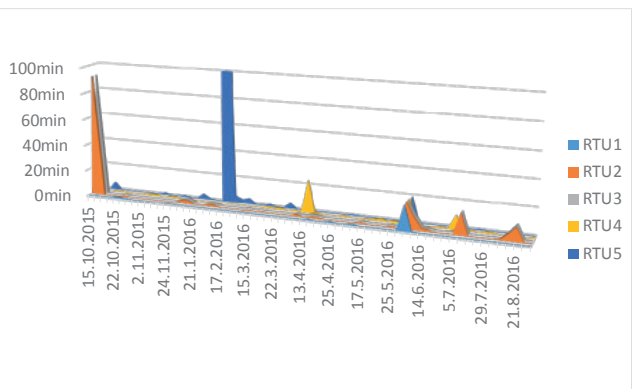
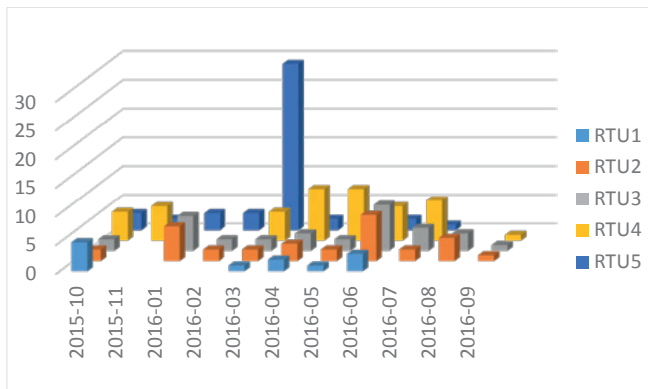


Figure 10. Unavailability of communication to RTUs, number of communication loss event (left), duration of communication loss (right).

Data available in SCADA systems are not sufficient to determine the cause of communication unavailability. Further detail analyses could be done if SCADA data are combined with telecommunication monitoring and asset management systems that can account for planned outages.

## ANALYZING MEASUREMENT VALUES

Transmission system control centers are primarily focused to ensure secure operation and control of a power system. SCADA systems provide continuous supervision of the whole network in real time but not all of this information is stored permanently in an archive. For measurement data this means that it is processed, downsampled and then put in permanent storage according to TSO rules. Minimum time resolution is 2 seconds for crucial data and 10 seconds for non-crucial data. Data is downsampled in other resolutions as well: 1 minute, 15 minute, 1 hour, and 1 day. Different time resolutions are used for different purposes.

This paper does not focus on usual analysis of measurements like calculation of total and peak load and generation of an area, which are usually done for purposes of accounting and reporting. In addition to old way of using measurement data, here is a proposition to use measurement data for asset management and maintenance planning.

### Transformer Measurement Data

Power transformer unit in transmission network is a crucial and expensive element, often unique and hard to replace. All of these are reasons that careful attention must be provided for a transformer during its lifetime. For this purpose transformer monitoring systems are widely used [5]. Transformer monitoring system are often custom made for specific power transformer and have complex specifications and design [6] [7]. Status and key performance indicators are tracked using three major sources of data: current or temperature monitoring [8], overvoltage monitoring and gas analyses. For gas analysis and monitoring of overvoltage inside windings there needs to be specialty equipment inside tank, but current and temperature is often available at SCADA as a normal measurement. The task of monitoring and calculating KPIs of transformers can be shifted to a SCADA system in control center. Almost all of the transformers at transmission system level and at power plants have measurements of at least power or current so they can be monitored, which is very valuable for asset management of the whole transformer fleet. Monitoring using current or power can be extended with other measurements, like oil and winding temperature [9], number of operating hours (days) in a year, number of tap changer operations. An example of information that can be gathered is shown in figure 11. These data can be used for calculating ageing rate of each transformer [10].

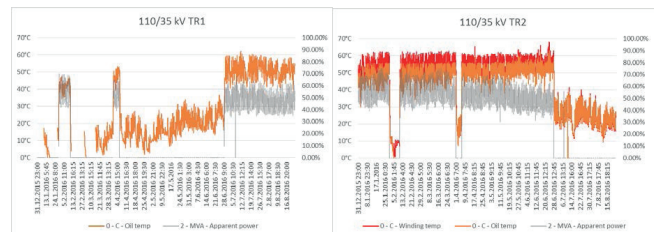


Figure 11. Temperature on left y-axis and power in percentage of rated power on right y-axis for two distribution transformers 110/35 kV in the same station.

On figure 11 charts from two transformers situated in the same station are shown. It can be seen that the transformers are not working in parallel, only one is in operation at a time. Older transformer does not have winding temperature measurement but only oil temperature (left).

### Hours in Operation

For operation and asset management, it is important to know the hours in operation for each equipment. Number of hours in operation can be calculated using energized state or using active power measurement when it is greater than zero. Working hours for transmission equipment during period of 60 winter days is presented in figure 12. In transformer stations, there are usually more than one transformer, and in normal operation only one is energized, which is the reason a lot of transformers have been in operation for less than 100% of the time. Most of the time lines are in operation, which is reflected in very few lines out of service. Shunts are not needed during this time, and none of them were in operation during period in consideration.

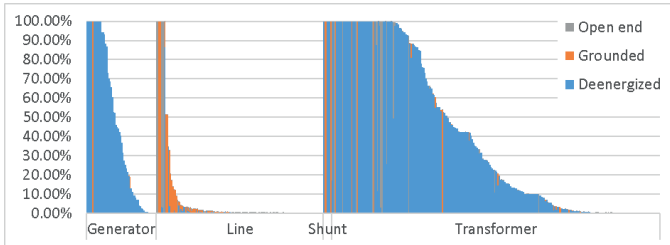


Figure 12. Percentage of hours not in operation of the total period considered.

## Off and on load tap changer operations

Statistics on change of tap positions should be recorded and analyzed because statistically more than third of transformers between 100 kV and 200 kV had failures on tap changing equipment [11]. This also allows for modification of maintenance procedures and optimal transformer maintenance schedule.

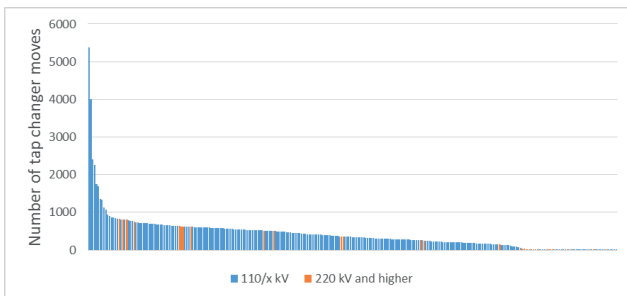


Figure 13. Number of tap changer operations during first 8 months of year 2016 per transformer (281 transformer units).

Using Figure 13, transformers can be classified into three groups. Just a small number of 110/x kV transformers have more than 4 tap changing actions per day (observed in 228 days) which are caused by lack of voltage controllers on some 400/110 kV and 220/110 kV transformers. This figure should indicate where increased maintenance of tap changers is required.

## BIBLIOGRAPHY

- [1] F. Li, W. Qiao, H. Sun, H. Wan, J. Wang, A. Xia, Z. Xu, P. Zhang, "Smart Transmission Grid: Vision and Framework," IEEE Transactions on smart grid, Vol.1, No.2, October, 2010, pp 168-177, doi:10.1109/TSG.2010.2053726.
- [2] N. Baranovic, P. Andersson, I. Ivankovic, K. Zubrinic-Kostovic, D. Peharda, J.E. Larsson, "Experiences from Intelligent Alarm Processing and Decision Support Tools in Smart Grid Transmission Control Centers," 2016 Cigre Session, D2-112.
- [3] R. Candy, J. Taisne, "Advanced Alarm Processing Facilities Installed on Eskom's Energy Management System – IEEE PES Power Africa 2007," Conference and Exposition, Johannesburg, South Africa, 2007.
- [4] J. Simunic, K. Zubrinic-Kostovic, B. Dobras, "Modelling of Information System using Object-Oriented Approach," The 14<sup>th</sup> Mediterranean Electrotechnical Conference, MELECON 2008, pp. 258-263, 5-7 May 2008.
- [5] Y. Han and Y. H. Song, "Condition Monitoring Techniques for Electrical Equipment – A Literature Survey," IEEE Trans. Power Del., vol. 18, no. 1, pp 4-13, Jan. 2003.
- [6] S. Dumitru, H. Lulian, P. Ion, "Compact local system designed for power transformer monitoring-Type Monitra control process" International universities Power Engineering Conference (UPEC), Universitatea Tehnica din Cluj-Napoca, Romania, 02-05 Sep 2014.
- [7] A. C. Leger, P. Laurent, C. Legrand, "On-line power transformer monitoring at Electricite de France" IEEE Porto Power Tech Proceedings, Porto Portugal, 10-13 September 2001.
- [8] E. Aburaghiega, M. E. Farrag, D. M. Hepburn, B. Garcia, "Power Transformer health monitoring: A Shift from off-line to on-line detection" International universities Power Engineering Conference (UPEC), Staffordshire University, UK, 01-04 September 2015
- [9] J. Q. Feng, P. Sun, W. H. Tang, D. P. Buse, Q. H. Wu, Z. Richardson, J. Fitch, "Implementation of a power transformer temperature monitoring system" in proc. International Conference on Power System Technology, PowerCon, Kunming China, 2002.
- [10] D. Peharda, I. Ivanković, N. Jaman, "Using Data from SCADA for Centralized Transformer Monitoring Applications", 4th International Colloquium "Transformer Research and Asset Management", Procedia Engineering, (PROENG\_396604), (1877-7058), (2017).
- [11] Cigré WG A2.37, "Transformer reliability survey", Cigré Technical Brochure no. 642, 2015.

## CONCLUSION

Croatian TSO set up its SCADA system to collect wide range of signals from substation equipment. This is used for the main task for SCADA system of TSO, which is the control of transmission network. Great amount of data in SCADA databases can be used for development of new processes and functions.

New technologies and standardization of SCADA data enables optimized and smarter approach to preventive and proactive maintenance, which is based on actual conditions of equipment by using real time information. Identifying anomalies in SCADA data can find single or series of faulty equipment. Making statistical reports and KPIs is important for measure of maintenance efforts. Goal is to improve the preventive based maintenance process and start using condition based maintenance and proactive maintenance. In first phase creating various reports from those data will be a starting point towards upgrading the maintenance rulebook. Analyses of SCADA data can be used to follow the efficiency of measures taken to improve systems or processes. EMS data combined with SCADA data can be used to extract valuable information on operating conditions of the equipment that can be used to determine if preventive maintenance is necessary or already scheduled maintenance can be postponed without big risks.

Crucial step of the project is standardization and unification of data points of the SCADA database in "Catalog of unified process information". Whole process of data engineering in bay, station computer, and SCADA system have to strictly follow those rules if advanced data analytics is to have good results. Quality of description of data points is directly correlated to the quality of conclusions made by analysis of the SCADA data. On the other hand use of SCADA data raises the quality of information on data points so it is important that cleaning of data points is done at the same time as use of SCADA data for analysis. Catalog should be a living documents requiring continuous work on updating the Catalog.

Next phase and continuous work should be updating the maintenance rulebook with proactive and condition maintenance, with mechanisms in place to have continuous monitoring of the effect of new and old rules on maintenance. Another piece of work is defining the Key performance indices for equipment data. Study has to be done in order to determine the proper values for those indices.

**IGOR IVANKOVIĆ**  
HOPS  
CROATIA

**VLADIMIR TERZIJA**  
UNIVERSITY OF MANCHESTER  
UNITED KINGDOM

**SRDJAN SKOK**  
UNIVERSITY OF RIJEKAY  
CROATIA

# Transmission network angle stability protection based on synchrophasor data in control centre

## SUMMARY

Angle stability appears in many forms in transmission network. There are small active power oscillations which do not endanger the normal operations whereas medium and large oscillations have implications on normal operations. These latter kinds of oscillations in some cases develop in out of step condition, which is dangerous disturbance with serious impact on transmission network and generating units.

Transmission network operator's challenges and obligations are to treat in the right manner angle stability issues in their network. Controlling and protecting network needs to be done in efficient way in order to disconnect disturbance quickly and prevent abnormal network operation without exporting disturbance in surrounding networks.

Synchrophasor measurements in control centre offer a platform, which responds in a new way on angle stability in transmission network. Those measurements which are collected in phasor data concentrators, which is a part of Wide Area Monitoring will be used for creating out of step protection. This is the first step to extended system to Wide Area Monitoring Protecting And Control (WAMPAC).

Paper gives progress of such project in Croatian Transmission Network Operator (HOPS). Firstly, there will be stated motives for development of new out of step protection based on synchrophasor measurements. Some feasibility aspect elaborated with emphasis on communications latency. Furthermore, designed Matlab model for transmission network and protection with small portions of simulations results and analyses presented in paper reveal potential of proposed solutions. This new protection is based on using voltage angles values from phasor data stream in phasor data concentrator.

## KEYWORDS

Angle stability protection – WAMPAC system – Active power oscillations – Out of step protection – Transmission lines protection – Synchrophasor data – Control centre applications – Matlab model.

## INTRODUCTION

Transmission system operator is obliged to constantly maintain angle stability. Deterioration of angle stability caused by disturbances manifests in oscillation of active power and if left unchecked out of step condition could develop [1]. Angle instability appears in time frames varying from very short (few seconds) to medium ones (few minutes). Synchrophasor based applications which run in control centres give TSOs new way of effectively handling and treating those disturbances [2]. Angle stability protection based on synchrophasor data can have alarming and protection functionality. Base for that functionality will be voltage and current synchrophasors data stream collected in control centres.

## Methods for active power oscillations monitoring and protection

Both standard well known and new methods are available as a response to active power oscillations and some of them are already in use while others are only in research phase. A list of basic features of different technical solutions for advanced protection systems is presented in Table 1. Each method has mentioned main issues for usage like a real time protection application.

Table 1. Basic features of out of step protection methods.

Method	Line End Measurement	Wide Area Measurement	Independent from setting process <sup>1</sup>	Real time application	Remarks
Impedance based	✓	✗	✗	✓	Source impedances dependent, Study work phase
Resistance based	✓	✗	✗	✓	Study work phase
Voltage based	✓	✗	✗	✓	Source impedances dependent, Study work phase
Swing voltage/ Speed acceleration criterion based	✓	✗	✗	✓	Voltage on source dependent, study work phase, system reduction (2 machines) approximation
Generator angle based	✓	✗	✓	✓	Availability of generator measurements, communication requirements
WAMPAC system	✓	✓	✓	✓	Communication requirements
Equal area based	✓	✗	✗	✗	Inertia values (H) for generators and parts of the system needed, system reduction, study work phase
Energy function based	✓	✗	✗	✗	Study work phase
Neural network based	✓	✗	✗	✗	Study work phase
Fuzzy logic/ clustering based	✓	✗	✗	✗	Study work phase

<sup>1</sup> Protection setting process is sensitive to network configurations.

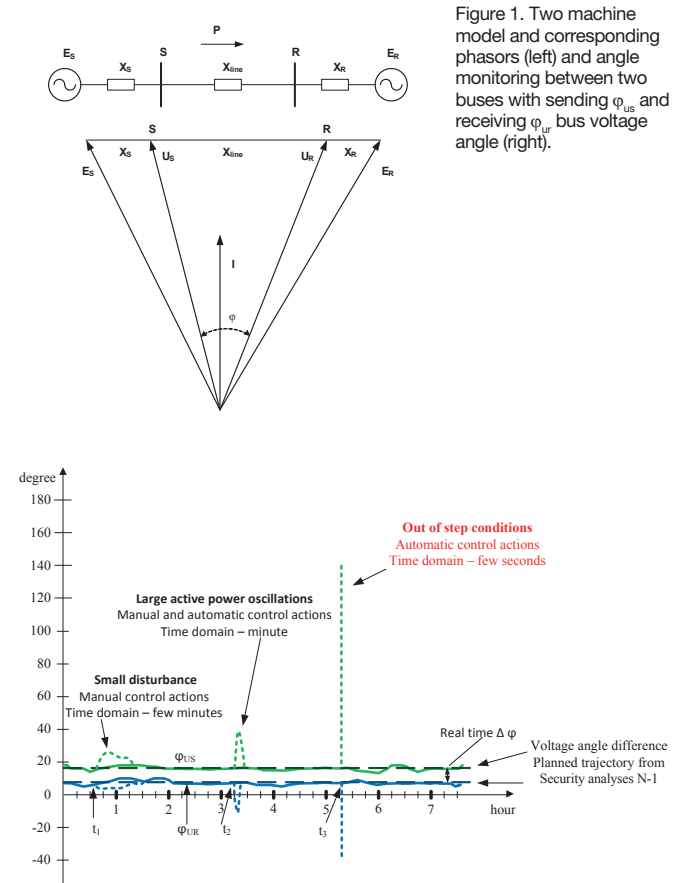
WAMPAC systems are critically dependent on the communication equipment and potential delays. Preliminary evaluation focused on execution time for such algorithms shows that communications infrastructure time has an acceptable time delay in range of 50 ms and the delay time on server machines in control centres (<10 ms) is not a limitation for protection reactions. This means that the transfer of developed applications in a simulations environment to the real technical world is possible and will be the focus of future work.

### Angle stability monitored with voltage angle data

Advanced transmission operation control in real time can be realized by angle voltage monitoring and by that manner the angle stability in 400 kV transmission grid in real time is monitored. Two machine model with phasor representation on both ends (sending and receiving) in transmission grid has been developed, Figure 1. Line loading P is defined with equation (1) where  $L_{line}$  is line reactance, sending end voltage is  $U_S$  and receiving end voltage is  $U_R$ . Angle between two phasor is  $\varphi$ .

$$P = \frac{U_S \cdot U_R}{X_{line}} \cdot \sin \varphi \quad (1)$$

Loading in this two machine model depends on angle  $\varphi$  and voltage ends  $U_S$  and  $U_R$ . Theoretically maximum line load will be at angle  $\varphi=90^\circ$ .



Angle difference values can be used to trace the behaviour of the transmission network. Any values deviation is noticed and appropriate control action (manual or automatic) or protection action can be launched. Figure 1 presents possible trajectory for angle difference obtained from calculations and in real time for a time span of a few hours. The Figure 1 illustratively shows different events that start at a different moment ( $t_1$ ,  $t_2$  and  $t_3$ ), have different duration and are of different severance. Angle difference deviations are presented with dashed lines. It is presumed that during disturbances appropriate control or protection action has been activated thus angle values return to levels before disturbances.

## FEASIBILITY ASPECT FOR USING SYNCHROPHASOR MEASUREMENT

Croatian transmission system operator (HOPS) has operating WAM system [3] in control centre (CC) where PMUs completely cover the vital part of transmission network, Figure 2, [4].

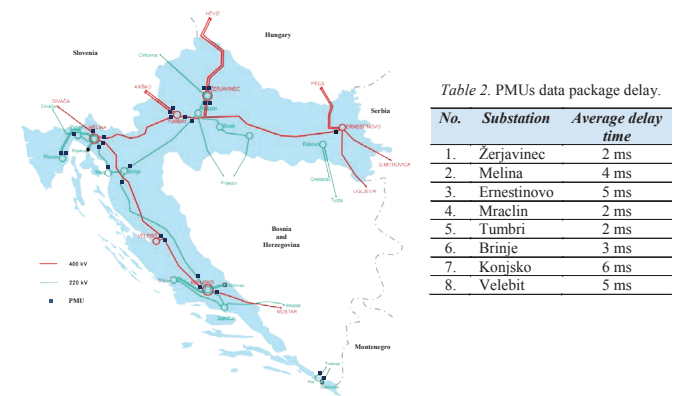


Figure 2. PMUs installation in 400 and 220 kV Croatian transmission network (left) and table with time delay values through communication infrastructure for PMUs data package (right).

Currently whole of internal 400 kV and most of 200 kV network has PMUs. PMU data collected from those devices is sufficient to get a good insight to neighboring states transmission networks and also in lower voltage transmission network (110 kV), [5].

Delay times [6] for particular connections are presented in Table 2. Those delays are fitted very well within project calculated values and are acceptable for use in wide area protection function based on synchrophasor data.

Statistical values for package delay  $t_{DEL}$  (4) were established for each PMU locations in WAM system. Table 3 has values of PMU package delays along with information about PMU type and type of communication link.

Table 3. Time delays recorded by PDC application.

No.	Substation	$t_{DEL}$ average (ms)	PMU type	Link type
1.	Žerjavinec line Tumbri	6,0	A	SDH (64k/bit/s - 2Mbit/s)
2.	Melina line Velebit	10,0	A	SDH (64k/bit/s - 2Mbit/s)
3.	Ernestinovo line Žerjavinec	9,6	A	SDH (64k/bit/s - 2Mbit/s)
4.	Konjsko line Velebit	10,6	A	SDH (64k/bit/s - 2Mbit/s)
5.	Žerjavinec line Ernestinovo	8,5	A	SDH (64k/bit/s - 2Mbit/s)
6.	Tumbri line Melina	7,0	A	SDH (64k/bit/s - 2Mbit/s)
7.	Konjsko line Brinje	10,6	A	SDH (64k/bit/s - 2Mbit/s)
8.	Melina line Tumbri	9,9	A	SDH (64k/bit/s - 2Mbit/s)
9.	Brinje line Konjsko	9,4	A	SDH (64k/bit/s - 2Mbit/s)
10.	Brinje line Mraclin	9,3	A	SDH (64k/bit/s - 2Mbit/s)
11.	Mraclin line Brinje	5,3	A	SDH (64k/bit/s - 2Mbit/s)
12.	Velebit line Melina	7,8	A	SDH (64k/bit/s - 2Mbit/s)
13.	Velebit line Konjsko	7,7	A	SDH (64k/bit/s - 2Mbit/s)
14.	Pehlin line Divača	20,8	B	WAN (10Mbit/s - Ethernet)
15.	Melina line Divača	21,6	B	SDH (64k/bit/s - 2Mbit/s)
16.	Peruća Generator 2	23,6	B	SDH (64k/bit/s - 2Mbit/s)
17.	Peruća Generator 1	24,1	B	SDH (64k/bit/s - 2Mbit/s)
18.	Tumbri line Krško 1	22,3	B	WAN (10Mbit/s - Ethernet)
19.	Control Centre PMU 1	19,3	B	LAN
20.	Control Centre PMU 2	19,3	B	LAN

PMU packages were received by PDC algorithm with average delay within 18 to 21 ms. Additional time needed to execute triggering algorithm can be neglected.

In a system where reaction time needs to be measured in milliseconds and consequences can be severe the analyses of whole communication chain from substation to WAMPAC system and back is very important. As a prerequisite for successful functioning of the proposed advanced protection algorithm testing of time delay issues in communications infrastructure was conducted. The principal flow chart for possible WAMPAC protection function operations is presented on Figure 3. It can be seen that it is a rather complex flow chart with dedicated equipment and communications paths and devices covering the whole path from the transmission line to the WAMPAC system.

On the flow chart the upper expected time delay in all three segments of the communication chain is presented. The real time measurements conducted on a real transmission system (Croatian transmission power system) show much smaller time delays (Tables 2 and 3). Time delays measured were done separately for different communication infrastructure on a TSOs Synchronous Digital Hierarchy (SDH) optical network with LAN and WAN configurations. The measured values presented in table (Table 2) include both main and reserve paths with distance from substation to control center of up to 300 km. Results for those measurements are presented in Table 2, for substations in 400 and 220 kV high voltage network.

This means that in practice with current infrastructure it is feasible to have advanced functions because of acceptable time delays. Consequently, the advanced angle instability protection is possible to implement in real transmission networks since the communications infrastructure offers reliable path with affordable time delays.

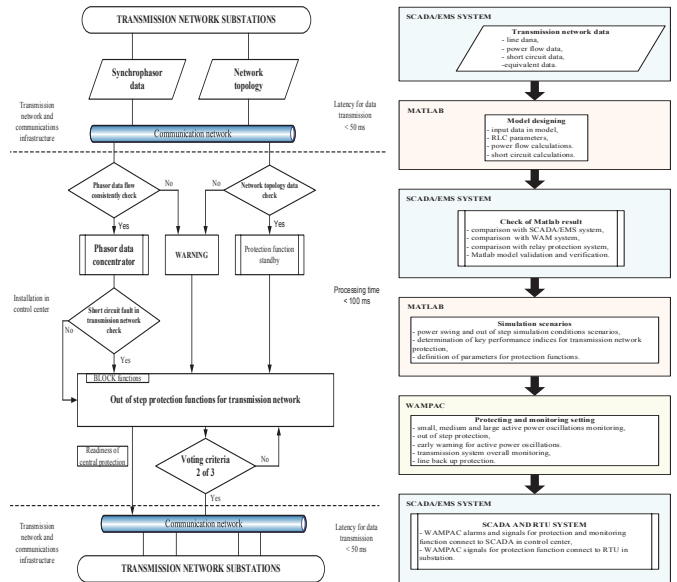


Figure 3. Principal flow chart for out-of-step protection in WAMPAC system in transmission network substations (left) and basic flow chart for designing and tuning Matlab model with protection function setting in WAMPAC system (right).

The whole process for implementing the new out of step protection function is presented in phases on the right side of Figure 3. Matlab model and its simulations possibilities were used for study work and analyses to gain parameters for settings of protection functions in WAMPAC [7], [8].

## MODEL FOR TRANSMISSION NETWORK AND PROTECTION

In order to accomplish the steps required for transitioning from the currently operational WAM system installed in the control centre towards a full capability WAMPAC system, a simulation environment of detailed model of Croatian 400 kV network with PMU devices installed on all lines, Figure 4, was developed in Matlab. At this stage, only positive sequence values were used. The model fulfils the following requirements:

- Three phase transmission network model,
- Implementation of power flow functionality with basic and intermediate characteristics,
- Adaptation of a simulations time domain in milliseconds,
- Simulation of line single and three phase short circuit faults,
- Capability for creation of different system disturbances, power swing and out of step,
- Designing the system protection function for out of step and monitoring capability for power swing in transmission network,
- Designing the scope of line back up protection functions, line differential, distance, overcurrent, voltage and others.

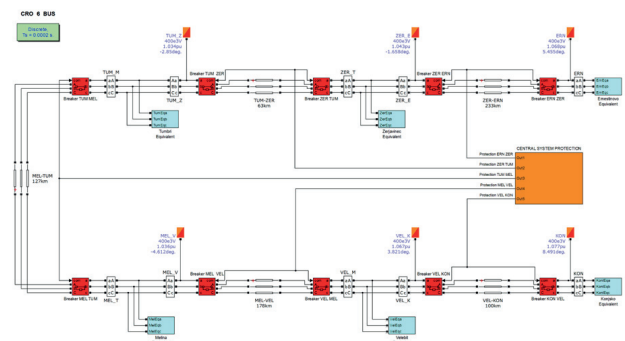


Figure 4. Matlab simulation environment with Croatian 400 kV transmission network model and central system protection in WAMPAC system in Control center.

Each 400 kV line in the model has its own three-phase voltage and current measurement module, which is a source for other monitoring and protection functions as shown in the block diagram, Figure 5. These protection functions are designed to be sensitive and capable of alarming and issuing triggering commands in a case of a complex disturbance in transmission network. Aforementioned disturbances are active power oscillations and out-of-step conditions. In addition, some of these functionalities will be used as an additional criterion in a decision process inside the protection model.

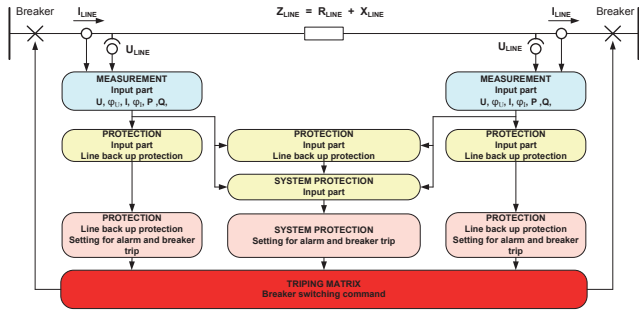


Figure 5. Developed Matlab model block diagram for line protection and monitoring functions.

Line back up functions will be used as remedial criteria for system protection function for out of step disturbance or some power swing disturbance [6].

## SIMULATIONS RESULTS FROM MATLAB PLATFORM

### Local oscillations in hydro power plant – real case

The oscillations originated from the hydro power plant Zakucac connected to 110 kV voltage level and propagated to 400 kV transmission network. WAM system recorded the oscillations generated by the generation units on the 400 kV transmission lines as shown on Figure 6. Highest oscillations were detected on the lines, which are closest to the source of the oscillations; in this case, the 400 kV lines Konjsko-Velebit (yellow line) and Melina-Velebit (blue line). Oscillations from 50 to 70 MW were detected on the 400 kV transmission line with oscillation frequency around 1 Hz (result from Prony analyses reveals frequency  $f_0 = 0.96$  Hz and damping factor  $\zeta = 0.057$ ). The damping factor has a positive value, which indicates existence of an undamped oscillation.

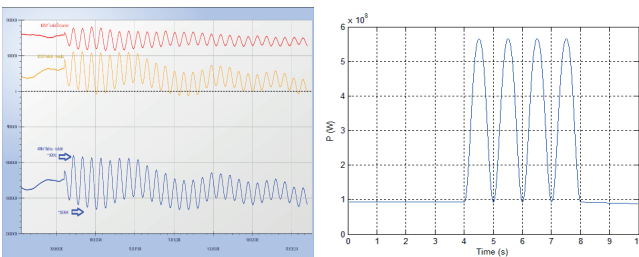


Figure 6. Active power oscillations recorded with WAM system in control center for three 400 kV lines (left). Simulated results in Matlab model (right).

The model was tuned to be able to simulate this particular disturbance which started in the mentioned power plant. The goal was to check if the impedance trajectory during this disturbance enters into any of the relay protection distance zones and power swing polygon. The results of these analyses in the R/X plane are presented on Figure 7. The impedance characteristic with the highest impedance setting is used for the power swing function. This particular polygon is the first one which is expected to be reached by the impedance trajectory.

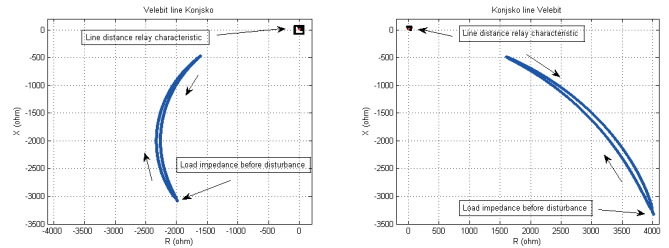


Figure 7. Line 400 kV Velebit-Konjsko, with line relay protection characteristic and impedance trajectory in R/X plane. Situation in Velebit station for line to Konjsko (left). Situation in Konjsko station for line to Velebit (right). Stations have different types of line distance relay.

### Large active power oscillations in R/X plane - simulations

In this chapter two hypothetical characteristic cases will be presented which cannot be compared with real situation because such disturbances do not exist in archives thus simulations scenarios were run on verified model.

On the same lines were induced large active power oscillations in one case and in another out of step conditions. Results of those simulations were presented for station Velebit, Figure 8. In the first case impedance trajectory will not enter in relay characteristic and there will be no protection activation. Whereas for second case trajectory passed through characteristic and activate some protection functions.

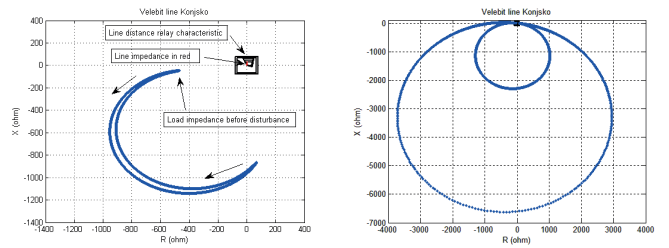


Figure 8. Line 400 kV Velebit-Konjsko, with line relay protection characteristic and impedance trajectory in R/X plane. Situation in Velebit station for line to Konjsko with large active power oscillations (left) and for an out of step conditions (right).

Study work mainly focused on all large active power oscillations. Special part of this work was analysing values for conditions when out of step develops from large oscillations. Those simulations gave a lot of insightful data because in real transmission network such events rarely happen.

### Out of step conditions with angle protection operations - simulations

Every internal 400 kV line is observed with two PMUs allowing us to study and trace angle  $\Delta\varphi$  values from which we derive some key performance indexes, Figure 9.

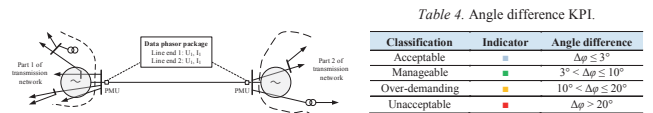


Table 4. Angle difference KPI.

Classification	Indicator	Angle difference
Acceptable	■	$\Delta\varphi \leq 3^\circ$
Manageable	■	$3^\circ < \Delta\varphi \leq 10^\circ$
Over-demanding	■	$10^\circ < \Delta\varphi \leq 20^\circ$
Unacceptable	■	$\Delta\varphi > 20^\circ$

Figure 9. Simplified two machine equivalent on a transmission network line equipped with PMU devices which send phasor data packages to WAMPAC system (left) and proposal for angle difference key performance index on transmission line (right).

Table 4 shows four KPI categories for angle  $\Delta\varphi$  values which can be used for monitoring the situation on each of transmission lines. Values above  $\Delta\varphi = 20^\circ$  are used as a setting parameter in synchrocheck functions on transmission lines. Values for inducing the out of step conditions in model are in Table 5.

Table 5. Simulation scenarios for out-of-step condition in Matlab model.

Disturbance origin	Disturbance characteristic	Network characteristic near disturbance origin
Konjsko	$\Delta f = 0.5 \text{ Hz}$ , $f = 0.2 \text{ Hz}$	Weak and radial type network, Oscillations on one transmission tie-line
Melina	$\Delta f = 0.5 \text{ Hz}$ , $f = 0.2 \text{ Hz}$	Weak and radial type network, Oscillations on one transmission tie-line
Ernestinovo	$\Delta f = 0.6 \text{ Hz}$ , $f = 0.2 \text{ Hz}$	Well connected network, Oscillations on four transmission tie-lines
Zerjavinec	$\Delta f = 0.6 \text{ Hz}$ , $f = 0.2 \text{ Hz}$	Well connected network, Oscillations on two transmission tie-lines, One internal transmission line disconnected

As seen values for  $\Delta f$  (amplitude of modulation) are slightly different in some parts of transmission network based on different characteristics of network part. Proposed protection technique which used  $\Delta\phi$  is demonstrated for two lines in model. In addition, differential line protection is used as remedial criteria. Right graph from Matlab presents a situation when protection actions are inhibited while left when protection functions operated and circuit breakers were tripped by out of step condition, Figure 10.

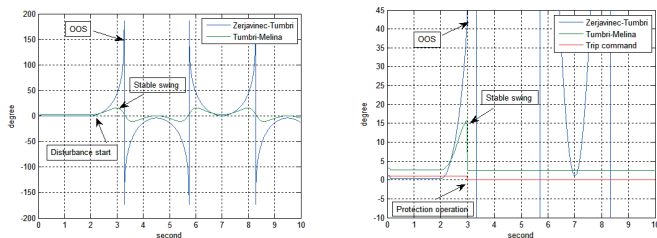


Figure 10. Active power oscillations on two 400 kV lines with voltage angle difference  $\Delta\phi$  and protection operations. On line Zerjavinec-Tumbri there is an out-of-step (OOS) condition and on line Tumbri-Melina there is a power swing condition (left). Detail presenting protection activations when protection setting is reached and tripped the Zerjavinec-Tumbri line while Tumbri-Melina remained in operation (right).

Line Zerjavinec-Tumbri is disconnected but oscillations on Zerjavinec side induced by simulation still exist because measuring module in model is placed between bus and breaker. Line affected only with stable swing, Tumbri-Melina (green line) after removing the disturbance returns in stable operation. Confirmations that breaker opened on line Zerjavinec-Tumbri is graph for current on those lines, Figure 11.

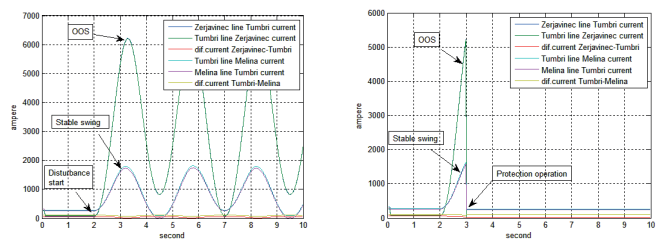


Figure 11. Remedial line protection criteria. Zerjavinec-Tumbri and Tumbri-Melina currents from both line ends with differential current protection ( $\Delta$ ). Out-of-step has developed on Zerjavinec-Tumbri line and on Tumbri-Melina line only stable power swing was present (left). Zerjavinec-Tumbri and Tumbri-Melina transmission line current with protection operations (right).

## BIBLIOGRAPHY

- M. Larsson, P. Korba, W. Sattinger, P. Owen, "Monitoring and Control of Power System Oscillations using FACTS/HVDC and Wide-area Phasor Measurements", CIGRE Session 44, August 26-31, 2012, Paris, France, paper B5-119.
- N. Baranović, P. Andersson, I. Ivanković, K. Žubrinić-Kostović, D. Peharda, J.E. Larsson, "Experiences from Intelligent Alarm Processing and Decision Support Tools in Smart Grid Transmission Control Centers", CIGRE Session 46, August 21-26, 2016, Paris, France, paper D2-112.
- M. Stojisavljević, D. Nemeć, I. Ivanković, "WAMS in Croatian Power System", 2nd International Conference, Monitoring of Power System Dynamics Performance, Saint Petersburg, April, 2008.
- S. Han, et. al. "PMU Applications in the Korean Power System: Wide-Area Monitoring And Control (WAMAC) System", CIGRE Session 45, August 24-29, 2014, Paris, France, paper C2-124.
- S. Skok, I. Ivanković, K. Frlan, Z. Zbunjak, "Monitoring and Control of Smart Transmission Grid Based on Synchronized Measurements", APAP2011, International Conference on Advanced Power System Automation and Protection, 16-20 October 2011, Beijing, China, paper No. 1447.
- CIGRE JWG 34/35.11, "Protection Using Telecommunications", August 2001.
- S. Skok, I. Ivanković, R. Matica, I. Šturić, "Multipurpose architecture model of phasor concentrator", CIGRE Session 43, August 22-27, 2010, Paris, France, paper D2\_B5\_101\_2010.
- V. Terzija, D. Cai, A. Vaccaro, J. Fitch, "Architecture of wide area monitoring systems and their communication requirements", CIGRE Session 43, August 22-27, 2010, Paris, France, paper D2\_B5\_110\_2010.
- B. Kasztenny, N. Fischer, K. Fodero, A. Zvorych, "Communications and Data Synchronization for Line Current Differential Schemes", Schweitzer Engineering Laboratories, Inc. 20110906, TP 6492-01, 2011.

Both graph present currents from each side with associated line differential currents [9]. After opening breakers Tumbri-Melina side of transmission network remains in stable operations with normal operating currents. With this proposed remedial criteria we can clearly and undoubtedly say that there are no short circuit fault on lines therefore reason for high current and power flow are oscillations somewhere in transmission network. This criterion can be considered as signal for out of step protection in WAMPAC system to be fully on standby and prepared for operation.

## CONCLUSIONS

Proposed technique for detection and protection will be centralized in control centres and have different approach from traditional line relay protection system for transmission lines.

Centralized protection applications use appropriated algorithm for fast and selective actions ensuring protection of transmission network from any kind of active power oscillations.

Algorithm uses voltage angle values from both transmission line ends. Algorithm effortlessly and smoothly covers whole range of possible active power oscillations in transmission network. With such applications in control centres, scarce information about wider transmission networks can be gathered too, not only lines with PMU devices. Besides monitoring any oscillations in transmission network, circuit breaker operations and short circuit faults can also be perfectly traced.

Current phasors are also available and are used for realisation of additional functionality such as a set of line protection and monitoring functions. Protection function based on phasor data are almost the same like traditional ones. Using them, some processes of supervising for traditional line protections can be developed. Alarms and events from those phasor data based protection will be forwarded to SCADA system. In the next phase of project real line back up protection is to be realized.

Crucial groundwork for having this particular protection solution is communication infrastructure across whole high voltage transmission network. This infrastructure must be reliable enough and redundant if we want to run protection functionality through them, which our TSO Company has.

**Goran Majstrovic**

**Drazen Jaksic**

**Martina Mikulic**

**Davor Bajs**

Energy Institute Hrvoje Pozar  
Croatia

**William Polen**

**Albert Doub**

United States Energy Association  
USA

# Impact of Adriatic submarine HVDC cables to South East European Electricity Market Perspectives

## SUMMARY

The ultimate goal in today's electricity business in Europe is market integration on pan-European level that will introduce transparency and competition between market players, incentives to clean energy development, as well as high quality of supply to the end-customers. To achieve these goals, in South-East Europe (SEE) there are number of barriers and uncertainties, one of which is linked with the possible new undersea HVDC connections between SEE and Italy.

With the support of the United States Agency for International Development (USAID) and coordination of the United States Energy Association (USEA), within the framework of the Southeast Europe Transmission System Planning Project (SECI), a detailed analysis has been accomplished on the impact of one or more undersea HVDC cables between Italy and SEE on power system operation and electricity market development [1]. Special emphasis to this analysis is given by the fact that SECI has been one of the longest running projects in the region. It started in 2001 with active participation of all regional TSOs, including continuous updating of power system and electricity market models and its harmonization of constant changes in power system planning. It is of utmost importance in the environment of constant changes of national power system development plans and needed further steps for full market opening and integration in the region.

SEE power systems and market<sup>1</sup> were modelled using the most relevant power system and market simulation and optimization softwares. Both system and market comprehensive models have been verified by all SEE TSOs.

Study analyses were divided in two parts: 1) market analysis and 2) network analysis. The market study investigated expected generation pattern, power exchanges and wholesale prices in SEE, taking into account regional market synergy, the new links with Italy, and high level of RES integration. Bulgaria and Romania are currently the main exporters in SEE. Significant power exchanges in the North-South/Southeast direction are related to the fact that the GR, MK, ME, HR and AL are mainly importing, plus the influence of Italy importing over new potential HVDC cable(s). Network analysis dealt with power flows, network bottlenecks and voltage profiles in given market scenarios.

Finally, the results of this comprehensive market simulation comprised of the following:

- Countries electricity balance (production, consumption and exchanges)
- Electricity prices for each country
- Cross-border power exchanges (MWh/h) for each border in the region on hourly basis
- HVDC link loadings (MWh/h) for each HVDC submarine cable on hourly basis
- Location and frequency of market congestions in SEE (NTCs full between areas with price difference)

All those analyses have been performed in two different transmission network development scenarios:

- Base case scenario: with planned HVDC ME-IT
- Alternative scenario: with planned HVDC ME-IT, and HVDC HR-IT, and HVDC AL-IT

In this way one of the most important uncertainties (new HVDC links SEE – Italy) for future power system and market operation in SEE, have been evaluated both in technical and market sense, using the most relevant inputs and model.

## KEYWORDS

South East Europe, HVDC submarine links, Italy, electricity market

<sup>1</sup> Albania (AL), Bosnia and Herzegovina (BA), Bulgaria (BG), Greece (GR), Croatia (HR), Hungary (HU), Kosovo (KS), Montenegro (ME), Macedonia (MK), Romania (RO), Serbia (RS), Slovenia (SI).

# INTRODUCTION

The case of new HVDC links between SEE (net exporter) and Italy (net importer) is relatively unique since we have two parallel uncertainties behind these large infrastructure investments that could change current electricity market positions: 1) strong development of SEE regional market and uncertain development of new generation portfolio and 2) strong development of generation (primarily RES) in Italy and potential change of existing country (importing) balance. The main target of this study was to evaluate impact of new HVDC links SEE – Italy on the future, expected electricity market and network in the region. The project has been divided in two phases:

- 1) preparation of common electricity market and power system model
- 2) detailed market and network analyses

In the first phase, relevant input data were collected, clarified and verified. It lasted for almost a year. The second phase aimed to assess perspective electricity market and system behavior in SEE considering influence of generation development involving RES, markets integration and the subsequent transmission investments.

## SOUTH EAST EUROPEAN ELECTRICITY MARKET AND POWER SYSTEM MODEL

The primary source of model input data has been provided by all regional TSOs, which is of utmost importance due to all market and network planning uncertainties [2]. For the remaining unavailable data, other verified and publicly available official data (e.g. ENTSO-E Pan European Market Modelling Database [3]) have been used along with internal documents and estimates. To perform market analysis SEE power systems have been modelled with electricity market simulation and optimization software PLEXOS, while for the network analyses PSS/E software platform was used. Starting with the data collected from the TSOs, the following modelling approach has been adopted for each country:

- Albania, Bosnia and Herzegovina, Bulgaria, Croatia, Kosovo, Macedonia, Montenegro, Romania and Serbia are modelled on plant-by-plant level of details,
- Greece, Hungary and Slovenia are aggregated per technology clusters (thermal by fuel type, hydro by type, RES by technology),
- Italy, Turkey and Central Europe region are modelled as external spot markets where the market clearing price series is insensitive to fluctuations of prices in SEE, constrained by transmission capacity.

Target year for these analyses was set to 2030 and the simulations have been carried out on hourly basis. Annual electricity demand was modeled on hourly basis. The generation cost function was also modeled, together with constraints of generation dispatch (must-run units, weather conditions, etc.). Market and grid models maintained compatible to run iteratively.

Considering the size of simulated system and the amount of collected data, each national market has been modelled as a single equivalent node to which all generators within the country were connected to. Nodes were connected by virtual transmission lines with maximum capacity equal to the nominal transfer capacities between the two countries.

Market model consists of 580 generating units in 12 SEE countries. It refers to 153 thermal power plants (TPPs), 6 nuclear power plants (NPPs), 124 storage hydro power plants (HPPs), 53 run-of-river (RoR) HPPs. Accordingly, this is the most detailed electricity market model in the region, verified by all TSOs. In addition, for each country one equivalent wind and one equivalent solar power plants have been modelled. Three external markets representing Italy, Turkey and Central Europe have also been modelled using simulated hourly price time series. This market model contains 28 cross-border lines and 4 submarine HVDC cables.

On the other side, regional power system model consists of more than 5500 nodes, 2000 power plants, 2200 generators, 9000 lines and 2800 transformers. It is the most detailed SEE power system model ever prepared.

## ELECTRICITY MARKET AND NETWORK DEVELOPMENT SCENARIOS

Impact of new regional candidate connections towards Italy was assessed by analyzing three scenarios, as shown on the following Figure:

- 1) Reference Case scenario: with existing HVDC Greece-Italy
- 2) Base Case scenario: with existing HVDC Greece-Italy and HVDC Montenegro-Italy (under construction)

3) Alternative Case scenario: with existing HVDC Greece-Italy, HVDC Montenegro-Italy (under construction), HVDC Croatia-Italy and HVDC Albania-Italy

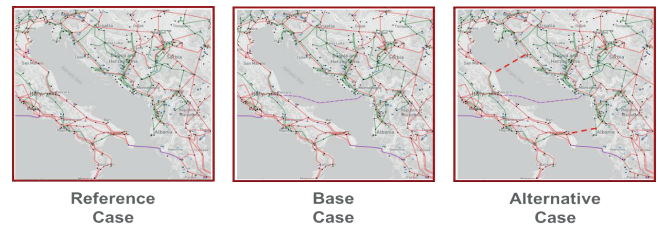


Figure 1: Illustration of analyzed scenarios

Reference Case scenario was created for comparison of the Base and Alternative Case scenario results. Reference Case scenario includes only the existing HVDC cable Greece-Italy and thus it presents current status of the regional interconnections to Italy. Base and Alternative Case scenario results are compared in terms of yearly electricity generation, average wholesale prices, net interchange, total transfer and cross-border loadings.

Important aspect of the market analysis lies in CO<sub>2</sub> emission prices that have also been included in the optimization objective function. Assumption on CO<sub>2</sub> emission prices is taken from ENTSOe Ten Year Network Development Plan 2016 [4] with the value of 17 €/ton. Additional set of scenarios (Reference, Base, Alternative) without Carbon Costs has also been analyzed for the evaluation of the effect of CO<sub>2</sub> emissions prices.

Network analyses have been based on the Market Analysis snapshots. For the Base Case and Alternative Case scenarios three study cases have been analyzed:

- 1) Highest consumption in SEE (18th of December 2030, 18:00h)
- 2) Highest RES penetration in SEE (9th of December 2030, 11:00h)
- 3) Lowest Consumption in SEE (28th May 2030, 03:00h)

Those three system snapshots have been identified as the most critical in terms of transmission system operational security. For two scenarios (Base and Alternative) and three characteristic regimes, total of six network (load flow) models have been created for the network analyzes. As a starting point SECI regional transmission system model (RTSM) for 2030 Winter Peak regime has been used.

## ELECTRICITY MARKET ANALYSES RESULTS

Regional wholesale prices are determined by marginal cost of generation and price on the external markets. These prices are comparable to actual market prices (due to input data and assumptions on fuel costs, generation cost curves, generation investments and demand increase, etc.). In SEE region wholesale electricity prices are mainly harmonized, with certain variations (for example in Greece). It assumes practically fully integrated SEE electricity market although several network congestions are still existing in the region.

Study results show that average market price in SEE is increased by 1.60 €/MWh in the Base Case and 3.75 €/MWh in the Alternative Case compared to results of the Reference Case, as shown on the following Figure. Thus, it can be concluded that additional HVDC links to Italy increase wholesale prices in SEE region up to 10%, but they also increase electricity generation and revenues.

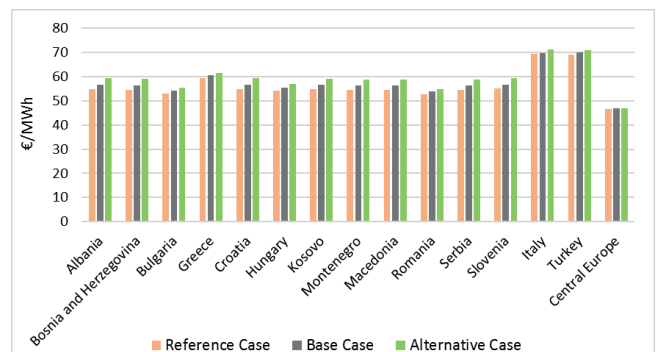


Figure 2. Comparison of average wholesale prices

Total generation in SEE is increased by 3.35 TWh (0.96%) in Base Case and 8.98 TWh (2.58%) in Alternative Case, compared to Reference Case scenario, as shown in the following Table. The most significant change occurs in Bosnia and Herzegovina – in Base Case yearly generation is

increased by 1.53 TWh compared to Reference Case, while in Alternative Case by 3.51 TWh. Certain increase of electricity generation can be also expected in Bulgaria, Romania and Serbia.

Table 1: Comparison of electricity generation in SEE region on country basis

Yearly generation (TWh)	AL	BA	BG	GR	HR	HU	KS	ME	MK	RO	RS	SI	TOTAL
Reference Case	10.75	15.59	50.99	51.11	15.06	40.04	12.07	4.57	10.42	88.44	35.18	14.31	348.53
Base Case	10.74	17.11	51.30	50.99	15.24	39.93	12.07	4.57	10.66	88.85	36.10	14.31	351.88
Change (TWh)	-0.01	1.53	0.32	-0.11	0.18	-0.11	0.00	0.00	0.24	0.41	0.92	0.00	3.35
Change (%)	-0.12	9.79	0.62	-0.22	1.18	-0.27	0.00	-0.01	2.33	0.46	2.61	0.01	0.96
Alternative Case	10.79	19.09	51.61	51.89	15.52	40.21	12.06	4.66	11.04	89.36	36.95	14.32	357.50
Change (TWh)	0.04	3.51	0.62	0.78	0.45	0.17	-0.01	0.10	0.62	0.92	1.77	0.01	8.98
Change (%)	0.36	22.50	1.22	1.53	3.02	0.43	-0.11	2.09	5.99	1.04	5.03	0.04	2.58

As expected, additional HVDC cables in the Base and Alternative Case increase net interchange to Italy. Italy is a net importer and in the Base Case scenario Italy imports 5,214 GWh more than in Reference Case, while in the Alternative 12,652 GWh more than in the Reference Case. With new HVDC link SEE region will become a stronger net exporter in the Base and Alternative Case. In the Base Case net interchange of SEE region is 3,284 GWh higher than in Reference Case, while in the Alternative Case it is 8,753 GWh higher than in the Reference Case.

Effect of CO<sub>2</sub> emission prices has been evaluated in additional set of scenarios without carbon cost. In all scenarios without carbon cost, electricity generation is expectedly increased. In the Base Case total SEE generation is 14.49 TWh higher, in the Alternative Case 14.52 TWh higher than in the main set of scenarios with Carbon Costs included. In scenarios with no carbon cost, the cost of generation is lower and thus market prices in SEE are lower. Average wholesale price in SEE region in scenarios without carbon cost is 5.60 €/MWh lower in the Base Case and 3.84 €/MWh lower in Alternative Case, which is quite significant. Based on the market analyses, the main findings of the network analysis are given as follows.

## ELECTRICITY NETWORK ANALYSES RESULTS

The analyses have shown that for some countries level of power exchanges presumed in initial SECI RTSM development model are different than the ones obtained from the Market Analyses in this study, i.e.:

- For Albania, Montenegro, Serbia and Slovenia, market analysis has shown these countries are importers rather than exporters, as it is initially individually expected
- For Greece and Macedonia, market analysis has shown these countries are exporters rather than importers, as it is initially presumed
- For other countries considered, initially planned exports or imports are in line with Market Analysis results, just with different total amounts

This brings us to the first conclusion: planned generation investments in all regional countries in given timeframe will significantly change individually expected country balances. Because of different exchange levels, load flow patterns will also be different. When compared to initial SECI RTSM 2030 Winter Peak model, main expected differences in power exchanges are the following:

- Flows from Hungary to Croatia are increased from 850 MW in the Base Case, to 1150 MW in the Alternative Case
- Flows from Romania to Serbia are increased from 600 MW in the Base Case to 1150 MW in the Alternative Case
- Flows from Greece to Albania are increased from 600 MW in the Base Case to 800 MW in the Alternative Case
- Flows from Bosnia and Herzegovina towards Croatia are decreased by 500 MW in the Base Case and increased by 500 MW in the Alternative Case.
- Flows in all analyzed regimes are in direction from Bosnia and Herzegovina to Montenegro, while it is opposite in SECI RTSM model
- Flows in all analyzed regimes are in direction from Greece to Macedonia, while it is opposite in SECI RTSM model

Finally, the biggest cross-border flow differences between SECI RTSM model and models based on market studies are shown on the following Figure.

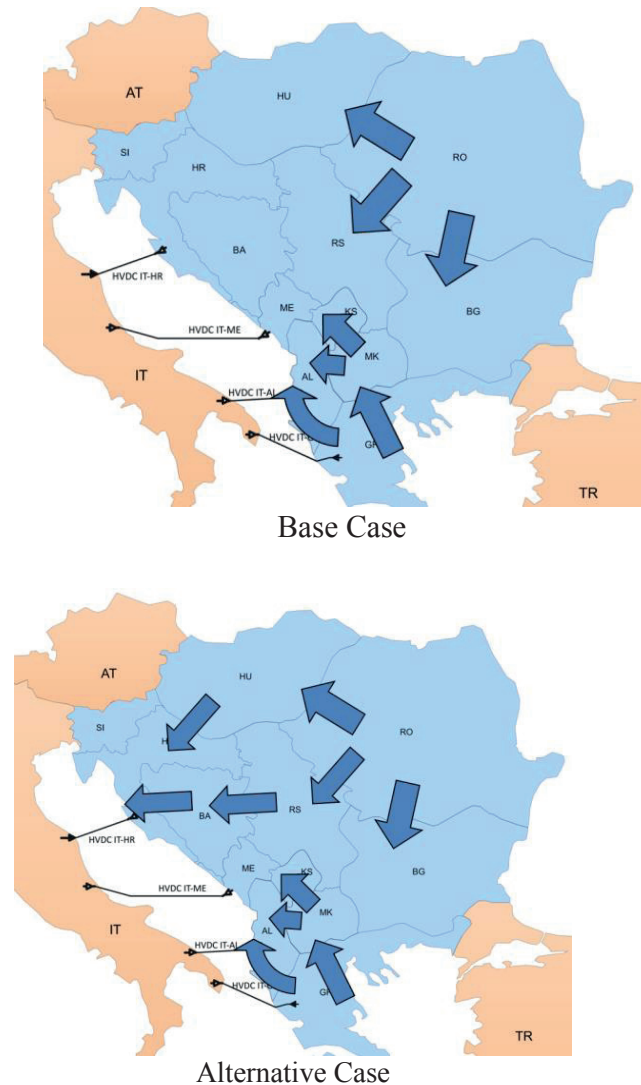


Figure 3: The biggest cross-border flow differences between SECI RTSM model and models based on market studies

For all above mentioned scenarios and characteristic regimes, load flow calculation, voltage profile assessment and (n-1) contingency analysis were carried out. Also, for significant planned projects in the region, TOOT analysis was additionally conducted, with the aim of evaluating their influence on overall security of the transmission network in SEE region, in market coupled conditions. TOOT (Take Out One at the Time) method consists of excluding grid element projects from the forecasted network structure on a one-by-one basis and to evaluate the load flows over the lines with and without the examined network reinforcement (a new line, a new substation, a new PST etc).

For all Base Case regimes, it was generally concluded that market coupling in SEE region introduced changes in load flow patterns. Changes in power flows in transmission networks of the SEE region will not lead to the network overloading if all network elements are available. In such network topology conditions, voltage levels will also be within allowed limits for Highest Consumption and Highest RES penetration regimes. For Lowest Consumption regime, the voltages are out of allowed limits and additional reactive compensation measures will need to be implemented to decrease high voltages.

Market simulations for Base Case scenarios have shown big congestions, with program flows reaching NTC values for many hours. Grid analyses have shown that, in terms of (n-1) security criteria assessment, Highest RES penetration regime was identified as the most critical one for the Base Case scenario. In this regime, outage of 400 kV OHL Portile de Fier (RO) – Resita (RO) causes overloading of 400 kV OHL Djerdap (RS) – Portile de Fier (RO). For other two regimes, Highest Consumption and Lowest Consumption, transmission networks in SEE region satisfy (n-1) security criteria.

Sensitivity analysis has been conducted for several planned projects by applying TOOT methodology. The results are as follows:

- Project 400 kV OHL Pancevo (RS) – Resita (RO) has shown significant influence on (n-1) security criteria, in Highest Consumption and Highest RES penetration regimes
- Project 400 kV OHL Banja Luka (BA) – Lika (HR) has shown small influence on (n-1) security criteria, in all analyzed regimes
- Project 400 kV OHL Bitola (MK) – Elbasan (AL) has shown small influence on (n-1) security criteria, in all analyzed regimes
- Project new 400 kV interconnections RS-BA-ME has shown small influence on (n-1) security criteria, in all analyzed regimes

On the other side, for all Alternative Case regimes, it was generally concluded that market coupling in SEE region also introduces changes in load flow patterns. Changes in power flows in transmission networks of the SEE region did not lead to overloadings if all network elements are in operation. Under these conditions, voltage levels were in permitted ranges for Highest Consumption and Highest RES penetration regimes. For Lowest Consumption regime again, additional reactive compensation measures will need to be implemented to decrease unacceptable high voltages.

In terms of (n-1) security criteria assessment, Highest Consumption regime was identified as the most critical one for Alternative Case scenario. In this regime, outage of 400 kV OHL Konjsko (HR) – Mostar (BA) and outage of 220 kV Konjsko (HR) – Zakucac (HR) are causing overloading of 220 kV OHL Zakucac (HR) – Jablanica (BA). For other two regimes, Highest RES penetration and Lowest Consumption, transmission networks in SEE region satisfy (n-1) security criteria.

Reported congestion on Croatia-BiH border in Highest Consumption regime, is a strong signal that in order to introduce estimated or higher levels of NTCs for target year between these two countries, additional network reinforcement has to be implemented to enhance electricity trade and to support higher social welfare (lower overall price). Sensitivity analysis conducted for several projects with TOOT methodology has shown that:

- Project 400 kV OHL Pancevo (RS) – Resita (RO) has shown significant influence on (n-1) security criteria, in all analyzed regimes
- Project 400 kV OHL Banja Luka (BA) – Lika (HR) has shown less influence on (n-1) security criteria, in all analyzed regimes
- Project 400 kV OHL Bitola (MK) – Elbasan (AL) has shown influence on (n-1) security criteria in Highest Consumption regime
- Project new 400 kV interconnections RS-BA-ME has shown influence on (n-1) security criteria in Lowest Consumption regime

It should be pointed out that Base Case models are more comparable to SECI RTSM initial model, than Alternative Case model, because in Alternative Case models four HVDC links are in operation while in SECI RTSM and Base Case models, only two of them are in operation. Nevertheless, market based models show significant differences in load flow patterns when compared to model based on individual information from each TSO's National Development Plan. Main reasons of such differences are in first place:

- market integration
- different initial assumption of countries balances
- different RES production profile

## CONCLUSIONS

Within this USAID/USEA project the most detailed South East European electricity market model has been developed and verified by all regional TSOs. In addition to the previously developed power system model (SEC), this study used the most relevant and detailed inputs for evaluation of large infrastructure investments on the regional network and market development. The study has shown that market based results gave very different generation footprint in the region when compared to predictions of individual TSOs. Main reasons for such differences is in additional market coupling introduced different country balances, different generation schedules than the ones based on individual TSO experience and higher RES penetration per country.

## BIBLIOGRAPHY

- [1] SECI Transmission System Planning Working Group: "Impact of Adriatic submarine HVDC cables to South East European Electricity Market Perspectives", EIHP/EKC (financed by USAID/USEA) 2017
- [2] 10-year network development plans of the SEE TSOs (ELES, HOPS, NOS BiH, EMS, MEPSO, KOSTT, OST, Transelectrica, CGES, NEK), 2015-2016
- [3] ENTSO-E Pan European Market Modelling Database, 2014
- [4] ENTSO-E TYNDP, 2016

After comprehensive electricity market study resulting wholesale prices are comparable to actual market prices. In SEE wholesale electricity prices are mainly harmonized, which presents practically fully integrated SEE electricity market although network congestions are still present in the region. Average market price in SEE region is increased by 1.60 €/MWh in the Base Case and 3.75 €/MWh in the Alternative Case compared to results of the Reference Case. It can be concluded that additional HVDC links to Italy increase wholesale prices in SEE region for up to 10%.

Total generation in SEE region is increased by 3.35 TWh (0.96%) in the Base Case and 8.98 TWh (2.58%) in the Alternative Case, compared to the Reference Case scenario. In the Base Case net interchange of SEE region is 3,284 GWh higher than in Reference, while in the Alternative Case it is 8,753 GWh higher than in the Reference Case scenario.

Dominant power exchange directions can be perceived through power transfer values and the occurrence of congestions. Total transfer sums up the absolute values of total yearly import and export, and Serbia has the highest total transfer in all scenarios, but transfer decreases in Base and Alternative Case compared to Reference Case. When looking at the power flow in just one direction, generally, in both Base and Alternative Case the highest power transit in SEE region can be expected from Romania and Bulgaria to the neighboring countries.

In terms of cross-border flows, significant congestions can be noticed in both Base and Alternative Case. In the Base Case congestions occur especially on the BG-GR, AL-GR, SI-IT borders and HVDC cable ME-IT, but only in one direction – to Greece and to Italy. Congestions can be also observed on CE-HU and CE-SI borders, in the direction from Central Europe. In Alternative Case total cross-border congestions are even higher than in Base Case scenario, but are more evenly distributed. Congestions mostly occur on CE-SI and CE-HU link in the direction from Central Europe, and on the BG-GR border in the direction to Greece, as in the Base Case. In Alternative Case congestions on RO-RS border can be also observed, in the direction from Romania to Serbia. Occurrence of congestions on these borders is a market signal for increasing cross-border capacity.

Effect of CO<sub>2</sub> emissions prices has also been evaluated. In all scenarios w/o Carbon Cost electricity generation is expectedly increased. In the Base Case total SEE region generation is 14.49 TWh higher and in Alternative Case 14.52 TWh higher than in main set of scenarios that include Carbon Costs. Since these scenarios do not include Carbon Cost, cost of generation is lower and thus market prices in SEE region are lower. Without Carbon Costs average wholesale price in SEE region is 5.60 €/MWh lower in the Base Case and 3.84 €/MWh in Alternative Case than in the main set of scenarios with Carbon Costs.

For the network analyses, it can generally be concluded that market coupling in SEE region introduces changes in existing load flow patterns. Changes in power flows in SEE transmission networks will lead to network overloading in the cases when all network elements are in operation. Under these network topology conditions voltage levels will be within permitted ranges for Highest Consumption and Highest RES penetration regimes. For Lowest Consumption regime network node voltages are out of acceptable limits.

In terms of (n-1) security criteria assessment, Highest RES penetration regime is identified as the most critical one for the Base Case scenario. In this regime, outage of 400 kV OHL Portile de Fier (RO) – Resita (RO) causes overloading of 400 kV OHL Djerdap (RS) – Portile de Fier (RO). For other two regimes, Highest Consumption and Lowest Consumption, transmission networks in SEE region satisfy (n-1) security criteria.

Highest Consumption regime is identified as the most critical one for (n-1) criteria in the Alternative Case scenario. In this regime, outage of 400 kV OHL Konjsko (HR) – Mostar (BA) and outage of 220 kV Konjsko (HR) – Zakucac (HR) are causing overloading of 220 kV OHL Zakucac (HR) – Jablanica (BA)

One of the findings was related to the voltage profiles in the region, in particular for the minimum system loading regime. The whole region is facing this issue for a longer time frame due to significant changes of the load pattern (heavy industry collapsed, larger share of households and services etc.). Therefore, detailed reactive power compensation studies in the region are necessary to resolve this issue on the regional level. It is one of the preconditions for sustainable and operationally safe integration of large network investments analyzed in this study.

**V. KOMEN\***HEP OPERATOR DISTRIBUCIJSKOG SUSTAVA  
CROATIA**A. ANTONIC**HEP OPERATOR DISTRIBUCIJSKOG SUSTAVA  
CROATIA**T. BARICEVIC,**ENERGY INSTITUTE HRVOJE POZAR  
CROATIA**M. SKOK**ENERGY INSTITUTE HRVOJE POZAR  
CROATIA**T. DOLENC**DALEKOVOD PROJEKT  
CROATIA

# Coordinated TSO and DSO network development plan on the islands of Cres and Lošinj

## SUMMARY

The paper presents an example of coordinated transmission and distribution network planning based on analyses conducted as part of the study on long term distribution network development plan for islands of Cres and Lošinj in Croatia. The observed area of two large and several smaller islands is supplied with electricity by one long radial 110 kV TSO owned line and parallel radial 35 kV DSO owned line. Due to transmission capacity of 35 kV line limited to 40% of the area peak demand, which is highly conditioned by tourism, the (N-1) criteria is not complied with in case of unavailability of 110 kV line during the two-month period in summer high season. Construction of the second 110 kV line as a common solution is extremely costly, due to necessity of laying down several kilometres of submarine cables. The paper provides the cost benefit analyses of this basic scenario and other possible alternative scenarios, including also investments in DSO network, to determine the most cost-effective solution. Due to the values of the demands and networks lengths, the presented example is close to a worst case scenario concerning the reliability of supply requirement, requesting thus some atypical distribution network analyses, elements and even conducted field tests of operation. The results clearly show that coordination of TSO and DSO planning is beneficiary concerning efficiency of investments in the networks. However, further analyses are recommended presuming contribution to satisfying the (N-1) criteria by use of non-traditional ("non-network" or "third party") solutions.

## KEYWORDS

(N-1) criteria, TSO/DSO alternatives and cooperation, high-temperature low-sag conductors, CBA

## INTRODUCTION

Islands of Cres and Lošinj as well as Silba and several surrounding small islands are supplied with electricity by one 110 kV TSO owned and operated line and one 35 kV DSO owned and operated line from TS 110/20/35 kV Krk, which is well connected with the main transmission network. As shown in Figure 1, electricity distribution on islands of Cres and Lošinj is provided from five TS 35/20 kV (Cres, Hrasta, Osor, Lošinj 1 and Lošinj 2) and one TS 35/0,4 kV. Considering also TS 35/10 kV Silba, which supplies

several distant smaller islands, it sums up to a total distance of about 110 km, or about 120 km of basically radial 35 kV overhead or cable lines. The corresponding transmission network supplying this area consists of just one radial 65 km long 110 kV line and TS 110/35 kV Lošinj, leaving the area with peak load of 24,8 MW without (N-1) criteria backup supply in case of unavailability of 110 kV line, except for limited capacity of up to 10 MVA through 20/35 kV 8 MVA transformer in TS 110/20/35 kV Krk and old Cu 3x50 mm<sup>2</sup> overhead lines along the islands of Cres and Lošinj.

## ALTERNATIVES FOR 110 kV AND 35 kV NETWORK DEVELOPMENT CONCERNING (N-1) CRITERIA

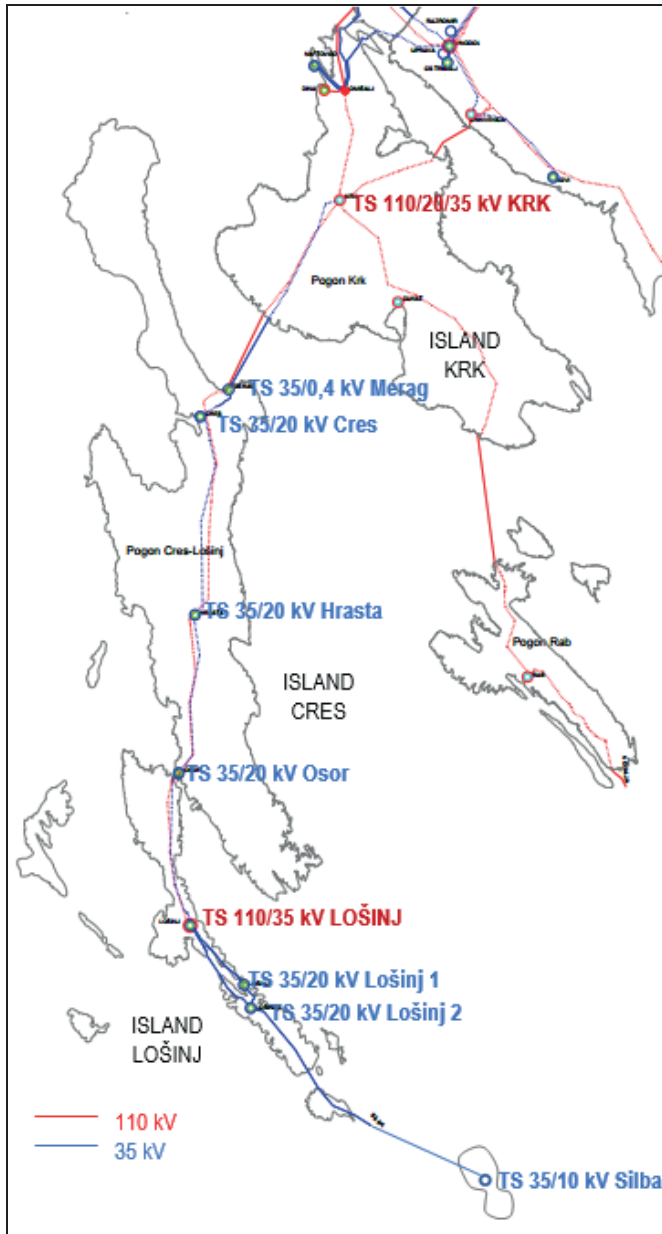


Figure 1: Transmission and distribution network for supplying the islands of Cres and Lošinj

Several alternatives for backup power supply according to (N-1) criteria in case of unavailability of 110 kV line Krk-Lošinj were analysed. The second 110 kV line to TS 110/35 kV Lošinj, as a traditional and technically favourable solution, requires laying down several kilometres of submarine cables, which is extremely costly, especially considering that demand of islands of Cres and Lošinj is highly conditioned by tourism and thus without backup supply according to (N-1) criteria only during one to two months in summer high season. Therefore, alternative solutions have been examined considering 35 kV distribution network, but the value and the location of most of the load in Lošinj area, about 70 km from TS 110/20/35 kV Krk as supplying point for 35 kV network, asked for atypical distribution network elements, such as of high-temperature low-sag conductors, three winding transformers 110/20/35 kV and long 35 kV submarine cables. Additionally, to deal with extreme voltage drops along 35 kV network, voltage regulation with two 110/35 kV transformers (in TS 110/35 kV Lošinj) operating in series (35/110 kV and 110/35 kV) is analysed and even examined in practice. Finally, for the case of long term unavailability of 110 kV submarine cable Krk – Cres, an emergency action plan for 110 kV overhead line connecting to 35 kV network is prepared.

Load flow calculations in case of peak load and unavailability of 110 kV line Krk-Lošinj are performed to determine backup power capacities of different alternatives for 110 kV and 35 kV network development, but also as a part of the process of detailed design of reconstructions of overhead 35 kV lines and assessment of the costs. One of important features of the study [1] is performing the load flow calculations for high loads inherent to (N-1) condition with the values of conductors resistances at temperatures of up to 120 °C, according to each line design parameters calculated based on IEEE Std. 738-2006.

The analyses were performed for the peak demand of the area of islands of Cres and Lošinj (with Silba) of 24,8 MW in 2016 and predicted increase to 34,3 MW in the observed 20-year period. Considering the existing network, the (N-1) criteria is: (1) complied with during the entire observed period in cases of unavailability of a single 35/10(20) kV transformer or 35 kV line, (2) complied with for the peak demand of 32,5 MW (16 years in the future) in case of unavailability of a 110/35 kV transformer, and (3) not complied with in the most severe case which is unavailability of 110 kV line Krk – Lošinj – the backup supply is in the current distribution network available only for 10 MW of peak demand, limited by the 20/35 kV 8 MVA transformer in TS 110/20/35 kV Krk,

Analyses of 110 kV and 35 kV network development alternatives aimed at satisfying (N-1) criteria were based on the following assumptions:

- Load flow calculations for cases of unavailability of single transformers 110/SN and 35/10(20) kV as well as 35 kV lines conducted with commonly used parameters for 20 °C
- Load flow calculations in case of unavailability of 110 kV line Krk – Lošinj:
  - Conductor resistance modified to design temperatures of up to 90 °C for cables and 120 °C for overhead lines (depending on the loading)
  - Due to very high active power losses (10% do 15%), as well as voltage drops and reactive power flows, transmission capacities (in MW) of the lines and transformers are up to 20% lower than nominal values.
  - Criteria for determination of backup supply limit at 35 kV network [2]:

Allowed overload of transformers<sup>1</sup> up to 20%.

Allowed voltage drop at 35 kV busbars in TS 35/20 kV up to 15%<sup>2</sup>. The analysed methods for voltage regulation: (1) use of voltage regulation 2x10x1,5% in TS 110/35 kV Lošinj (sectionalised 35 kV busbars and transformers in series: 35/110 kV and 110/35 kV), (2) use of capacitor banks (limited effects due to high voltage drops and consequently even higher required reactive power), and (3) use of autotransformers at 35 kV level.

- All network development alternatives assume replacement of TR 20/35 kV 8 MVA Krk with new transformer of minimal nominal rating of 20 MVA<sup>3</sup>.
- Concerning the reconstruction of the 35 kV lines Cres – Hrasta – Osor – Lošinj (total length of 42,5 km), three scenarios are analysed: replacement of the existing Cu 3x50 type conductors with the same new lines, conductors of ZTACIR 3x79 type or ACCC 3x115 type.

The following investments in 110 kV and 35 kV network have been analysed:

*Base scenario:* no investments in network development (reconstruction of overhead 35 kV line Cres – Lošinj with the same Cu 3x50 type conductors);

0. *Reference scenario:* 35 kV submarine cable Novalja – Silba (24 km), reconstruction of overhead 35 kV line Cres – Lošinj with ACCC 3x115 type conductors and 2 x TR 110/20/35 kV 40/20/20 MVA (Krk and Novalja);

1. *Alternative 1:* reconstruction of overhead 35 kV line Cres – Lošinj with ACCC 3x115 type conductors and selection of one sub-alternative for transformer in TS 110/20/35 kV Krk:

1 Overload of overhead lines is not considered, because the observed cases include extreme power flows lasting several hours in summer evenings, with high probability of high ambient temperature and absence of wind.  
 2 There are no 35 kV customers in 35 kV distribution network in this area.  
 3 Precondition for use of recently completed new submarine 35 kV cable Krk – Cres and reconstructed overhead line (with ZTACIR 3x79 type conductors). Selection of a transformer has been subject of the analyses.

1. TR 20/35 kV 20 MVA,
  2. TR 110/20(35) kV 20 MVA,
  3. TR 110/20(35) kV 20 MVA and existing TS 20/35 kV 8 MVA, or
  4. TR 110/20/35 kV 40/20/20 MVA;
2. *Alternative 2:* parallel 110 kV overhead line Krk – Cres operating at 35 kV, reconstruction of overhead 35 kV line Cres – Lošinj with ACCC 3x115 type conductors and TR 110/20/35 kV 40/20/20 MVA Krk;
  3. *Alternative 3:* 110 kV line Krk – Cres, reconstruction of overhead 35 kV line Cres – Lošinj with ACCC 3x115 type conductors and TS 110/35/20 kV Cres constructed as:
    1. simple single-transformer substation with TR 110/20/35 kV 40/20/20 MVA transported from TS 110/20/35 kV Krk, or
    2. standard two-transformer substation;
  4. *Alternative 4:* TS 110/20/35 kV Cres with TR 110/20/35 kV 40/20/20 MVA transported from TS 110/20/35 kV Krk and reconstruction of overhead 35 kV line Cres – Lošinj with ACCC 3x115 type conductors; depending on size of substation and rated power of TR 110/20/35 kV there are four sub-alternatives:
    1. simple single-transformer TS 110/20/35 kV Cres with TR 110/20/35 kV 40/20/20 MVA,
    2. standard two-transformer TS 110/20/35 kV Cres with TR 110/20/35 kV 40/20/20 MVA,
    3. simple single-transformer TS 110/20/35 kV Cres with TR 110/35/20 kV 40/40/20 MVA, or
    4. standard two-transformer TS 110/20/35 kV Cres with TR 110/35/20 kV 40/40/20 MVA;
  5. *Alternative 5:* second 110 kV line Krk – Lošinj and reconstruction of overhead 35 kV line Cres – Lošinj with ACCC 3x115 type conductors;
  6. *Alternative 6:* second 110 kV line Krk – Lošinj, reconstruction of overhead 35 kV line Cres – Lošinj with ACCC 3x115 type conductors and TS 110/35/20 kV Cres in one of two sub-alternatives:
    1. simple single-transformer substation with TR 110/20/35 kV 40/20/20 MVA, or
    2. standard two-transformer substation.

Overview of analysed investment alternatives in 110 kV and 35 kV network to satisfy (N-1) criteria is shown in Figure 2 and in more details in Table 1. The results are sorted in increasing order of available backup supply for demand rising from 24,8 MW to 34,3 MW in 20 years.

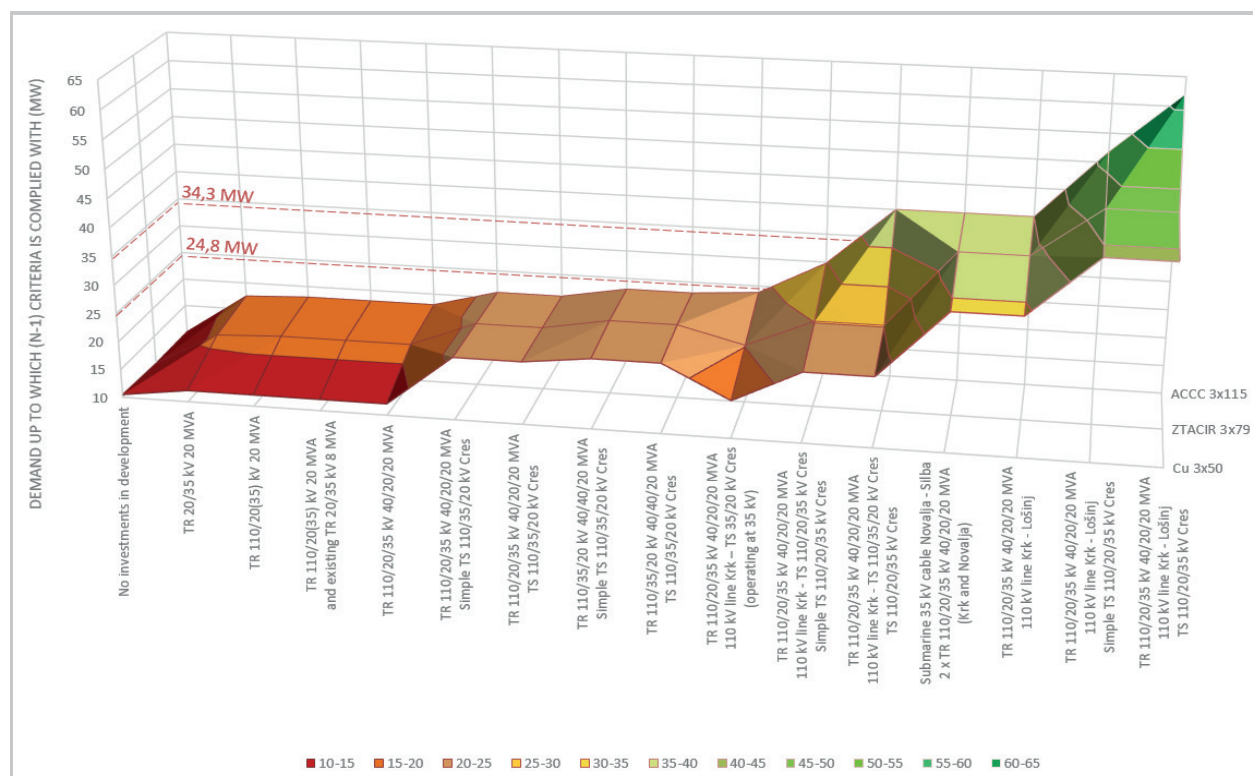


Figure 2: The demand of the islands of Cres and Lošinj (with Silba) up to which (N-1) criteria is complied with for different investment alternatives of 110 kV and 35 kV networks development

A specific scenario is analysed for the case of long term<sup>4</sup> unavailability of 110 kV submarine cable Krk – Cres. The emergency action plan assumes (1) connecting of 110 kV overhead line to the new 35 kV submarine cable and (2) use of 35 kV overhead line with the old 35 kV submarine cable<sup>5</sup>, enabling thus double 35 kV line Krk – Lošinj. Due to transmission capacity limit of the old 35 kV submarine cable of 9,7 MVA and high voltage drops, (N-1) criteria is complied with up to the 25,8 MW of demand of islands of Cres and Lošinj (with Silba), regardless of the types of conductors of 35 kV lines (Cu 3x50, ZTACIR 3x79 or ACCC 3x115).

1. The conclusions of the analysis aimed to satisfy (N-1) criteria are the following:
2. For full (N-1) criteria up to the existing load at least one more 35 kV line Krk – Cres is needed.
3. For full (N-1) criteria until the end of the observed 20-year period one more line is needed to Lošinj area (at 110 kV or cable line at 35 kV).
4. For full (N-1) criteria for longer period at 35 kV (DSO only investment) requires reconstruction of overhead 35 kV line Cres – Lošinj with ACCC 3x115 type conductors and new submarine 35 kV cable Novalja - Silba.
5. Alternative to 35 kV cable Novalja – Silba is construction of second 110 kV line to TS 110/35 kV Lošinj.
6. Concerning reconstruction of 35 kV overhead lines and supply from TS 110/20/35 kV Krk (and Novalja), ZTACIR 3x79 type conductors are only marginally better than Cu 3x50 type ones.
7. TS 110/20/35 kV Cres is required concerning (N-1) criteria in case of the demand of islands of Cres and Lošinj (with Silba) larger than 40 MW, with condition that backup supply of TS 110/35 kV Lošinj is provided at 110 kV level (i.e. another 110 kV line constructed). In that case simple single-transformer TS 110/20/35 kV Cres 40/20/20 MVA is sufficient.
8. Considering transmission capacity of 35 kV network and operating flexibility, optimal transformer for TS 110/20/35 kV Krk (and Novalja) is TR 110/20/35 kV 40/20/20 MVA.

4 Up to several weeks, including time needed for special equipment to arrive on site.  
 5 This solution includes the assumption that the existing old submarine 110 kV oil cable is taken out of the sea after the new cable is laid down.

# COST BENEFIT ANALYSIS OF ALTERNATIVES FOR 110 kV AND 35 kV NETWORK DEVELOPMENT CONCERNING (N-1) CRITERIA

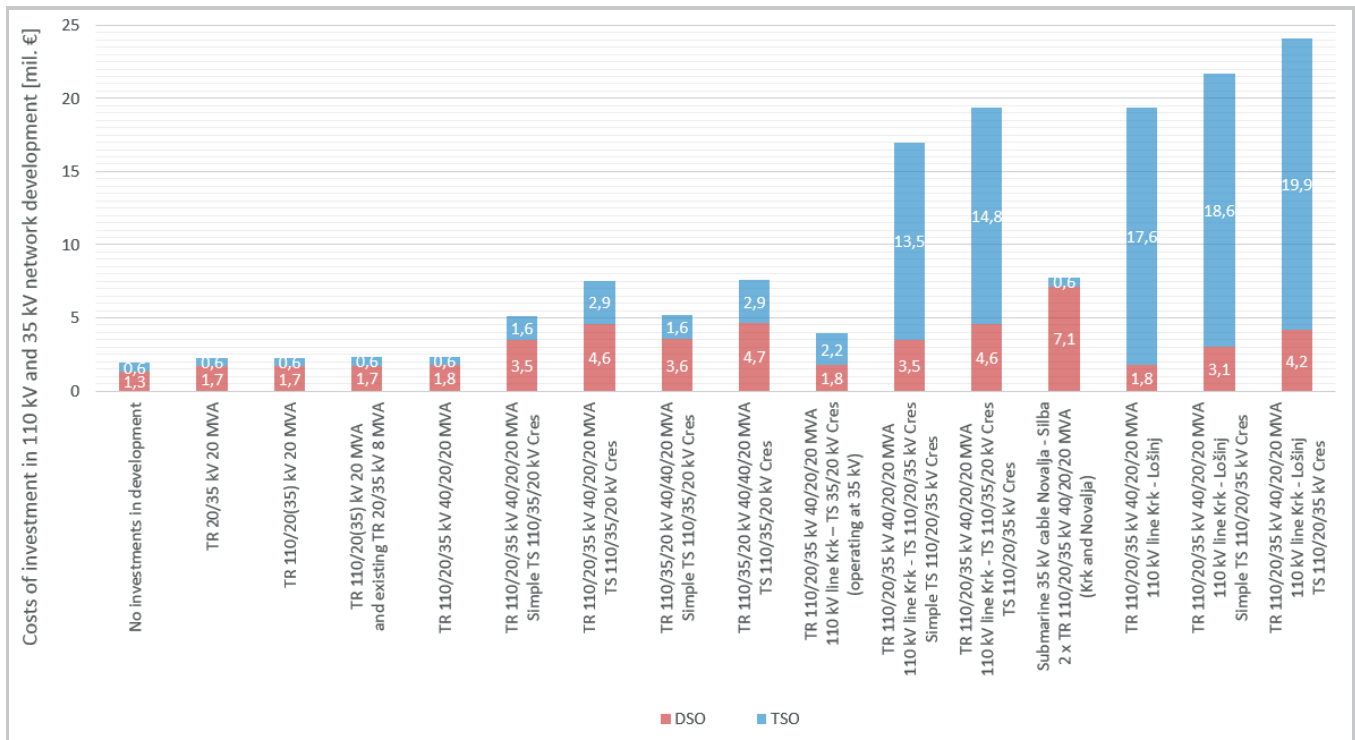
Overview of the results of backup supply determination for different investments in 110 kV and 35 kV network development concerning (N-1) criteria in case of unavailability of 110 kV line Krk – Lošinj is provided in Table 1. For each alternative the list of main investments is provided, including total nominal costs for DSO and TSO.

Table 1: Overview of alternatives of 110 kV and 35 kV network development concerning costs of investments and demand up to which (N-1) criteria is complied with

Alternative	Main investments	Investment (€) DSO TSO	Demand of islands of Cres and Lošinj (with Silba) up to which (N-1) criteria is complied with (MW)		
			Cu 3x50	ZTACIR 3x79	ACCC 3x115
			1.063.000	1.148.000	1.275.000
No investments	No investments in development	255.000 600.000	10,5		
Alternative 1	1 TR 20/35 kV 20 MVA	404.000 600.000	12	16	17,5
	2 TR 110/20(35) kV 20 MVA	401.000 600.000	12	16,5	18
	3 TR 110/20(35) kV 20 MVA and existing TR 20/35 kV 8 MVA	452.000 600.000	12	16,5	18
	4 TR 110/20/35 kV 40/20/20 MVA	486.000 600.000	12	16,5	18
Alternative 4	1 TR 110/20/35 kV 40/20/20 MVA Simple TS 110/35/20 kV Cres	2.219.000 1.600.000	21	21	21
	2 TR 110/20/35 kV 40/20/20 MVA TS 110/35/20 kV Cres	3.319.000 2.900.000	21	21	21
	3 TR 110/35/20 kV 40/40/20 MVA Simple TS 110/35/20 kV Cres	2.284.000 1.600.000	22,3	23	23
	4 TR 110/35/20 kV 40/40/20 MVA TS 110/35/20 kV Cres	3.384.000 2.900.000	22,3	23	23
Alternative 2	TR 110/20/35 kV 40/20/20 MVA 110 kV line Krk – TS 35/20 kV Cres (operating at 35 kV)	486.000 2.170.000	16,6	20,1	23,8
Alternative 3	1 TR 110/20/35 kV 40/20/20 MVA 110 kV line Krk - TS 110/20/35 kV Cres Simple TS 110/20/35 kV Cres	2.219.000 13.480.000	22,3	25,1	29,8
	2 TR 110/20/35 kV 40/20/20 MVA 110 kV line Krk - TS 110/35/20 kV Cres TS 110/20/35 kV Cres	3.319.000 14.780.000	22,3	25,1	40
Reference plan: (N-1) at 35 kV	Submarine 35 kV cable Novalja - Silba 2 x TR 110/20/35 kV 40/20/20 MVA (Krk and Novalja)	5.871.000 600.000	34	38,5	40
Alternative 5	TR 110/20/35 kV 40/20/20 MVA 110 kV line Krk - Lošinj	486.000 17.630.000	34	38,5	40
Alternative 6	1 TR 110/20/35 kV 40/20/20 MVA 110 kV line Krk - Lošinj Simple TS 110/20/35 kV Cres	1.786.000 18.630.000	44,3	47,1	51,8
	2 TR 110/20/35 kV 40/20/20 MVA 110 kV line Krk - Lošinj TS 110/20/35 kV Cres	2.886.000 19.930.000	44,3	47,1	62

The observed nominal costs for DSO and TSO are shown in Figure 3. They include evaluation of the existing TR 20/35 kV 8 MVA and TR 110/20 kV 20 MVA in TS 110/20/35 kV Krk, while for the second transformer in TS 110/35/20 kV Cres using of an old one is assumed (at no costs). For all alternatives except »No investments in development« reconstruction of overhead 35 kV line Cres – Lošinj with ACCC 3x115 type conductors is assumed, as the only feasible short term solution. The comparison of costs shows that all investments that require laying down new submarine 110 kV cable Krk – Cres are more than twice as expensive as other observed alternatives. Therefore, the study [3] relied predominately on the investments in 35 kV network, including reconstruction of overhead 35 kV line Cres – Lošinj with ACCC 3x115 type conductors, new submarine 35 kV cable Novalja – Silba and two new TR 110/20/35 kV 40/20/20 MVA (Krk and Novalja), as the reference scenario.

Figure 3: DSO and TSO costs for different investment alternatives of 110 kV and 35



KV network development on islands of Cres and Lošinj (with Silba)

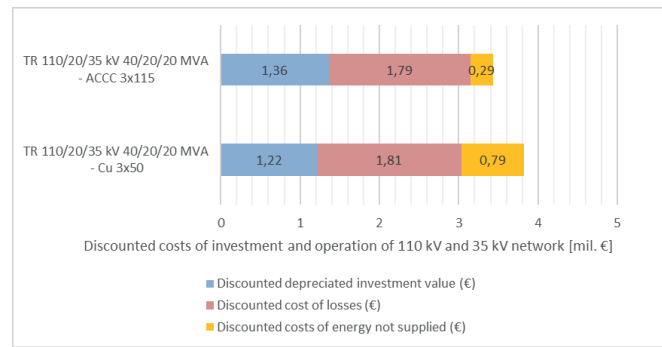
For the selection of optimal alternative of network development besides investment costs also operational costs of energy losses and energy not supplied during the observed 20-year period have to be considered. The common method of comparison of total discounted costs of depreciation, losses and energy not supplied has been applied [4].

Evaluation of losses and energy not supplied is conducted based on one-year SCADA hourly load data of all transformers in 110 kV and 35 kV network, considering also the predicted increase of demand up to 38% in the observed 20-year period. The following input parameters have been applied: (1) price of power losses dependent on load 97 €/kW, (2) price of power losses non-dependent on load 410 €/kW, (3) off-season (October-May) price of energy not supplied 2,5 €/kWh, (4) high-season (June-September) price of energy not supplied 5 €/kWh, (5) price of power not supplied 0,75 €/kW, (6) peak load duration for energy not supplied evaluation 2.828 h, (7) duration of losses dependent on load 1.084 h and (8) discount rate 8%. Assuming overall (including low voltage network) 40% share of energy losses non-dependent on load, the equivalent price of energy losses used in economic evaluation is 72 €/kWh. The prices of energy not supplied are derived based on income and energy consumption related to (1) tourism and (2) all other activities. The equivalent price of energy not supplied is 3,6 €/kWh.

The energy not supplied was evaluated separately for overhead 110 kV line and submarine 110 kV cable Krk-Cres, which, although unlikely, could require an extremely long time to repair (several weeks). For the overhead line backup supply capacities for different alternatives as shown in Table 1 have been considered. For the submarine cable higher of the same values or the value for emergency operation of 110 kV line at 35 kV level (25,8 MW) have been considered. For the overhead line the total yearly unavailability of 4 h is conservatively assumed based on the past unavailability data for all 110 kV lines in Croatian Primorje region. For the submarine cable a very radical model of unavailability during high-season weeks with probability of 5% has been assumed. However, considering the backup power supply of at least 25,8 MW in emergency operation, the contribution of the submarine cable to the total energy not supplied is much lower than the contribution of the overhead line.

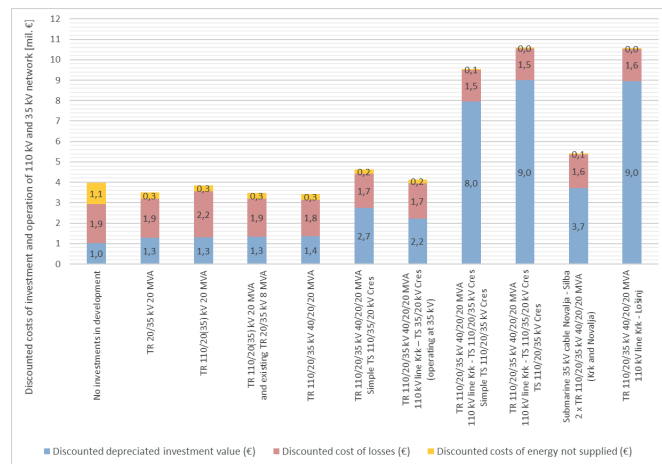
The result of economic justification of reconstruction of overhead 35 kV line Cres – Lošinj with ACCC 3x115 type conductors instead of Cu 3x50 type ones is shown in Figure 4. Nominal investment cost is 20% higher and discounted depreciated cost is 12% higher. However, with discounted costs of losses 1,4% lower and discounted costs of energy not supplied 64% lower, the total discounted costs of investments and operation are 10% lower. Considering the same discount rate of 8%, use of ACCC 3x115 type conductors is economically justified with nominal investment costs up to 75% higher than using Cu 3x50 type conductors.

Figure 4: DSO and TSO costs of different investment alternatives of 110 kV and 35 kV



kV networks development on islands of Cres and Lošinj (with Silba)

Figure 5 shows discounted investment and operation costs for observed



alternatives of 110 kV and 35 kV network development on islands of Cres and Lošinj with ACCC 3x115 type conductors applied.

The following conclusions summarize the findings of the conducted technical and economic evaluation:

Optimal investment complied with (N-1) criteria up to 18 MW of backup supply includes TR 110/20/35 kV 40/20/20 MVA Krk and reconstruction of overhead 35 kV line Cres – Lošinj with ACCC 3x115 type conductors (Alternative 1). The total nominal investment is 2.361.000 €, with DSO share

of 1.761.000 €, and TSO share of 600.000 €.

Optimal long-term investment complied with (N-1) criteria up to 40 MW of backup supply includes 2xTR 110/20/35 kV 40/20/20 MVA (Krk and Novalja), submarine 35 kV cable Novalja - Silba (24 km) and reconstruction of overhead 35 kV line Cres – Lošinj with ACCC 3x115 type conductors (Reference scenario). The total nominal investment is 7.746.000 €, with DSO share of 7.146.000 €, and TSO share of 600.000 €.

Additional alternative with costs in between the above values, complied with (N-1) criteria up to 23,8 MW of backup supply, includes TR 110/20/35 kV 40/20/20 MVA Krk, parallel 110 kV overhead line Krk – Cres operating at 35 kV and reconstruction of overhead 35 kV line Cres – Lošinj with ACCC 3x115 type conductors (Alternative 2). The total nominal investment is 3.931.000 €, with DSO share of 1.761.000 €, and TSO share of 2.170.000 €. However, this is only a temporary solution, assuming use of old submarine 110 kV oil cable (subject to evaluation of the risk to environment) or old submarine 35 kV cable with limited transmission capacity of 9,7 MVA.

Figure 5: Comparison of discounted investment and operation costs for observed 110 kV and 35 kV network development alternatives on islands of Cres and Lošinj

## CONCLUSION

The paper presents an example of coordinated transmission and distribution network planning based on analyses conducted as part of the study on long term distribution network development plan for islands of Cres and Lošinj in Croatia. Considering all conducted analyses, optimal network development aimed to satisfy (N-1) criteria in 110 kV and 35 kV network envisages backup supply of islands of Cres and Lošinj (with Silba) through two new transformers 110/20/35 kV 40/20/20 MVA (Krk and Novalja), 24 km of new submarine 35 cable Novalja – Silba and reconstruction of overhead 35 kV line Cres – Lošinj with ACCC 3x115 type conductors. This investments provide similar reliability of supply as would a second 110 kV line, but at 2,5 times lower nominal investment costs or 2 times lower discounted investment and operation costs. The provided results clearly show that coordination of TSO and DSO planning is beneficiary concerning efficiency of investments in both networks. In case the legal obligation of the investment to satisfy (N-1) criteria is at one network operator and investing by the other network operator provides significant reduction of costs, the network operators could decide to request from the regulator special treatment of the investment, if needed. However, they should in any case prove that also “non-network” (or “third party”) solutions have been considered as alternatives contributing to addressing the issue of satisfying (N-1) criteria. Further work on the network development alternatives in this region will focus on such analyses.

## BIBLIOGRAPHY

- [1] "Criteria and Methodology for Distribution Network Planning" (EIHP, 2013)
- [2] "Rule on Capital Projects Assessment in Transmission and Distribution Network" (REPOWER Kosovo, 2017)
- [3] "Detailed Design Documentation for Revitalisation of 35 kV Overhead Lines Krk – Cres and Cres – Lošinj" (Dalekovod projekt and EIHP, 2017)
- [4] "Study of Development of Distribution Network in Elektroprimorje Rijeka areas Skrad, Crikvenica, Krk, Rab and Cres-Lošinj for the Period of 20 Years" (EIHP, 2018)

